Phenotypic Plasticity of the Teleost Brain: Relationships Between Predation Pressure, Personality, and Stress Coping Style

Brendan J. Joyce

A thesis in the

Department of Biology

Presented in partial fulfillment of the requirements

for the Degree of Doctor of Philosophy at

Concordia University,

Montréal, Québec, Canada

December 2022

CONCORDIA UNIVERSITY

SCHOOL OF GRADUATE STUDIES

This is to certify that the thesis prepared

By: Brendan Joyce

Entitled: Phenotypic Plasticity of the Teleost Brain: Relationships Between Predation Pressure, Personality, and Stress Coping Style

and submitted in partial fulfillment of the requirements for the degree of

Doctor Of Philosophy (Biology)

complies with the regulations of the University and meets the accepted standards with respect to originality and quality.

Signed by the final examining committee:

Dr. Uri Shalev _____ Chair

Dr. Dennis Higgs _____ External Examiner

Dr. Wayne Brake _____ External to Program

Dr. Robert Weladji _____ Examiner

Dr. Emma Despland _____ Examiner

Dr. Grant Brown _____ Thesis Supervisor

Approved by Dr. Grant Brown _____
Graduate Program Director

Dr. _____
Dean

Abstract

Phenotypic Plasticity of the Teleost Brain: Relationships Between Predation Pressure, Personality, and Stress Coping Style

Brendan J. Joyce, Ph.D.

Concordia University, 2023

Teleosts exhibit extensive, ongoing neuroproliferation within their brains even as adults, which facilitates indeterminate growth and permits them to recover from injuries to their central nervous system which would be catastrophic in higher vertebrates. As a result, the brains of teleosts show considerable phenotypically plasticity, adopting different morphologies in response to stimuli from the environment. This plasticity manifests as differential regional growth rates within the brain, with the balance between the rates of neuroproliferation and apoptosis determining if a region grows or shrinks. Their adaptive plasticity is constrained by the elevated metabolic cost of neural tissue, which penalizes excess investment in underutilized parts of the brain but also permits patterns of investment to change, leading to substantial intraspecific variation in brain morphology. The plasticity which leads to the morphological variation seen within species can exceed that seen between species and presents both obstacles to and opportunities for those who study teleosts or used them as model species. In this thesis, I set out to explore the potential ramifications of neuroplasticity in the teleost brain.

I begin with a review of the literature (Chapter 1), identifying factors known to influence brain morphology and the predominant methods and model species used to measure it. In Chapter 2, I tested the impact of exposure to predation risk on the brain morphology of juvenile Atlantic salmon (*Salmo salar*) and adult northern redbelly dace (*Chrosomus eos*). I found that gross brain morphology can change in under 14 days of elevated predation risk. Chapter 3 expands on this, finding that predation pressure lead to smaller hypothalami and bolder individuals. I also demonstrate that hypothalamic size correlates with shyness (i.e. risk averse phenotypes). In Chapter 4, I used predation-induced brain morphology to test how olfactory and hypothalamic investment influence anti-predator behaviour in proactive and reactive individuals. Finally, in Chapter 5 I conclude with an experimental validation of the methodology used for quantifying brain morphology (cross-sectional area); I tested its performance against the widely used ellipsoid estimation; in most circumstances, they were found to perform comparably. Together, my research provides strong evidence that short-term exposures to local stressors (i.e. predation, captivity) lead to predictable changes in brain morphology; changes that correlate well with studies of behavioural phenotypes.

Acknowledgments

The completion of this thesis would not have been possible had it not been for the support and encouragement of those around me. Concordia University and the National Science and Engineering Research Council provided financial support. I would like to express my gratitude to my supervisor Dr. Grant Brown, for his support, guidance, and, above all, his patience throughout this endeavor. This project could not have succeeded without those who volunteered their time: Laure-Ann Dubuc-Karary**,** Allison Winiewski, and Félixe Dumaresq Synnott assisted with dissections; also, Ebony Demers, Lauren Gazzard, and Anna Vallinakis were invaluable in the field. I credit much of my success to those who came before me and kindly shared their knowledge before moving on, Patrick Malka, Michelle Leblanc, and Dr. Chris K Elvidge. The long days and late nights at the Catamaran brook field site were made better by the company of my colleagues and fellow students, Caroline Bilhete, Amanda Jeanson, Arun Dayanandan, Victoria Chicatun, and Ashley Watt. Also, I have been fortunate to work with several outstanding undergraduates on their independent studies, Braeden Donaldson, Wyatt Toure, Alex Popescu, Annick Singh, and Nia Kastova. My thanks to Dr. Gray Stirling, Dr. Catherine Calogeropoulos, and Dr. Gregor Kos for their encouragement over the years. Finally, I would like to thank my family and friends for their ongoing support on this long road to completion. All work here was conducted in accordance with the guidelines set by the Concordia Animal Research Ethics Committee.

Contributions of Authors

Chapters 2-5 were written for and published in peer-reviewed journals. B.J. contributed to the conception, planning, collecting of data, data analyses, and preparation of all chapters. G. E. Brown contributed to the conception, planning, data analyses, and editing of all manuscripts.

Chapter 1 is in preparation for submission to a peer-reviewed journal.

Chapter 2 has been published:

Joyce, B.J., Brown, G.E., 2020. Rapid plastic changes in brain morphology in response to acute changes in predation pressure in juvenile Atlantic salmon (*Salmo salar*) and northern redbelly dace (*Phoxinus eos*). Can. J. Zool. 98, 186–194. https://doi.org/10.1139/cjz-2019-0131

Chapter 3 has been published:

Joyce, B.J., Brown, G.E., 2020. Short-term captivity drives hypothalamic plasticity and asymmetry in wild-caught northern red bellied dace (*Chrosomus eos*). J Fish Biol 97, 577–582. https://doi.org/10.1111/jfb.14408

Chapter 4 has been published:

Joyce, B.J., Brown, G.E., 2022. Olfaction and reaction: The role of olfactory and hypothalamic investment in the antipredator responses to chemical alarm cues by northern redbelly dace. Current Zoology https://doi.org/10.1093/cz/zoac086

Chapter 5 has been published:

Joyce, B.J., Brown, G.E., 2022. Estimating the volume of biological structures from a single 2D image: considering apparent cross-sectional area as an alternative to the ellipsoid method. Evol Ecol. https://doi.org/10.1007/s10682-022-10211-7

All authors reviewed the final manuscript and approved of the contents.

Table of Contents

List of Tables……...……viii

List of Figures……..…….. ix

List of Appendices……..……..... xi

General Introduction……... 1

Chapter 1: Environmentally Induced Intraspecific Diversity in the Brains of Fish…….…. 8

Introduction…… 8

Methods…….. 9

Results……... 10

Discussion……...…….. 15

Chapter 2: Olfaction and Reaction: The Role of Olfactory and Hypothalamic Investment in the Antipredator Response of Northern Redbelly Dace (*Chrosomus eos*) to Chemical Alarm Cues……...……...… 25

Introduction…….. 25

Methods…… 27

Results……... 31

Discussion……...…….. 31

Chapter 3: Rapid plastic changes in brain morphology in response to acute changes in predation pressure in juvenile Atlantic salmon (*Salmo salar*) and northern redbelly dace (*Phoxinus eos*)……...… 40

Introduction……... 40

Methods…… 41

Results…….. 42

Discussion……...…….. 43

Conclusions……...…... 43

Chapter 4: Short-term captivity drives hypothalamic plasticity and asymmetry in wild-caught northern red bellied dace (*Chrosomus eos*)…….. 48

Introduction……... 48

Methods……. 49

Results……... 52

Discussion……. 54

Chapter 5: Estimating the Volume of Biological Structures from a Single 2D Image: Considering Apparent Cross-Sectional Area as an Alternative to the Ellipsoid Method……. 63

Introduction……...…..... 63

Methods……. 65

Results ……...…... 68

Discussion……...…….. 69

General Discussion……...… 76

References……..… 80

Appendices……..…… 103

List of Tables

Introductory Table A: Table of predictions and associated chapters

Table 1.1: List of studies comparing the performance of two or more methods of quantifying teleost brain morphology, denoting which methods were found to be comparable (≈), which were recommended (✓), or to be used with caution (!)

Table 1.2: List of recent papers introducing methodologies suitable for use in teleost brains

Table 2.1: Mean values for parameters measured for juvenile Atlantic salmon (*Salmo salar*) in heightened vs. ambient risk conditions

Table 2.2: Mean values for parameters measured for dace (*Phoxinus eos*) in heightened risk, ambient risk, or wild caught conditions.

Table 3.1: Mean values for parameters measured for *Chrosomus eos* exposed for 14 days to either water, conspecific disturbance cues, repeated handling, skin extract simulating the injury death of a conspecific, and wild subjects caught at two locations.

Table 3.2: Parameters Estimates for the generalized linear mixed models (GLMM) of emergence time, hypothalamic asymmetry, and relative hypothalamic investment

Table 4.1: Predictions and outcomes for a) predation-induced morphological and behavioral changes and b) correlations between brain morphology and behavior

Table 4.2: Spearman's Rho correlations between the $\log_{10}$ transformed size of brain regions for dace in the ambient vs. heightened risk treatments, classified as having a strong or weak antipredator response phenotype or, classified as early or late emergers.

Table 4.3: Spearman Rho correlations between relative olfactory or hypothalamic investment vs. the change in vertical area use, activity level, and time spent stationary.

Table 5.1: 3D model metrics and mean estimates

Table 5.2: The percent differences by echinoderm specimen between full/half ellipsoid estimates, top-down / side-on orientations for ACA, and the optimal choice between methods

List of Figures

Fig. A: Diagram depicting the processes of a) neurogenesis – (i) a neural stem cell gives rise to a (ii) neuronal precursor cell which (iii) differentiates in a neuron; and b) apoptosis where (i) mature neuron undergoes chromatin condensation followed by (ii) nuclear fragmentation while the cellular membrane destabilizes; (iii) macrophages remove the debris

Fig. B: An illustration depicting: (i) the ship of Theseus (SoT) with the commander at the stern; (ii) lookouts standing at the height of the original mask (black) and new mast (grey); (iii) the apparent distance to the horizon increases with height (dashed line versus dotted line) such that; (iv) other ships may be spotted sooner

Fig. 1.1: Diagram showing the major subdivisions of the teleost brain; a) dorsal view of a juvenile Atlantic salmon (*Salmo salar*) brain; b) dorsal and c) ventral view, of a northern redbelly dace (*Chrosomus eos*) brain; OB – olfactory bulbs, TE – telencephalon, OT – optic tecta, CE – cerebellum, HYP – hypothalamus, PT – pituitary, MO – medulla oblongata; scale bar 4mm

Fig. 1.2: The cumulative total of papers published (blue squares) and the number of papers published by year (green circles)

Fig. 1.3: a) Bar chart showing the comparison count for all species with ≥4 comparisons; b) pie chart showing the species grouped by family – Salmonidae (Atlantic, chinook and coho salmon, rainbow and brown trout), Gasterosteidae (three-spine and ninespine stickleback), and the order Cyprinodontiformes which includes the families Rivulidae (Hart's rivulus) and Poeciliidae (Trinidadian guppy)

Fig. 1.4: Bar graph showing the number of cases by methodology for the period of 2001-2013 (light green bars) and in total for all years (dark purple bars)

Fig. 1.5: Bar chart showing the percentage of cases reporting by brain region; OB – olfactory bulbs, TE – telencephalon, OT – optic tecta, CE – cerebellum, HYP – hypothalamus, PT – pituitary, MO – medulla oblongata, WB – whole brain

Fig. 1.6: Pie chart showing the proportion of cases by category of experimental comparisons

Fig. 2.1: Procrustes analysis of the juvenile Atlantic salmon (*Salmo salar*) showing (A) the configuration of landmarks and polygons used in the analysis overlaid on two example Atlantic salmon brains, which exhibit the sort of variation observed in (B) a principal components (PC) plot of the distribution of brain shapes by treatment

Fig. 2.2: The mean relative regional areas of the (a) optic tecta and (b) olfactory bulbs by treatment for the northern redbelly dace (*Phoxinus eos*)

Fig. 2.3: Procrustes analysis of the northern redbelly dace (Phoxinus eos) showing (a) the configuration of landmarks and polygons used in the analysis overlaid on an example of a typical northern redbelly dace brain, which exhibits the sort of variation observed in (b) a principal

components (PC) plot for brain shape by treatment and (c) wireframe plo…ts representing the shape configurations, at either end of the PC1 axis, as deformations (warps) of the mean shape for all specimens.

Fig. 3.1: – Scatterplots of (a) $\log_{10}$ transformed latency to emerge from shelter versus hypothalamic area and (b) the ratio of right and left inferior hypothalamic lobe areas; in *Chrosomus eos* (Cope 1861). Insert: ventral image of a *C. eos* brain, showing the pituitary and asymmetric inferior hypothalamic lobes.

Fig. 4.1: Diagrams of (a) the rafts used to suspend the mesh enclosures, (b) the single camera setup for recording multiple tanks for behavioural testing, (c) an experimental test tank with 3x3 grid, and (d) a refuge used for emergence time testing.

Fig. 4.2: (a) The dorsal surface of a dace brain, showing the positions of the landmarks and semi-landmarks used for morphometrics; (b) a wireframe showing the mean configuration of landmark points for all specimens following Procrustes alignment; and (c) the ventral surface of a dace brain showing the left and right inferior lobes of the hypothalamus.

Fig. 4.3: (a) Bar chart showing the number of individuals in each combination of early/ late emergers and weak/ strong antipredator responders for ambient and heightened risk treatments. Notable differences in mean brain morphology and symmetry by (b) background risk– ambient/heightened risk, and (c) by antipredator response - strong (reactive)/weak (proactive) responders.

Fig. 4.4: The standardized values for (a) relative hypothalamic investment controlling for body size versus log10 transformed latency to emerge from shelter; and (b) relative olfactory investment versus the change in the number of intervals spent stationary on the substrate.

Fig. 5.1: The brain of an adult northern redbelly dace (*Chrosomus eos*); showing the subregions of the brain – the olfactory bulbs (1), the telencephalic pallium (2), the optic tectum (3), the cerebrum (4) and hypothalamus (5) as measured by ACA and EM.

Fig. 5.2: (a) Two distinctly different pears with identical lengths and widths. (b) Percent error for estimates comparing volume and area values for the center pear using polygons with 8, 16, 24, 32, 34, and 36 points.

Fig. 5.3: (a) Log_{10} transformed volume estimates versus known volume. Percent error of ACA and EM estimates versus apparent (b) circularity and (c) solidity.

Fig. 5.4: Scatterplot showing the average circularity and solidity of nine echinoderm specimens, with their silhouettes shown. Inset: bar chart showing the mean percent error for top-down and side-on, and mean ACA estimates, full/half-ellipsoids, and for EM when the optimal model is selected for each specimen.

List of Appendices

Appendix A: Supplementary materials for Chapter 1

Appendix B: Abstract for Chapter 2

Appendix C: Abstract for Chapter 3

Appendix D: Abstract for Chapter 4

Appendix E: Abstract and Supplementary materials for Chapter 5

General Introduction

While adult neurogenesis is a common feature of vertebrates, it is most pronounced in teleosts, which continuously produce new neurons (Kaslin et al., 2008). As compared to mammals and birds, where neurogenesis only occurs in some small regions, in teleosts neurons are supplied by neuroproliferation zones found throughout their brains (Kaslin et al., 2008). For instance, it is estimated that in zebrafish (*Danio rerio*), circa 12,000 new neurons are generated per hour (Hinsch and Zupanc, 2007). This ongoing neurogenesis is complimented by apoptosis (Fig. A), which serves to remove old and damaged cells through programmed cell death (Zupanc, 2008). Working in concert, neurogenesis and apoptosis are involved in the day-to-day growth or maintenance of the teleostean brain; which occurs depending on the ratio of the rates at which neurons are added versus removed (Puschina and Obukhov, 2011).

Neuroplasticity and the Teleost Brain

To maintain brain size, similar numbers of neurons must be generated and eliminated, whereas, lasting brain growth occurs when the rate cellular proliferation exceeds the rate of apoptosis (Pushchina and Obukhov, 2012). Notably, growth rates within the teleost brain may vary regionally, such that regions may grow (or shrink) at different rates (Zupanc, 2006). The ability to modulate regional growth rates also makes teleosts exceptionally good at repairing neuronal damage (Zupanc, 2006). Teleosts can repair or replace damaged neural tissue through neurogenesis and apoptosis, enabling them to rapidly recover from serious injuries. Small teleosts like zebrafish have been known to recover from brain lesions (Kishimoto et al., 2012; Kroehne et al., 2011) or repair a severed spinal cord (Cigliola et al., 2020; Sîrbulescu and Zupanc, 2011), in a matter of weeks. Regeneration experiments such as these, which involve recovery from plainly visible injuries, highlight how neuroplastic processes at the cellular level (neuroplasticity) can impact the gross brain morphology (phenotypic plasticity) of teleosts over short periods.

Phenotypic Plasticity of Teleost Brains

The brains of teleosts are known to be phenotypically plastic, with the potential to produce distinct morphologies in response to the environment (Gonda et al., 2009; Alexander Kotrschal et al., 2012). Plasticity is most pronounced during ontogeny (Pittman et al., 2013), but their capacity for morphological plasticity persists into adulthood (Fuchs and Flügge, 2014). This phenotypic plasticity enables individuals to respond to their environment by prioritizing investment in regions that might increase fitness, such as situationally relevant sensory regions while downregulating the growth of underutilized regions. For example, nine-spine sticklebacks (*Pungitius pungitius*), raised with reduced visibility (water with black dye) shifted their morphology to favors their ability to smell (larger olfactory bulbs) and reduced investment in their vision centers (smaller optic tecta) (Pike et al., 2018). This parallels the morphological adaptations of cave-dwelling shortfin molly (*Poecilia mexicana*) which, living in darkness, also have severely reduced optic tecta (Eifert et al., 2015).

Traditionally when such divergence was observed between populations it was attributed to long-acting natural selection (Soares and Niemiller, 2013). However, in the previous example of shortfin molly, common garden experiments suggest a strong plastic component to the apparent morphological divergence between the cave and surface-dwelling populations (Eifert et

al., 2015). The reduction of the optic tecta in both species illustrates an important concept that unpins the interpretation of brain morphology in fish, the investment-utility principle. This principle is rooted in the expensive tissue hypothesis (Tsuboi et al., 2016) and it contends that owing to energetic constraints regional size denotes utility to the individual (Iglesias et al., 2018; Kotrschal et al., 2017).

The Investment-Utility Principle

The performance of neural tissue is subject to the law of diminishing returns on investment (Niven and Laughlin, 2008). The energetic cost of growth and maintenance of brain tissue is especially high; the brains of ectotherms typically weigh less than 1.5% of body mass but consume around 3% of an individual's energy budget (Soengas and Aldegunde, 2002). The formation and heightened metabolism of neural tissue often require energetic tradeoffs with other "expensive tissues" such as the gut (Tsuboi et al., 2015), or visceral fat stores (Tsuboi et al., 2016). Correspondingly, regional size (a proxy for total energetic investment) is believed to be indicative of the importance (utility) of that region to the individual. Thus, for the shortfin molly in caves, the utility of full-sized optic tecta (vision) fails to outweigh their energetic cost (5-15% of the resting metabolism); for them, smaller tecta consuming closer to 4% suffices (Eifert et al., 2015; Moran et al., 2015).

The investment-utility principle is also supported by studies where regional morphology (size/shape) has been observed to correlate with a fish's behaviour. For example, in Rusosuomunsyöjä (*Perissodus microlepis*) the disparity between the size of the left and right tecta correlates with the lateralization of their feeding behaviour (Lee et al., 2017). Similarly, in northern redbelly dace, the size and symmetry of their hypothalami correlated negatively with boldness (Joyce and Brown, 2020b). Studies such as these suggest that in some instances gross brain morphology may contextualize and potentially explain some interindividual variation in behaviour. By extension, phenotypic/neuroplasticity is likely to correspond with intraindividual changes in behaviour. Overall, the investment-utility principle provides a practical framework for interpreting the morphology and experience-dependent neuroplasticity of teleosts.

The experience-dependent neuroplasticity of teleosts presets both opportunities and obstacles to the study of teleost brain morphology. On one hand, it opens new avenues for inquiry for both the study and potential exploitation of inducible brain morphology (Gonda et al., 2013). On the other, it complicates the interpretation of evolutionary relationships between species, since morphological variation within and between species can be comparable (Gonda et al., 2013; Hall and Tropepe, 2020). To parse the difference between obstacle and opportunity it can be helpful to employ a conceptual framework that reflects the dynamic nature of teleost brain morphology (Nicholson, 2018). When viewed in the context of the continual turnover of neurons, changes in brain morphology are the result of the aggregation of innumerable small changes where new material is introduced and old material is removed.

The Ship of Theseus

An ancient thought experiment - the ship of Theseus paradox - provides a means to conceptualize how to address either form of this question; in it a mythical ship is maintained through the gradual replacement of its parts, such that one day no original parts remain. The ship of Theseus (SoT) paradox is frequently invoked in biology when considering objects and

organisms which persist through time and are maintained by the gradual replacement of old parts for new ones (Nicholson, 2018). The paradox inherent in the classical form of the SoT story, mirrors the question posed about the persistence of individuality considering the neuroplasticity of teleosts:

> If all an object's parts are gradually replaced or modified – is it still the same object?

As implied by its name, the SoT paradox is subject to interpretation, as is the definition of what is meant by "the same"; correspondingly, the paradox has no universally accepted solution (Pickup, 2016). However, when asked the intuitive answer given by many is that, maintaining form and function is equates to the retention of individual identity; but modification tends to be viewed as producing something new (Hall, 1998).

A fish's neuroplastic brain can be likened to Theseus's ship; the person in command corresponds to the individual's personality and an observer studying the ship's movements from a distance represents an experimenter performing a behavioural assay. By exploring the parallels between the SoT and the phenotypic plasticity of teleostean brains it is possible to identify elements of the problem with plasticity and which may be relevant to those who study teleost brains and behaviour. Consider Theseus's ship with a new taller mast (Fig. B). The additional height of the mast permits a lookout at its top to spot enemy ships further away and act sooner and, as with a fish, what action is taken on depends on the personality of the decision maker.

A distant observer unaware of the lookout's new vantage point may misinterpret the significance of a quicker response to the enemy. For instance, if familiar with Theseus's past actions, the observer might misinterpret the reduced reaction time as a change in Theseus himself. Alternatively, a naïve observer might assume that the ship always could respond as quickly. In both cases, by thinking of the form of the ship as static and failing to consider the possibility of remodeling (adaptive plasticity), the observers reach erroneous conclusions, and the true significance of the ship's responses only becomes clear when past and present forms of the ship are considered. In the absence of this context, the observers must allow for the possibility of recent change and temper their conclusions accordingly.

How concerned an observer should be about the potential for misinterpretation depends on how likely it is that significant remodeling has occurred, the extent to which modifications are expected to impact the ship's performance, and if the significance of the modifications depends on who is at the helm. Similar questions may be applied to teleosts to avoid misinterpreting the significance of morphological and behavioural measures. The goal of this thesis was to explore how rapidly and thoroughly the phenotypic plasticity of the teleost brain might manifest and changes in both brain morphology and behaviour (Table 1.1).

Experimental questions and hypotheses

Like those observing the SoT, researchers routinely make inferences based on direct observations of behaviour (Jolles et al., 2017). Insofar as the brain governs behaviour responses, and its morphology reflects its function (Gonda et al., 2013) it is reasonable to suppose that underlying changes in morphology might produce corresponding changes in behaviours. So, our first line of inquiry was to explore what factors were known to influence morphology and

determine what was known about how quickly macroscopic changes might occur. We began with a preliminary review of the literature, which was later expanded to encompass what has been learned over the past twenty years (Chapter 1).

Our review found that intraspecific comparisons of brain morphology in teleosts were increasingly common but primarily confined to interpopulation comparisons or tested the effect of interventions during ontogeny, when extensive plasticity is expected (Pittman et al., 2013). Thus, although several environmental variables were known to influence brain morphology, including environmental enrichment (Kihslinger and Nevitt, 2006) and predation pressure (Burns and Rodd, 2008); relatively little work had examined the role or rapidity of adult neuroplasticity in teleosts (Fuchs and Flügge, 2014).

Previously lesion studies in neuroscience had shown that adult teleosts could regenerate substantial portions of their brains in less than a month (Kishimoto et al., 2012; Zupanc, 2006). This capacity for rapid healing led us to hypothesize that (1) plastic changes in morphology in response to a stimulus could occur on short timescales. We tested this hypothesis in Chapter 2 by manipulating the perception of predation risk with conspecific alarm cues (Dupuch et al., 2004), in juvenile Atlantic salmon and mature northern redbelly dace. Having established that the brain morphology of adult northern redbelly dace exhibited substantial plasticity, the results from Chapter 2 formed the basis for the methodology of subsequent studies in Chapters 3 and 4.

A study in ninespine stickleback (*Pungitius pungitius*) found that exposure to predator cues led subjects to produce smaller hypothalami (Gonda et al., 2012), and in Chapter 3, we hypothesized that (2) morphological divergence between groups subject to different levels of predation would correspond with differences in group behaviour. Furthermore, we hypothesized that (3) individual morphology would correlate with behaviour. The hypotheses of Chapters 2 and 3 were revisited in Chapter 4 when based on the results of a study that suggested that patterns of neuronal activation in teleosts are influenced by stress coping style (Butler et al., 2018), we hypothesized that (4) an individual's stress coping style may interact with its morphology in determining behaviour.

During the expansion of the literature review in Chapter 1, it became apparent that the methodology employed for Chapters 2-4, which uses cross sectional area as a proxy for volume (Burns and Rodd, 2008), had been surpassed by another long used approach based on treating brain regions as ellipsoids. While both methods have been validated, primarily by comparing them to one another or other methods (Park and Bell, 2010; White and Brown, 2015), little was known about the absolute performance of either, nor had the limits of their applicability been explored. Based on the results of previous validations we hypothesized that (5) the optimal volume estimation methodology would depend on how much the measured objects deviates from an ideal ellipse. We tested this hypothesis using an *in-silico* validation with virtual objects of known volume in Chapter 5. These predictions are summarized in Introductory Table A.

Introductory Table A – Predictions and associated chapters

Predictions	Chapters
(1) Plastic changes in the brain may occur rapidly	1, 2, 3
(2) Morphological divergence correlates with behavioural divergence between groups	2, 3
(3) Individual morphology correlates with behaviour	2, 3
(4) Morphological and behavioural correlates vary with and are contextualized by an individual's stress coping style	3
(5) The optimal method of estimating the volume of brain regions from photographs depends on the shape of the region	5

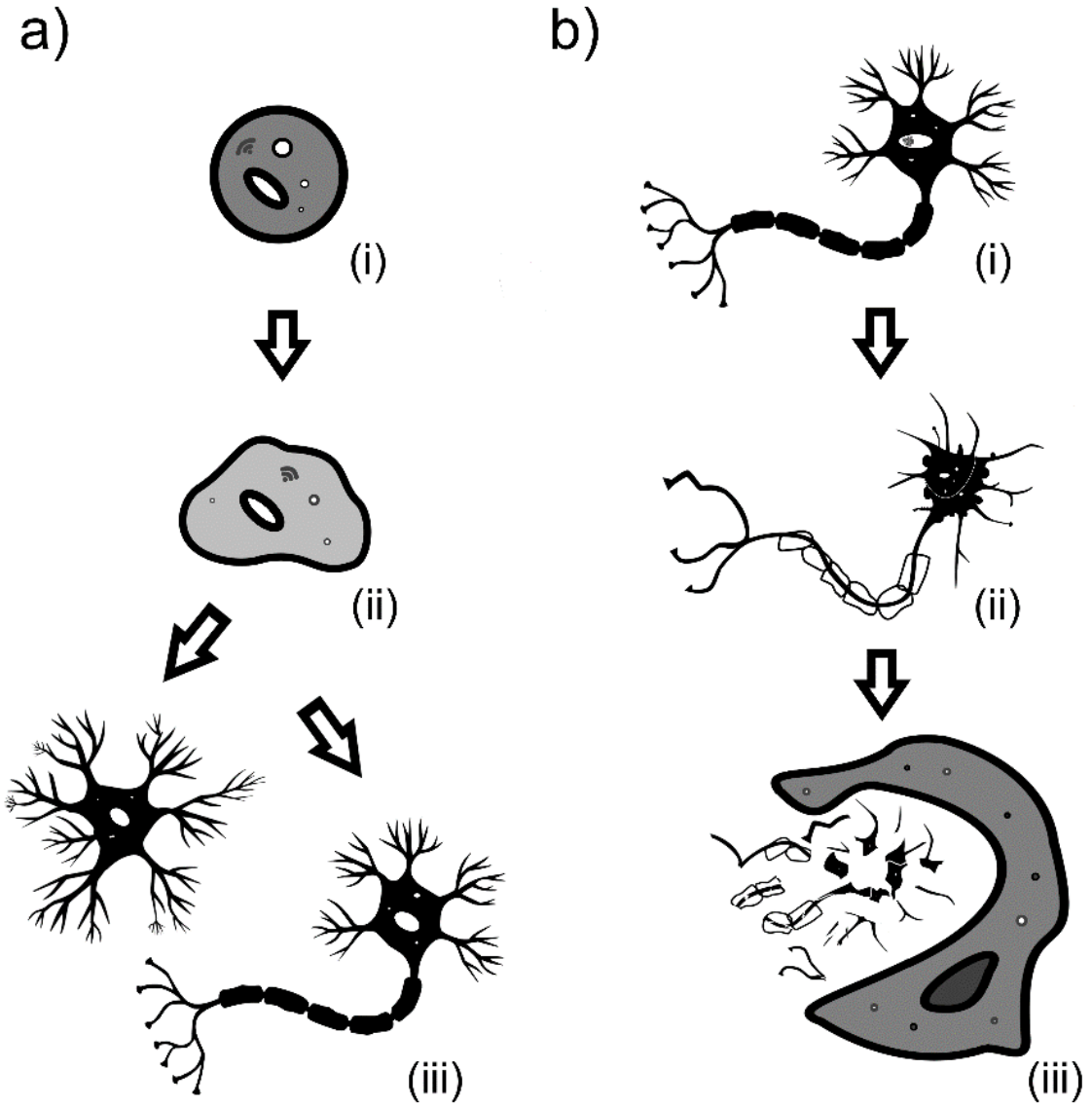

Figure A – Diagram depicting the processes of a) neurogenesis – (i) a neural stem cell gives rise to a (ii) neuronal precursor cell which (iii) differentiates in a neuron; and b) apoptosis where (i) mature neuron undergoes chromatin condensation followed by (ii) nuclear fragmentation while the cellular membrane destabilizes; (iii) macrophages remove the debris

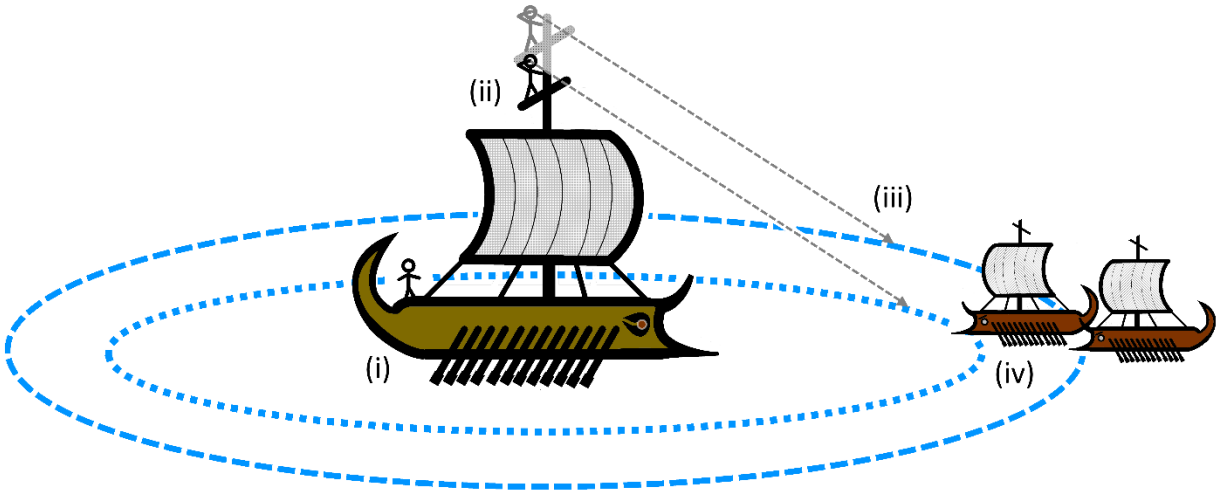

Figure B – An illustration depicting: (i) the ship of Theseus (SoT) with the commander at the stern; (ii) lookouts standing at the height of the original mask (black) and new mast (grey); (iii) the apparent distance to the horizon increases with height (dashed line versus dotted line) such that; (iv) other ships may be spotted sooner

Chapter 1: Environmentally Induced Intraspecific Diversity in the Brains of Fish

1.1 Introduction

Historically, explanations for observed differences in brain morphology between teleost species have focused on evolutionary divergence as the primary mechanism, and were grounded on the assumption that interspecific variation exceeds intraspecific variation (Eifert et al., 2015; Gonda et al., 2013). However, more recently it has been shown that variation in the brain morphology of teleosts has a large plastic component, and this phenotypic plasticity can lead to morphological variation within species being comparable to that seen between species (Hall and Tropepe, 2020). This complicates the separation of correlations from causes, especially when comparing the morphology of distantly related species, and to combat this studies using intraspecific variation in brain morphology have become increasingly common (Gonda et al., 2013; Hall and Tropepe, 2020).

In their review, Gonda et al. (2013) identify intraspecific brain evolution as a rapidly growing field. They argue that intraspecific studies have the conceptual advantage of examining microevolutionary adaptation as a means of identifying the roles played by evolutionary adaptation and phenotypic plasticity (Gonda et al., 2013). They, and others (Gonda et al., 2013; Hall and Tropepe, 2020), have called for more studies focusing on what the phenotypic plasticity and diversity seen within and between populations can reveal about the interaction between genes, the environment, and individual fitness. Since then, interest in comparative intraspecific brain morphology has rapidly grown, along with our understanding of adult neuroplasticity (Fuchs and Flügge, 2014). The study of intraspecific brain morphology has benefitted from a confluence of interest from the disparate disciplines concerned with the ramifications of environmentally induced morphology for individual fitness as well as for the evolution of populations and species. Much of this work has been done in the most diverse and neuroplastic group of vertebrates, (Ito et al., 2007; Zupanc, 2008), the teleosts.

The extensive phenotypic plasticity of teleost brains (Zupanc, 2008) coupled with the relative ease of quantifying their gross morphology (Ullmann et al., 2010; White and Brown, 2015), makes them suitable model organisms for a variety of research interests. In addition to the study of fish for ecological, evolutionary and conservation research, they are also commonly used as model organisms by other disciplines such as genetics (Dahm and Geisler, 2006), toxicology (Planchart, 2016), and endocrinology (Blanco et al., 2018). Teleosts are well suited for comparative neuroanatomy and much is known about their brains is thanks to neuroscience's perennial favourite, the zebrafish (*Danio rerio*) (Kalueff et al., 2014). The major subdivisions, delineated by the creases and furrows where they meet, are plainly visible (Fig 1.1), owing to their lack a neocortex (Ito and Yamamoto, 2009; Krauzlis et al., 2018). The phenotypic variation between individuals and populations is believed to reflect and arise from differences in the regional growth rates (Pushchina and Obukhov, 2012; Zupanc, 2006). The patterns of differential

growth, in turn, suggests which parts of the brain have been prioritized (Iglesias et al., 2018; Kaslin et al., 2008).

In teleosts and other ectotherms, brain tissue typically accounts for less than 1.5% of total body weight while accounting for approximately 3% of the body's energy consumption (Soengas and Aldegunde, 2002); making neural tissue very expensive to grow and maintain (Tsuboi et al., 2016). The extensive neuroplasticity of teleosts allows for substantial morphological and phenotypic plasticity of the brain (Fuchs and Flügge, 2014; Gonda et al., 2013), but investment is constrained by resource availability (Závorka et al., 2021) and by their genotype (Gonda et al., 2012). In recent years, the number and diversity of papers reporting on intraspecific variation in the brains of teleosts has grown substantially. Correspondingly, the list of environmental variables which might influence brain morphology encompasses a range of biotic, abiotic and social conditions. Which, by extension, may influence cognition and behaviour, an awareness of which these factors can inform the design of future experiments, by helping to account and control for potentially confounding variables.

In this qualitative review, we set out to characterize research regarding morphological variation in the gross brain morphology of teleosts reported in the past two decades. First, we explore trends in publication of the studies, looking at the number of papers published by year and which species were used. Second, we look at which methodologies were used to quantify brain morphology and contrast the predominant practices with the methods recommended in the literature. Finally, we examine the list of variables used for comparisons which may either induce changes in teleost brain morphology or contextualize extant morphology.

1.2 Methods

We conducted a literature review using the Web of Science and Google Scholar databases searching for papers published since early 2001. The Boolean search terms included were: (fish or teleost or teleostei) and (brain or neural or cerebral) and (plasticity, morphology, or size). The inclusion criteria were:

1) Published in a peer-reviewed journal between Jan 2001 and Dec 2021
2) Reported the result of an intraspecific comparison of gross morphology of the whole brain and/or brain regions in a teleost

A preliminary review of titles and abstracts was used to identify candidates for further examination. Those papers were then retrieved and checked against the inclusion criteria. As expected, the results from the two databases included substantial overlap (Martín-Martín et al., 2021) and reference management software (Zotero) was used to eliminate duplicates. Eligible studies were then re-examined and their information, including: the species used, the type of study (interpopulation, common garden etc.), the life stage of the subjects, the nature of the comparison, and the reported results were extracted and summarized in a table (Table A.1).

1.3 Results

Our search found 603 results on Google Scholar, and 2164 results from Web of Science. Of those, 318 papers were retrieved for closer examination and 79 papers satisfied the selection criteria which were included in the review. Several of those studies included more than one set of results, often from more than one species, in these cases, the results of each comparison were considered and tabulated separately; from those 80 papers, we identified a total of 150 comparisons (Table A.1).

1.3.1 A growing field

As seen in Fig 1.2, the number of papers reporting intraspecific comparisons of brain morphology in fish has grown substantially in the past two decades. Notably, the number of papers published in the interval between 2014 and 2021 is nearly twice as large as the number published between 2001 and 2013 (50 vs 29). Looking at the number of comparisons made between 2001 and 2013 (60 cases) versus those made between 2014 and 2021 (90 cases), and the number of species used (19 versus 37), we see that the comparative intraspecific brain morphology of teleosts as a field has substantially expanded and diversified in recent years. Although our review was limited to a few fish genera and included various types of studies, our results broadly align with the findings of Gonda et al. (2013) in suggesting that interest in intraspecific comparisons of brain morphology continues to grow.

1.3.2 Species diversity

The studies we identified employed a total of 48 different species; of those 20 appear once and only 8 species (17%) were well represented, appearing in four or more cases. Those 8 species represent approximately 55% of all the cases we examined (Fig 1.3a). Grouping the well-represented species by family, (Fig 1.3b), it became apparent that most of the species are from two families, the Gasterosteidae (sticklebacks), which are popular as model organisms in evolutionary ecology (Merilä, 2013; Reid et al., 2021), and the Salmonidae (salmon, trout, and charr) which collectively represent multiple economically and ecologically important species of fish (Naish et al., 2007).

1.3.3 Sticklebacks

The most encountered species in our sample was the three-spined stickleback (*Gasterosteus aculeatus*), which, along with the ninespine sticklebacks (*Pungnitus pungnitus*), made up 25% of cases (Fig 1.3b). The disproportionately high number and diversity of studies using three-spined sticklebacks (18% of cases), is illustrative of their ubiquity and long-established reputation as a model organism for studying adaptation and plasticity (Bell and Sih, 2007; Buechel et al., 2019; Noreikiene et al., 2015). Sticklebacks are small fish that occupy diverse habitats (marine, brackish, and freshwater) and that, coupled with their well-characterized neuroanatomy and genomes (Reid et al., 2021; Sanogo et al., 2011) makes them an attractive option for comparative neuroanatomy. Notably, several studies in ninespine sticklebacks provide an important insight into teleost neuroplasticity, that plastic responses to

factors such as predation, environmental complexity, and group size, are constrained by evolutionary history; seen as different patterns of investment in marine and freshwater populations (Gonda et al., 2009; Gonda et al., 2012). These evolutionary constraints can produce divergent brain morphologies between populations and in their descendants under common garden conditions (Gonda et al., 2013).

1.3.4 Salmonids

The second largest grouping of well-represented species was the salmonids (26 cases, 17%, Fig 1.3b). This number increased to 35 cases (24%) when five less well-represented species of salmonid were included (Coho salmon (*Oncorhynchus kisutch*, 3 cases), lake trout (*Salvelinus namaycush*, 2 cases), bull trout (*Salvelinus confluentus*, 2 cases), Arctic charr (*Salvelinus alpinus*, 1 case), and brook charr (*Salvelinus fontinalis*, 1 case). The family Salmonidae includes numerous species which provide vital ecosystem services (Watz et al., 2022), and some of which are classed as 'at risk' of extirpation (Irvine et al., 2005). Efforts to combat this have included conservation programs using hatchery-raised fish to restocking wild habitats (Bacon et al., 2015), and the promotion of farmed fish as an alternative to the continued depletion of wild stocks (Fluet-Chouinard et al., 2018; Guillen et al., 2019). Correspondingly, the conservation and farming of salmonids and other fishes are of increasing concern, and much attention is paid to their welfare while in captivity (Conte, 2004; Kristiansen et al., 2020). Upon closer examination of the salmonid subset, (Table A.1) it is unsurprising that a large proportion of them (21/32) explicitly concern hatchery conditions (i.e., population density, feeding regime, and environmental enrichment) or compare captive-bred and wild stocks. Based on this, it appears that brain morphology research in salmonids represents a subset of the field which is primarily oriented towards the goal of identifying possible interventions to improve efforts at conservation and aquaculture.

1.3.5 Poeciliids

Another prominent species in our sample was the Trinidadian guppy (*Poecilia reticulata*), which is a popular model organism for evolutionary ecology and genetics (Nakajima and Taniguchi, 2001; Reznick and Travis, 2019; Zandonà et al., 2017). They are small live-bearing fish and being easy to raise and breed, are a popular choice for laboratory studies and behavioural research (O'Neill et al., 2018; White and Brown, 2015). In our sample, we found that guppies were used in approximately 9% of cases, and the majority of these (9/14) used experimental manipulations of the physical or social environment. The remaining cases looked at the impact of predation on brain morphology using interpopulation and common garden approaches.

Guppies are frequently used to study predation pressure in the lab and the wild (Kotrschal et al., 2017; Vega-Trejo et al., 2022). In the wild, natural and interventional experiments using guppies are facilitated by the availability of multiple populations experiencing different levels of predation (Fraser and Gilliam, 1987; Reznick and Travis, 2019). Notably, one paper took this a step further and, using female guppies from 16 wild populations, found significant relationships between brain morphology and which predators were present in the environment (Kotrschal et

al., 2017). Similar results have been found for the total brain size of male guppies exposed to heightened predation pressure (Reddon et al., 2018). Taken together these results suggest that guppies are a good model for elucidating evolutionary and plastic responses to predation, however, as with the sticklebacks, it highlights the perils of assuming that all members of a species are equal in the potential for plasticity.

As interest in the comparative neuroanatomy of conspecific teleosts has grown so too has the diversity of the species studied. That said, most of the studies/cases which we examined used either small well established model organisms (poecilids and gasterosteiformes) primarily for basic research or looking at salmonids primarily with a focus on improving aquaculture practices. The results from these three families provides a firm base on which to build and researchers approaching comparative brain morphology in fish would be well advised to review their findings for new insights and potential confounds to avoid in their own work.

1.3.6 *Methodologies*

One major limitation to comparisons across studies comes from the diversity of methodologies that have been used to measure brain morphology by 1) making it difficult to select the appropriate approach and 2) by making it difficult to compare the results between studies. There is a range of methodologies, which can be categorized broadly as mass metrics (wet or dry weight), area metrics (2D cross-sectional area or centroid size), volume metrics including ellipsoid approximations, estimates from histology, and advanced imaging, i.e., magnetic resonance imaging (MRI) and computerized tomography (CT) scanning. Figure 1.4 contrasts the distribution of the methodologies employed before 2014 to the total number of cases for 2001-2021.

As seen in Table 1.1, histology and the ellipsoid method were the methods most often included and the methods most cautioned against as being likely to introduce measurement error, either through tissue shrinkage when performing histology, or through over/underestimation when objects deviate from an ellipsoid form. Also, the only methods to receive unambiguous endorsements were the advanced imaging techniques, MRI, and microCT. Of the two, microCT has received the most attention recently, in part due to its superior resolution for structures <1mm in size (Ziegler et al., 2011); as seen in Table 1.2, several papers have been published outlining advancements in using microCT in zoological research.

Remarkably, none of the studies in Table 1.1 included brain mass for comparison despite the prevalence of papers using brain mass as a proxy for brain size (Fig 1.4). Wet mass can be a good proxy for volume in that neural tissue has a density near that of water, in the range of 0.99-1.04g/cm^{3,} (Beckmann et al., 1999), however dry mass is also sometimes used. Wet brain mass is a relatively crude measure that ignores shape and infers size, as does dry mass. As a result, neither is an attractive option for morphological quantification considering other available methods. However, a recent report has highlighted a situation where the combination of wet and dry weight was useful to assess the water content of the brain. Yin et al., (2019) found that black rockfish (*Sebastes schlegelii*) exposed to microplastics had significantly higher water content. Given the apparent ubiquity of microplastics in aquatic environments (Amelia et al., 2021), brain

water content may be worth examining as a possible influence on brain morphology. On a related note, another recent report suggests that, for assessing the water content of small brain samples, vacuum drying is superior to heat-drying (Sebastiani et al., 2017).

A common theme among the quantification methodology papers (Tables 1.1 & 1.2) and among papers that advocate for the study of intraspecific morphological variation (Gonda et al., 2013; Hall and Tropepe, 2020) is that more advanced methods like MRI and CT should be used when available. They have several advantages, not least of which is foregoing the need to dissect the specimens, but also the ability to measure tissue *in situ* and potentially *in vivo* (Camilieri-Asch et al., 2020b; Clark et al., 2022). However, as discussed in the methodological comparison by White and Brown, (2015), another consideration is the availability and affordability of the training and equipment used in CT and MRI. Notably, the authors found CT to be more affordable in terms of equipment, time, and consumables than MRI but were still more costly than the next option, histology (White and Brown, 2015).

Histology offers an intermediate choice between advanced imaging and cruder measures like the ellipsoid method, and it has the advantage of revealing the underlying structure of the brain. However, it is still associated with considerable time and consumables costs as compared to estimates made from photographs (White and Brown, 2015). This coupled with the potential for distortions introduced during fixation and staining (Udagawa et al., 2019; Weisbecker, 2012), makes histology the least suitable option for quantifying the gross morphology of the teleost brain and its subdivisions. Correspondingly, relatively few histology papers were found reporting volumes, and there has been only a modest increase between 2014 and 2021.

The two most popular approaches used in the past twenty years were the ellipsoid method and 2D area approaches (Fig 1.4); both methods are forms of photographic volume estimation. Photographs are taken of the brain and analyzed to extract either length, width, and height, or its apparent cross-sectional area by measuring its silhouette (Joyce and Brown, 2022). The essential equipment for both approaches consists of a camera and freely available image analysis software such as ImageJ (Schneider et al., 2012). Despite concerns about over and underestimation resulting from treating all structures as ellipsoids, the ellipsoid method has seen widespread acceptance (Fig 1.4).

2D area approaches, which as of 2013 were well represented (Fig 1.4), failed to gain the traction of the ellipsoid method. However, a recently introduced method for estimating the brain volume of small fish using transillumination of the skull (Näslund, 2014a) has contributed to renewed interest in this approach. This simple, noninvasive methodology allows the brain to be measured in vivo and the field, facilitating high throughput and repeated measures (Jenkins et al., 2021; Mitchell et al., 2020). Although photographic approaches are comparatively crude, provided the differences are sufficiently pronounced, they are suitable for detecting variation in morphology, and they continue to be the most used methods (Fig 1.4). While we echo the assertions of others in saying that tools such as microCT are preferable when available, often they are not and, while photographic approaches are not as good, it appears that they have been widely accepted as good enough – at least from preliminary studies.

1.3.7 Regional Reporting

The subdivisions of the teleost brain visible dorsally are the: olfactory bulbs, telencephalic pallium, optic tecta, cerebellum, and medulla (Fig 1.1a); the pituitary and hypothalamic lobes are found ventrally (Fig 1.1b). A review of the tabulated results (Table A.1) revealed that some brain regions have received more attention than others (Fig 1.5). In addition to total brain size, the region most often reported on was the telencephalon, which appeared in 77% of cases. Conversely, the pituitary and medulla, which incidentally are the two regions that are often partially obscured by adjacent regions (the hypothalamus and cerebellum respectively), were the most frequently omitted regions. The two regions most often explicitly omitted due to damage during the extraction were the olfactory bulbs and hypothalamus.

Approximately 13% of cases only reported whole brain size and the majority of these (85%) were from studies that used wet or dry weight. The period following 2013 saw an increase (≈26%) in the frequency of papers reporting on the optic tecta and cerebellum, there was also a modest increase in the reporting rate for the hypothalamus (10%) and medulla oblongata (9%); the rates for the remaining regions were similar. Despite the increase in attention, the lack of reporting on the medulla may present an opportunity for future inquiry. The medulla oblongata, also known as the myelencephalon or brain stem, serves to relay messages between the brain and the spinal cord, and is tied to auditory perception (Sreekala, 2011) and an increase in its inclusion in future studies may be warranted.

1.3.8 *Comparisons*

The studies in our sample all involve one or more comparisons made between two or more groups of teleosts, and which tested an assortment of disparate hypotheses. Each case was categorized by the type of study (interpopulation, intrapopulation, common garden, etc.), and given a tag describing the nature of the differential (Table 1.1). Then the variables were broadly categorized (Fig 1.6), as relating to comparing habitats (within and between populations), investigating the impact of environmental factors both biotic (e.g., predation pressure and social environment) and abiotic (e.g., temperature and time of year), as well as the role of endogenous factors (e.g., energetic and reproductive condition).

As seen in figure 1.6, two categories stand apart from their parent groups, sex, and enrichment. Experiments involving environmental enrichment accounted for 14% of cases. It has been known for some time that the complexity of habitat has consequences for neural development (Mohammed et al., 2002; van Praag et al., 2000) which can influence brain morphology during ontogeny (Näslund et al., 2012), and in recent years, habitat enrichment has been promoted as a means of improving the welfare of teleosts in aquaculture (Jones et al., 2021; Näslund and Johnsson, 2016). Mounting evidence suggests that the level of enrichment in microhabitats can influence brain morphology, neuroplasticity, and cognitive performance (Fong

et al., 2019; Pereira et al., 2020; Salvanes et al., 2013). Future investigations should consider the potential importance of enrichment, and if employed to promote plasticity, any enrichment should be consistent across all treatments.

Approximately 11% of cases involved testing for sexual dimorphism, which taken together strongly suggest that many teleosts exhibit sexual dimorphism in their brains (Buechel et al., 2019; Jadhao et al., 2001), and also in their capacity for neuroplasticity (Ampatzis et al., 2012; Ampatzis and Dermon, 2007). The nature and direction of the sexual dimorphism seen in teleosts depend on the evolutionary history of the fish involved and may vary between populations; for example, marine threespine stickleback males typically care for young and have larger brains than females, whereas the pond-dwelling 'white' morph has no parental care and both sexes have similarly sized brains (Samuk et al., 2014). Consequently, patterns of sexual dimorphism are not readily generalized, and when employing both sexes, it should be accounted for. When doing so it is advisable to consider the sex ratio within any group, as the social environment may also influence outcomes (Kotrschal et al., 2012).

1.4 *Discussion*

In this review, we have examined the current state of research involving the comparative brain morphology of teleosts and our findings show that interest in this field continues to grow. As a field, this research has benefited from the diversity of disciplines that have taken an interest in teleostean brains. In addition to aiding in the study of brain evolution, teleosts have also provided convenient models in areas such as environmental toxicology (Pereira et al., 2016; Puga et al., 2016), the study of cognition (Pike et al., 2018; Yamamoto, 2009), and psychology (do Carmo Silva et al., 2018; Vallortigara, 2006). The studies seen here were conducted using many species; however, most of the studies seen here relied on three families, with much of what is known comes from the three-spine stickleback and various salmonids. Future studies should involve a greater diversity of taxa to allow researchers to assess the generalizability of trends and/or mechanisms.

Likewise, while most of the methodological studies advocate for more advanced methodologies, most of the work has used photographic volume estimates which, while crude, is often sufficient for detecting substantial morphological variation. Both the choice of methodology and the selection of which regions to study appear to be influenced by their difficulty and expediency. Most studies employed the ellipsoid method, which requires the fewest measurements of all the methods discussed, except weight; also, most studies reported the volume of the telencephalon, while the volume of the medulla oblongata, which tends to be poorly delineated, was usually omitted. While less than ideal, focusing on the simplest means of collecting the least ambiguous morphological measures is a reasonable approach, at least for pilot studies. Considering the changeable nature of teleost brain morphology, beginning with a pilot study approach may be advisable. As we have seen, there is a myriad of factors that may influence their morphology and, in turn, their behaviour and recent evidence suggest that these

changes may occur rapidly, potentially altering brain morphology with as little as 14 days of treatment (Donaldson and Brown, 2022; Joyce and Brown, 2020b).

Findings such as these underscore the importance of treating teleost brain morphology as dynamic as opposed to static (Fuchs and Flügge, 2014; McCallum et al., 2014). In this sense, the significance of any given morphological configuration is best understood in context and relative to preceding forms. For instance, wild-caught Northern redbelly dace kept in captivity for two weeks had measurably different brain morphology (smaller hypothalami) and became significantly less risk-averse (Joyce and Brown, 2020a); changes which were only apparent when captives were compared to contemporaneously caught controls. Results such as these indicate that short-term holding conditions may lead to considerable deviation from the morphology and behaviour of the source population and their influence should not be discounted. Our review of the research published since 2001 shows that interest in brain morphology continues to be a fruitful area of research; however, there is a bias towards a limited diversity of species and a range of methodologies, where both limit the generalizability of findings to other genera. The results to date suggest that teleost brain morphology can be highly labile, providing a powerful tool for the experimental manipulation of teleost brains and behaviour. However, they also highlight the range of endogenous and exogenous variables which might influence brain morphology; underscoring the importance of controlling for potential confounds. Overall, our review show that the study of teleost brain morphology and its plasticity is potentially relevant to anyone concerned with using teleosts to investigate the underlying regulation of behaviour and the role of phenotypic plasticity in the evolution of complex behavioural phenotypes.

Table 1.1 – List of studies comparing the performance of two or more methods of quantifying teleost brain morphology, denoting which methods were found to be comparable (≈), which were recommended (✓), or to be used with caution (!)

Histology	Ellipsoid	2D Area	Centroid Size	MRI	microCT	Reference
≈	≈					(Pollen et al., 2007)
	≈	≈				(Burns and Rodd, 2008)
!	!			✓		(Ullmann et al., 2009)
≈		≈	≈			(Park and Bell, 2010)
≈				≈		(Ullmann et al., 2010)
!	!				✓	(White and Brown, 2015)
	≈	≈				(Joyce and Brown, 2022)

Table 1.2 – List of recent papers introducing methodologies suitable for use in teleost brains

Method	Contribution	Reference
2D Area	Introduces the use of 2D area as a proxy for volume in teleost brains	(Burns and Rodd, 2008)
MRI	Describes the use and optimization of magnetic resonance histology in the zebrafish brain	(Ullmann et al., 2009)
Morphometrics	Outlines a method using 2D geometric morphometrics to quantify the size and shape of teleost brains	(Park and Bell, 2010)
2D Area	Introduces a method of estimating brain volume in vivo in small subjects by transillumination of the skull	(Näslund, 2014a)
microCT	Proposes a high throughput methodology for use with microCT	(Weinhardt et al., 2018)
microCT	Explores the use of microCT for examining structures in fish	(Udagawa et al., 2019)
microCT	Introduces diceCT a new CT methodology useful for visualizing the nervous system of fish	(Camilieri-Asch et al., 2020b)

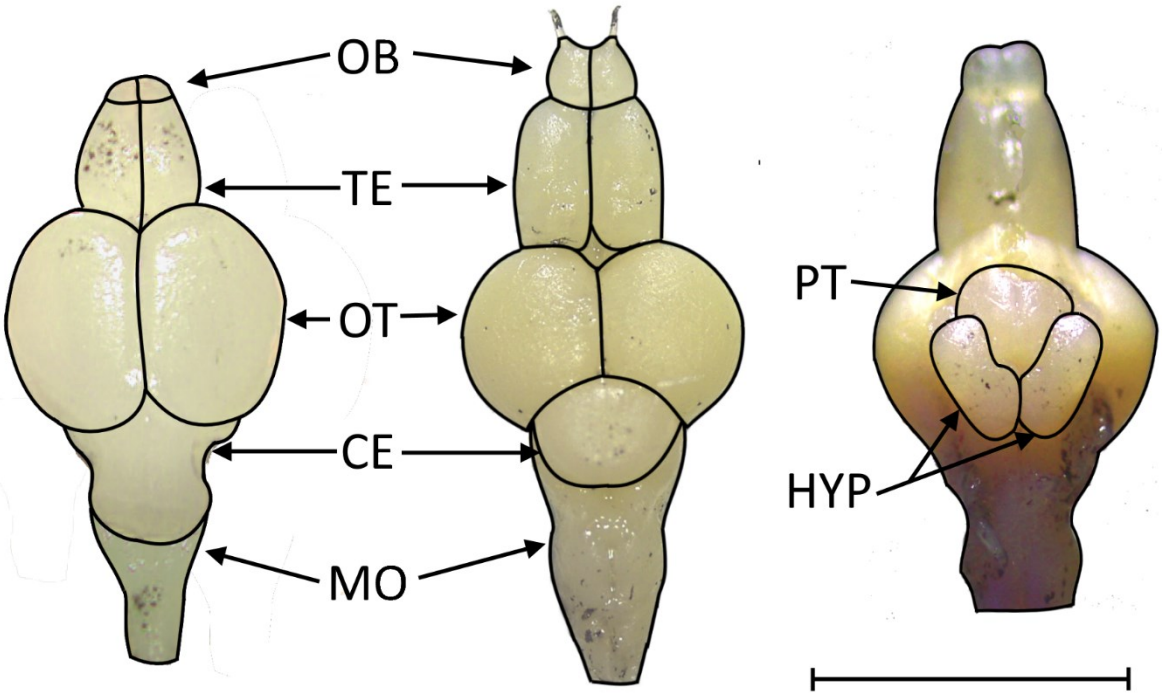

Figure 1.1 – Diagram showing the major subdivisions of the teleost brain; a) dorsal view of a juvenile Atlantic salmon (*Salmo salar*) brain; b) dorsal and c) ventral view, of a northern redbelly dace (*Chrosomus eos*) brain; OB – olfactory bulbs, TE – telencephalon, OT – optic tecta, CE – cerebellum, HYP – hypothalamus, PT – pituitary, MO – medulla oblongata; scale bar 4mm

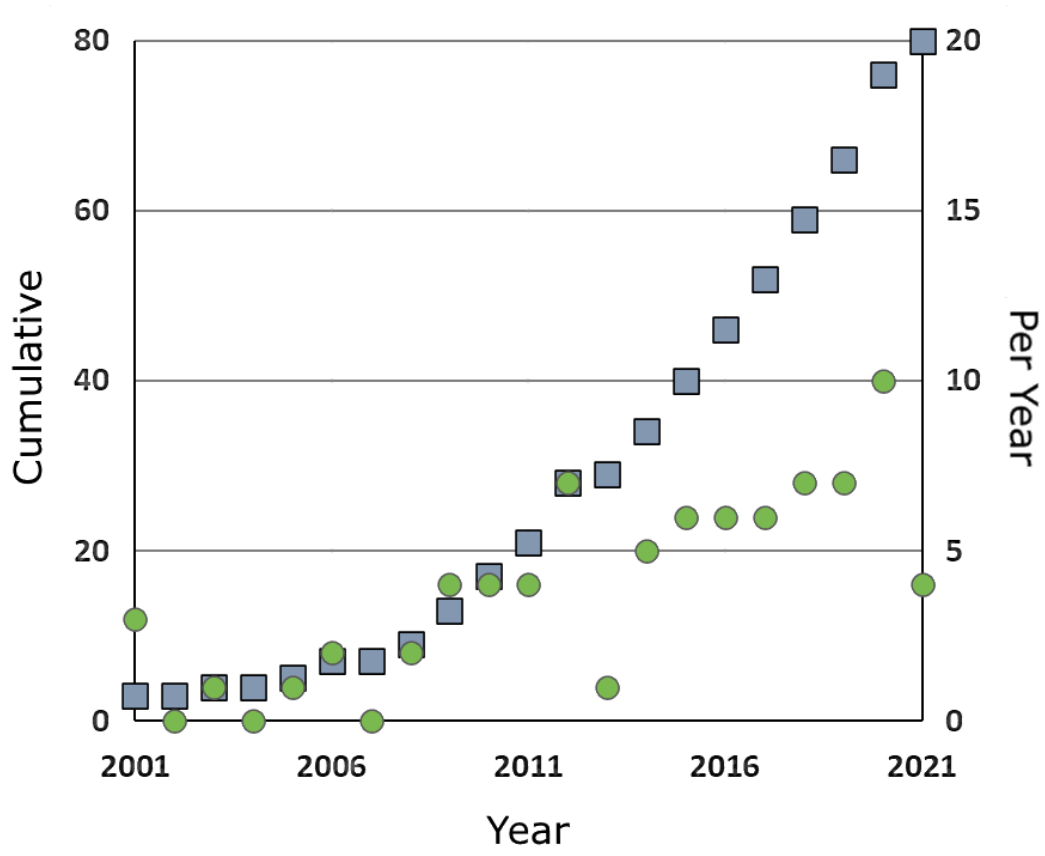

Figure 1.2 – The cumulative total of papers published (blue squares) and the number of papers published by year (green circles)

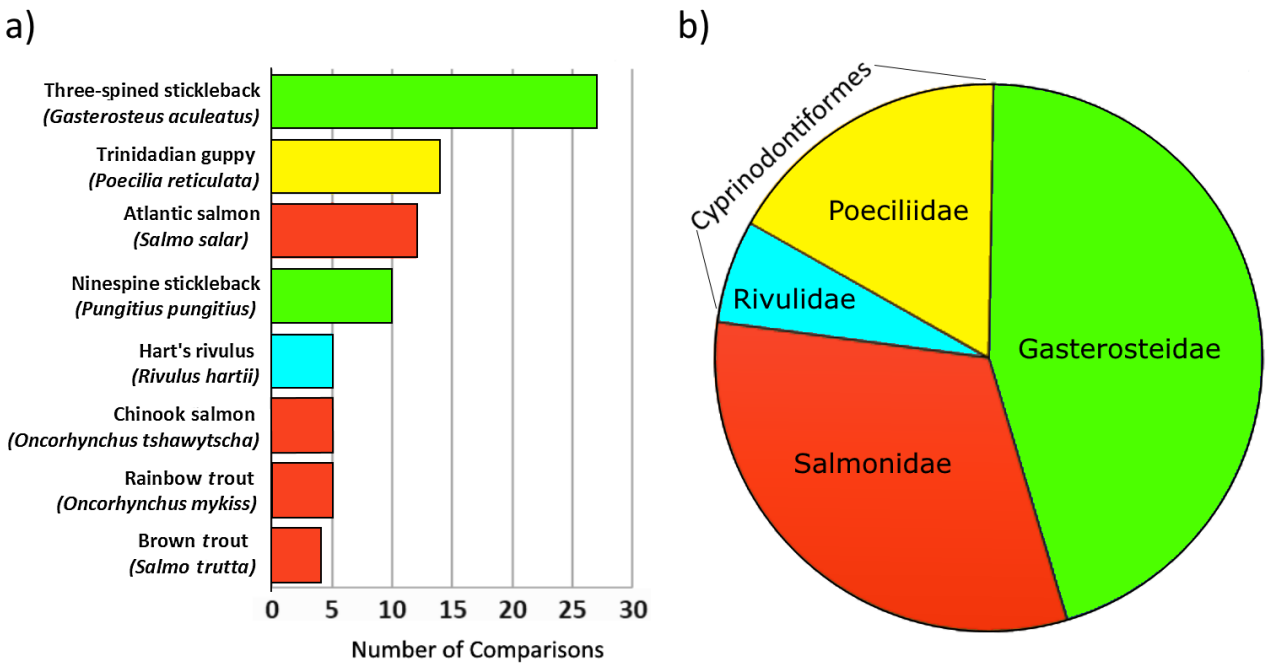

Figure 1.3 – a) Bar chart showing the comparison count for all species with ≥4 comparisons; b) pie chart showing the species grouped by family – Salmonidae (Atlantic, chinook and coho salmon, rainbow and brown trout), Gasterosteidae (three-spine and ninespine stickleback), and the order Cyprinodontiformes which includes the families Rivulidae (Hart's rivulus) and Poeciliidae (Trinidadian guppy)

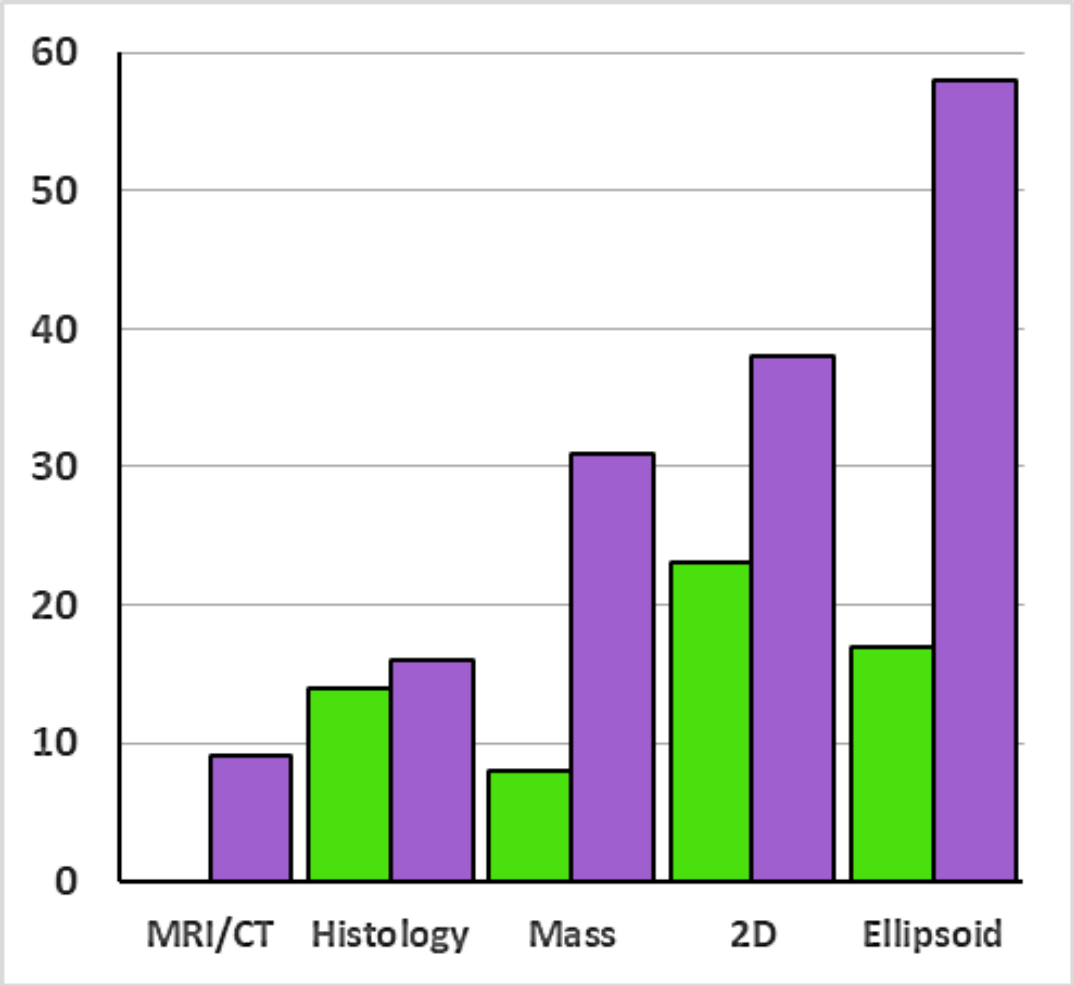

Figure 1.4 – Bar graph showing the number of cases by methodology from 2001 through 2013 (light green bars) and in total for all years (dark purple bars)

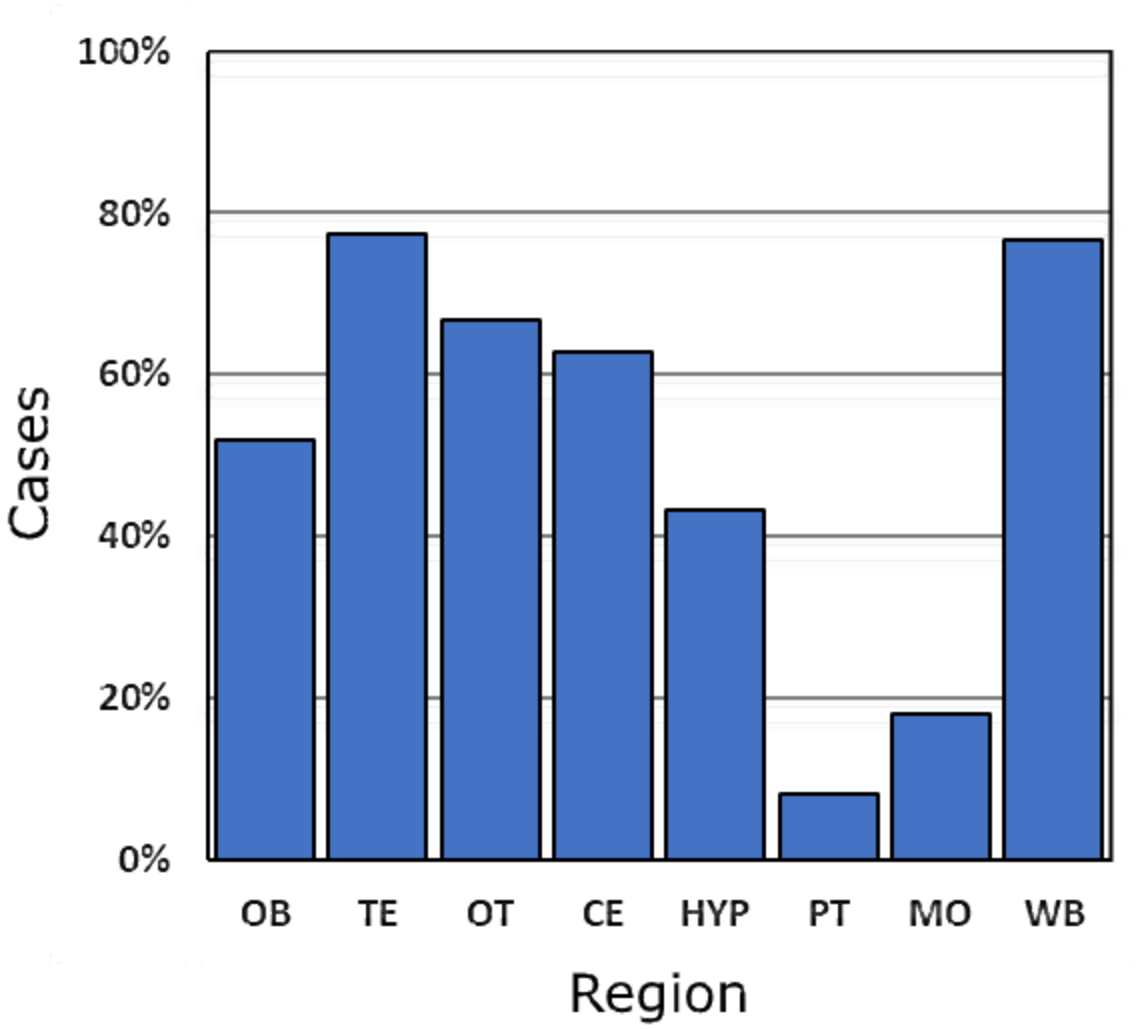

Figure 1.5 – Bar chart showing the percentage of cases reported by brain region; OB – olfactory bulbs, TE – telencephalon, OT – optic tecta, CE – cerebellum, HYP – hypothalamus, PT – pituitary, MO – medulla oblongata, WB – whole brain

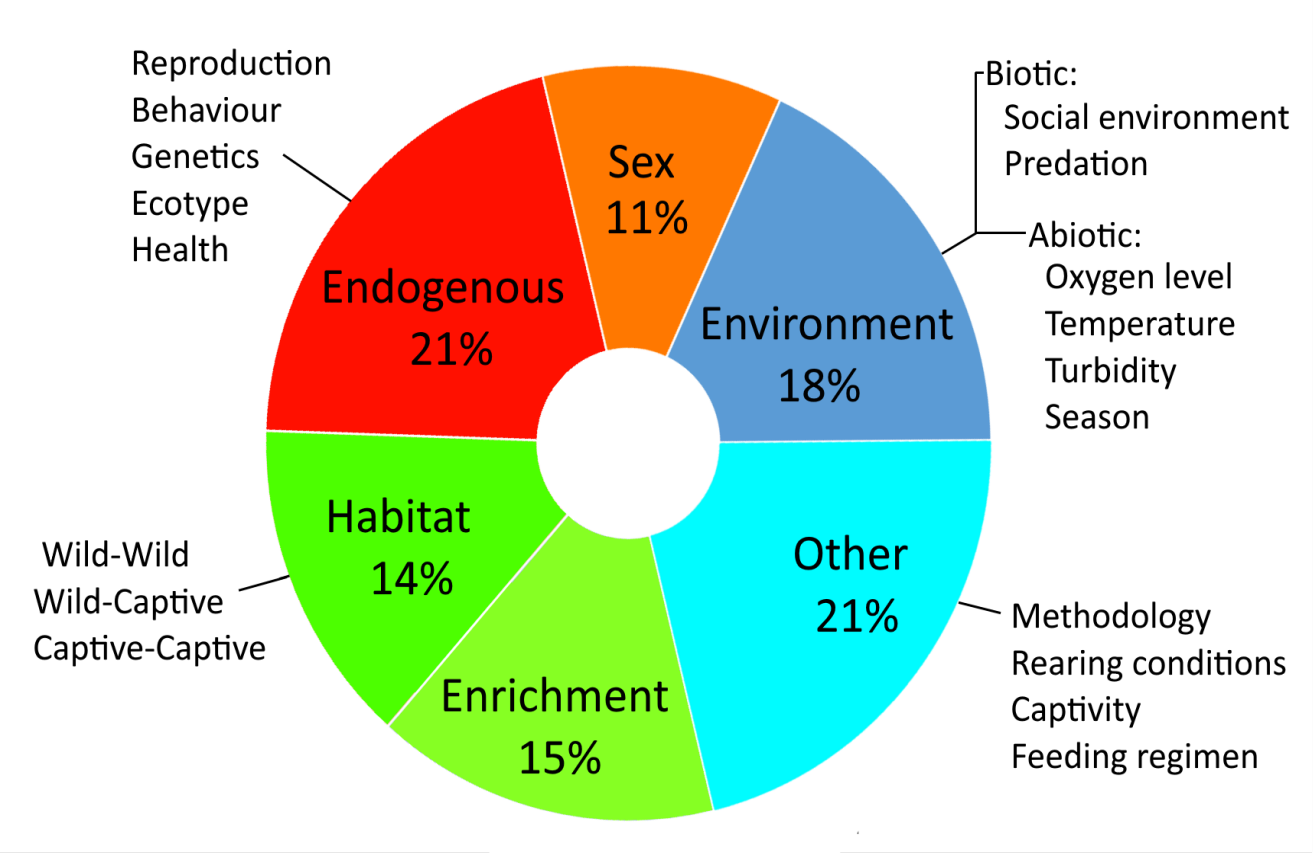

Figure 1.6 – Pie chart showing the proportion of cases by category of experimental comparisons

Chapter 2: Rapid plastic changes in brain morphology in response to acute changes in predation pressure in juvenile Atlantic salmon (*Salmo salar*) and northern redbelly dace (*Phoxinus eos*)

2.1 *Introduction*

Studies have demonstrated high degrees of variability in the brain morphology of teleost fishes, both within and between species (Kotrschal et al., 1998). Within species, variation in brain morphology between populations is often attributable to differing local ecological parameters (Cadwallader, 1975; Ebbesson and Braithwaite, 2012). For example, cave-dwelling populations of the shortfin molly (*Poecilia mexicana*, Steindachner, 1863) have severely reduced optic tecta compared with surface populations (Eifert et al., 2015). In the teleost brain, cell proliferation and neurogenesis occurs continuously (Kaslin et al., 2008; Zupanc, 2006) and may account for a high degree of adaptive phenotypic plasticity in brain morphology (Eifert et al., 2015; Gonda et al., 2013; Olivera-Pasilio et al., 2017).

This plasticity in brain morphology is often measured as differences in the size of distinct brain regions relative to whole brain size or body size (Gonda et al., 2013). Additionally, as a result of neurogenesis, subregions also exhibit considerable variation (Boulanger-Weill and Sumbre, 2019), resulting in changes in shape independent of relative size. As a result, the impacts of ecological parameters on brain morphology may be measured as differences in relative size of specific regions and (or) overall shape.

The dorsal surface of a teleost brain has four visually distinct regions: the olfactory bulbs, telencephalic pallium, optic tectum, and cerebellum. The metabolic cost of neural tissue is high, and the expense of producing and maintaining it is believed to impose strong constraints on brain size (Aiello and Wheeler, 1995; Tsuboi et al., 2015). Consequently, variation in the relative size of brains and their structures between populations of a species reflects energetic investment which correlates with the utility of that region for a population (Kaslin et al., 2008; Kotrschal et al., 2017, 2015). Recent studies have identified an array of factors that may influence the relative size of these regions. For example, under hatchery conditions, high population density in Atlantic salmon (*Salmo salar* Linnaeus, 1758) results in larger telencephalons and cerebella (Näslund et al., 2017), while captive rearing produces larger optic tecta in juvenile coho salmon (*Oncorhynchus kisutch* (Walbaum, 1792)) (Kotrschal et al., 2012). Ninespine sticklebacks (*Pungitius pungitius* (Linnaeus, 1758)) raised in a social environment have been shown to invest more in their optic tecta and less in olfaction (Gonda et al., 2009). These studies demonstrate the plasticity of teleost brains with respect to their environment.

Perceived predation risk can likewise shape brain morphology. Laboratory experiments with fish raised under elevated predation, such as freshwater ninespine sticklebacks, male guppies (*Poecilia reticulata* Peters, 1859), and Panamanian bishops (*Brachyrhaphis episcopi* (Steindachner, 1878)), have shown differential investment in overall brain size and (or) specific regions, including relatively larger olfactory bulbs and optic tecta, smaller hypothalami, and altered patterns of brain lateralization (Brown et al., 2004; Gonda et al., 2012; Reddon et al., 2018). Notably, these patterns can vary across environments (e.g., marine vs. freshwater) and contexts (e.g., the hunting strategy of local predators) both within and between species and this may result from local adaptation (Eifert et al., 2015; Gonda et al., 2012; Kotrschal et al., 2017;

Samuk et al., 2014). These results are echoed by comparisons between populations with differing degrees of predation in the wild across several species, including ninespine stickleback and guppies (Gonda et al., 2012; Kotrschal et al., 2017; Reddon et al., 2018). Additionally, recent work with guppies has found complex associations between mass of brain regions and predation pressure (Kotrschal et al., 2017; Reddon et al., 2018). Male guppies from high-predation streams and those raised in the laboratory with cues of elevated predation risk invest more in neural tissue than conspecifics from low-predation conditions (Reddon et al., 2018). In female guppies, exposure to predatory prawns (species of the genus Macrobrachium Bate, 1868) was correlated with larger brains and increased telencephalic investment, whereas the biomass of the blue acara cichlid (Andinoacara pulcher (Gill, 1858)) was associated with reduced olfactory bulb and hypothalamus size (Kotrschal et al., 2017).

Typically, this type of study has been conducted using either wild-caught or laboratory (hatchery) strains of prey exposed to some degree of chronic predation (Gonda et al., 2011; Handelsman et al., 2013; Kotrschal et al., 2017). The related laboratory studies have employed long periods of conditioning with levels of perceived risk elevated for one or more months (Gonda et al., 2009; Gonda et al., 2013, 2012; Näslund et al., 2017). In both the wild and the laboratory, subjects exposed to elevated predation for extended periods exhibited distinct brain morphologies. However, predation can be highly variable, both within an animal's range and across its lifetime (Schauber et al., 2009); predation's propensity for change combined with its lethal nature is expected to exert a strong selective pressure on the phenotypes of prey (Lima and Dill, 1990; Relyea, 2002).

Phenotypic plasticity in life history, morphology, and behaviour enables prey species to reduce their risk of consumption when confronted with an elevation in perceived predation pressure (Benard, 2004). Of the three, behaviour is often the most plastic and least costly (Murren et al., 2015; Snell-Rood, 2013). Individuals exposed to an increase in risk display antipredator behaviour immediately upon exposure and develop distinct behavioural phenotypes in a matter of days (Brown et al., 2015; Ferrari, 2014; Joyce et al., 2016). Teleost behaviour has been shown to correlate with brain morphology (Burns and Rodd, 2008; Gonda et al., 2009; Ito et al., 2007; Schnitzlein, 1964).

Here, we set out to determine if differences in brain morphology are detectable on a time scale commensurate with the behavioural plasticity previously observed in fish. We used conspecific chemical alarm cues, which are released from damaged skin and serve as a reliable indicator of an injured conspecific, to manipulate perceived predation risk (Mirza and Chivers, 2003; Wisenden et al., 2010). We used two species of teleost fish known to employ such cues: juvenile Atlantic salmon and northern redbelly dace (*Phoxinus eos* (Cope, 1861) = *Chrosomus eos* Cope, 1861) (Brown et al., 2011; Dupuch et al., 2004).

Our choice of a 2-week time frame for these experiments was informed by observations in several related fields of study. First, a reasonable upper limit for the time required for detectable plastic changes in the brain was established. We based this on the time required to regenerate an olfactory bulb damaged by lesioning, approximately 3 weeks in zebrafish (*Danio rerio* (Hamilton, 1822)), or complete removal, 4 weeks in goldfish (*Carassius auratus* (Linnaeus, 1758)) (Paskin et al., 2011; Zippel et al., 1993). Second, a lower limit was suggested by work in

threespine sticklebacks (*Gasterosteus aculeatus* Linnaeus, 1758), which after 6 days of exposure to predator cues had significant transcriptomic changes in their brain tissue (Sanogo et al., 2011).

Finally, as mentioned, often the first outwardly observable changes in an organism in response to elevated predation are behavioural (Elvidge et al., 2014; Mirza and Chivers, 2003; Wisenden et al., 2010). Evidence from studies conducted under natural conditions, such as with the Panamanian bishop, suggest that predation pressure selects for bolder behavioural phenotypes (Archard and Braithwaite, 2011; Brown et al., 2005). Work in threespine sticklebacks suggests that plastic changes in personality can occur rapidly, with increased boldness being detected 1 week following exposure to a live salmonid predator (Bell and Sih, 2007). Based on these combined observations, we hypothesized that macroscopically detectable differences in the relative size of brain regions and (or) overall brain shape, in response to additional predation risk, may be expected to manifest within 14 days.

2.2 *Materials and methods*

2.2.1 *Stimulus preparation*

We collected alarm cues from 16 Atlantic salmon (experiment 1) and 27 northern redbelly dace (experiment 2). Alarm-cue donors were euthanized by cervical dislocation in accordance with Concordia University's Animal Research Ethics protocol (AREC 30000255). We removed their skin by dissection and recorded the dimensions of the skin fillets. The fillets were homogenized with distilled water, filtered through polyester fiber, and diluted to a final concentration of 0.15 cm^2/mL. The resulting alarm cue was divided into 10 mL aliquots in plastic bags and frozen at −20 °C until needed.

2.2.2 *Collection, preservation, and sample storage*

The subjects were euthanized using an overdose of clove oil (prepared in accordance with Concordia University's Animal Research Ethics protocol AREC 30000255), weighed, and photographed. The subjects were individually preserved in 20 mL glass scintillation vials containing a solution of 3.7% paraformaldehyde in phosphate-buffered saline (PBS). Upon transfer to the laboratory, the preservative was replaced with fresh solution and the samples refrigerated at 4 °C.

2.2.3 *Sample preparation*

Brains were extracted by removing the neurocranium and severing the optic nerves and the spinal cord at the entrance of the vertebral column (Noguera et al., 2015). Once removed, they were placed beside a millimetric grid on high-contrast magenta felt saturated with PBS, which facilitated positioning and prevented them from drying out. The dorsal surface of each brain was photographed using a 3MP microscope camera affixed to an 8× to 35× binocular dissection scope using a small halogen spot lamp as a light source. Specimens, or portions thereof, damaged during dissection were coded, but only intact specimens were used in morphometric and multivariate size analyses.

2.2.4 *Photographic analysis*

Our approach to photographic analysis was adapted from and modified to also permit Procrustean analysis with the geomorph package in R version 3.03 (Adams et al., 2017), which

enabled us to estimate regional area and to analyze an additional aspect of the data (i.e., brain shape) that should reflect differences in relative regional investment. Procrustean analysis allowed regional size or shape variation to be visualized and compared between treatments.

Using ImageJ (Schneider et al., 2012), all images were coded, blind to treatment, and in random order by the addition of landmarks, corresponding to readily identifiable anatomical points, thereby defining each brain region (Fig. 2.1A). Cross-sectional areas were estimated as the area of the resulting n-sided polygon for each region and used as a proxy for regional size. Damaged specimens showing signs of separation between the telencephalon and the optic tectum were excluded from morphometric analysis and encoded with additional landmarks to permit estimation of cross-sectional area when landmarks were no longer shared between otherwise intact regions. Example brains were selected from samples collected in 2016, from the same source populations, and photographed with a 5MP Leica™ EZ4W HD dissecting scope using incident and oblique LED illumination. The images were isolated from their backgrounds, converted to grayscale, and overlaid with landmarks and polygons using Adobe Photoshop.

2.3 *Experiment 1: juvenile Atlantic salmon*

2.3.1 *Fish collection*

We obtained hatchery-raised Atlantic salmon from the Miramichi Salmon Conservation Centre and transported them to Catamaran Brook (46°52.7=N, 66°06.0=W), which is a nearby natural salmon habitat with parameters similar to those in the hatchery. Fry (n = 20) were haphazardly distributed into and held in 60 L transparent plastic bins (Sterelite™, 60 cm × 40 cm × 34 cm). We modified the totes cutting three windows (15 cm × 15 cm) in each of the long sides and covered them in 3 mm hardware cloth. The four bins were anchored in the Catamaran Brook to a steel I-beam, filled with a shallow layer of gravel substrate from the stream bed, and separated from one another by 0.5 m and with a water depth of 0.4 m. The windows were perpendicular to the water flow to enable drift fodder to enter for natural feeding. During the experiment, the mean (±SD) current velocity, adjacent to the enclosures, was 0.33 ± 0.01 m/s and the mean (±SD) water temperature was 20.6 ± 1.8 °C.

2.3.2 *Alarm-cue exposure*

To manipulate background predation risk, we created two groups: heightened risk (HR group), exposed to 10 mL of salmon alarm cue, and ambient risk (AR group), exposed to stream water, twice per day for 14 days. Ambient risk was selected to reflect the potential for exposure to alarm cue from wild salmon upstream. The cue was released while moving the syringe back and forth along the bin's windows and approximately 5 cm upstream. In an effort to enhance the perceived risk and reduce predictability, the exact timing of the morning and evening treatments was varied. The lids of the bins were opened daily for welfare checks; on three occasions, the elevated risk subjects were exposed with the lids open. Exposure occurred over approximately 14 days with the last treatment occurring 24 h prior to euthanasia.

2.3.3 *Morphometric analysis*

A statistical analysis of shape variation and covariation of shape with risk was performed in RStudio running the geomorph package (Adams et al., 2017). First, each data set underwent a generalized Procrustes analysis (GPA) employing the raw landmark coordinates and scaling data

obtained with ImageJ. GPA calculates the centroid size (CS) of each brain as the square root of the sum of squared distances from each landmark to the specimen's centroid. GPA also rotates all landmark configurations to a shared coordinate system and unit size and generates shape data as the Procrustes distances between specimens (Adams et al., 2013; Sherratt 2014). The Procrustes distance between two specimens is a measure of the difference between two sets of coordinates following Procrustes superimposition, calculated as the square root of the summed squared distances between the landmarks (Mitteroecker et al., 2013).

We evaluated our shape data graphically for outliers by treatment, using the plotOutliers function on the Procrustes aligned coordinates by group, and none were found. Then the data were tested for shape covariation, with centroid size serving as a proxy for brain size, using the procD.allometry function that included a test for homogeneity of slopes; no significant allometric relationships were found and the slopes were homogeneous. The output of the GPA was used to run a Procrustes ANOVA with shape as the dependent variable, risk as a fixed factor, and CS as the covariate, including a risk by the CS interaction term.

Procrustes ANOVAs employ a permutation procedure to generate random test statistics for comparison with the original and requires a user-specified number of iterations (Sherratt 2014). To minimize the variance around the reported p values, all analyses were carried out at 5500 permutations (Adams and Anthony, 1996). No significant interaction between risk and CS was found in Atlantic salmon or northern redbelly dace ($p > 0.05$) and the interaction was omitted from later analysis. Principal components analysis (PCA) including deformation grids were generated using the geomorph function plotTangentSpace (Adams et al., 2017).

2.3.4 *Size analysis*

Areas were obtained for each lobe separately and totaled by region: olfactory, telencephalic pallium, optic, and cerebellar. The sum of these areas was total brain area. The allometric relationship of brain with body size was controlled for by log10 transformation of the regional values (Kotrschal et al., 2012). Measures of standard length (SL) and mass (M) were $\log_{10}$-transformed and we computed Fulton's condition factor as $K = 100 \times M \times SL^{-3}$. Our data were analyzed using IBM SPSS Statistics for Windows version 25.0 (IBM Corp., Armonk, New York, USA).

The same initial multivariate GLM analysis was used for both species. First, the residuals for all transformed variables were assessed for normality with Shapiro–Wilk W tests ($p > 0.05$). Our model included all four brain regions with risk level as a fixed factor and the log10 of standard length as a covariate. The model was run with the inclusion of a length × risk interaction term; no significant interaction was found ($p > 0.05$) and non-significant interaction terms were excluded from subsequent analysis (Kotrschal et al., 2012). We followed up on significant results from the full factorial model with univariate GLM, initially including enclosure as a random factor and a length × enclosure interaction term. No effect of enclosure was found ($p > 0.05$) and it was excluded from the final model.

2.4 *Experiment 2: northern redbelly dace*

2.4.1 *Fish collection*

Our subjects were northern redbelly dace, a common and widely distributed bait fish (Stasiak, 2006). They were from an isolated population inhabiting a man-made pond (0.25 ha) in Kenyon township, Ontario, Canada, and were collected using baited (white bread) Gee's Improved minnow traps. Upon capture, we identified the northern redbelly dace visually by comparison to reference images (Froese and Pauly, 2018; Lyons 2018). They were separated from the bycatch, which consisted primarily of similarly sized finescale dace (*Phoxinus neogaeus* (Cope, 1861) = *Chrosomus neogaeus* (Cope, 1867)) and northern redbelly dace × finescale dace (*P. eos* × *P. neogaeus*) hybrids; the bycatch was subsequently released.

Upon being sorted, we transferred all of the captured northern redbelly dace to a 40 L glass aquarium fitted with an air stone and charcoal filter and held them for 24 h to assess their health and confirm their species prior to distribution. We distributed the northern redbelly dace across 10 containers haphazardly with 10 per container. Two of the containers were randomly selected as wild-caught controls and sacrificed by anesthetic overdose and preserved immediately.

The northern redbelly dace enclosures were 19 L white plastic buckets, which we modified with six 7.6 cm diameter holes (two on the base and four on the sides) covered by 6.5 mm galvanized hardware cloth fastened with steel rivets. These were suspended in the pond at the field site such that the northern redbelly dace occupied approximately 16 L. To deter possible predation and prevent jump outs, we covered them with bird netting. The buckets in each group were spaced 30 cm apart, the distance between the groups was 133 cm, and they were arrayed along the shoreline of a peninsula, projecting into the pond, with their holes oriented to ensure visual isolation between them. The meshed holes provided a combined 270 cm^2 of interface with the environment and permitted the northern redbelly dace to feed on drift fodder passing through the holes. Additional food in the form of tropical fish flake food (Nutrafin Max™, Hagen) was provided once daily at dusk. Excess food and waste exited the enclosure through two mesh-covered holes in the base. The enclosures were held over water 1.5 m deep, and during the experiment, the mean (±SD) noon water temperature was 21.3 ± 1.4 °C.

2.4.2 Alarm-cue exposure

Similar to experiment 1, we employed HR and AR groups; 10 mL of alarm cue or water was introduced into the enclosures twice a day. This was introduced by syringe via a length of airline tubing that led to a fixed release point approximately 5 cm below the water line. The cue was allowed to disperse within the enclosure for 5 min before the enclosures were flushed by pushing water through the enclosures laterally by means of a boat oar. The timing of the treatments and the interval between first and second injections varied from day to day in an intentionally unpredictable fashion, resulting in the only reliably risk-free period being between midnight (0000) and 0600. Exposure occurred over approximately 14 days with the last treatment occurring 36 h prior to euthanasia.

For northern redbelly dace, we conducted the same analysis as described above for Atlantic salmon. As our northern redbelly dace results included a wild-caught (WC) control group, we added two additional statistical comparisons. First, we included post hoc comparisons (least-squared difference) to the GLM tests of brain area. Second, we compared the Procrustes variance (morphological variation) for the shape data of the three groups (Adams 2018). The

relative areas of the olfactory and optic regions, by treatment and corrected for standard length, were calculated as $\log_{10}$(area)/ $\log_{10}$(length).

2.5 *Results*

2.5.1 Atlantic salmon

We found that Atlantic salmon from the HR and AR groups did not differ significantly from each other with respect to standard length, body mass, condition index, or total brain area (one-way ANOVA, $p > 0.05$; Table 2.1). The log10-transformed variables for regional areas, as well as the covariate, were normally distributed with respect to factors risk and enclosure (Shapiro–Wilk W test, $p > 0.05$). Multivariate GLM was insignificant for treatment (Pillai's trace = 0.13, $F_{[4,34]} = 1.24$, $p = 0.31$). Procrustes ANOVA found a significant effect of risk on brain shape ($F_{[1,17]} = 2.19$, $p = 0.02$), driven primarily by variation in the position of landmarks defining the optic tecta and cerebellum in the hind brain (Figs. 2.1A–2.1C), but not for overall centroid size or shape × size ($p > 0.8$ for both). The plotTangentSpace function reported 21 principal components (PC) with the proportion of variance for PC1 and PC2 being 0.34 and 0.15, respectively.

2.5.2 *Northern redbelly dace*

The HR, AR, and WC conditions were not significantly different in standard length, mass, or condition index (one-way ANOVA, $p > 0.05$; Table 2.2). There was a significant effect of treatment on total relative brain area (univariate GLM, $F_{[2,30]} = 8.94$, $p < 0.01$). As the olfactory bulbs were the region most frequently detached or damaged, we followed up with a GLM of total brain area without the olfactory bulbs vs. treatment, which was also significant ($F_{[2,68]} = 6.41$, $p < 0.01$). Post hoc least-squared difference testing showed that the HR fish had significantly larger brains than the AR (mean difference = 1.26 mm^2, $p < 0.01$) and WC (mean difference = 1.18 mm^2, $p = 0.01$) groups. As with the Atlantic salmon, the response variables were normally distributed (Shapiro–Wilk W test, $p > 0.05$). Multivariate GLM analysis for all intact specimens was significant for risk (Pillai's trace = 0.559, $F_{[8,56]} = 2.713$, $p = 0.013$) and univariate GLM found a significant effect of treatment for the olfactory bulbs ($F_{[2,30]} = 5.62$, $p < 0.01$) and optic tecta ($F_{[2,30]} = 5.756$, $p < 0.01$) (Figs. 2.2A–2.2B). Follow-up univariate GLM of all specimens with intact optic tecta was also significant ($F_{[2,68]} = 8.248$, $p = 0.001$). The telencephalic palliums did not differ significantly in size across treatments, nor did the cerebella ($p > 0.05$).

Procrustes ANOVA found a marginally non-significant effect of treatment for both groups ($F_{[2,27]} = 1.69$, $p = 0.07$) and log10transformed centroid size ($F_{[1,27]} = 1.7$, $p = 0.08$) (Figs. 2.3A–2.3C). The test of morphological disparity among the three groups showed the Procrustes variance (PV) for the AR group was significantly greater than for the HR and WC groups ($PV_{AR} = 0.004$, $PV_{HR} = 0.0025$, $PV_{WC} = 0.0025$, $p < 0.01$ for both).

2.6 *Discussion*

Our results suggest that exposure to conditions of elevated predation risk for as little as 2 weeks is sufficient to induce differential brain morphologies in two species of freshwater fish. Interestingly, our two focal species were at very different life-history phases (juvenile Atlantic salmon and sexually mature northern redbelly dace), consistent with the observation that teleosts

retain neuroproliferation throughout their life. In Atlantic salmon, these differences were primarily detectable as a difference in shape, whereas in northern redbelly dace, differences in proportional investment in different brain regions were most pronounced.

In experiment 1, we employed hatchery-raised Atlantic salmon and exposure to heightened risk produced no significant differences in brain size relative to controls, suggesting similar degrees of investment in neural tissue; however, there was a demonstrable difference in brain shape. Brain regions, such as the optic tectum, are heterogeneous structures composed of various subregions and cell populations (Boulanger-Weill and Sumbre, 2019). Just as differences in size reflect investment at the regional level, our observed differences in shape may reflect differential patterns of growth at the subregional level.

Our experiment with the northern redbelly dace, in some ways an inversion of our Atlantic salmon work, changed fewer abiotic parameters, with the primary alteration being the imposition of confinement to a single location within the pond. Here heightened risk produced larger brains compared with ambient risk and wild-caught controls with detectably larger olfactory and optic tecta but did not result in a significantly distinct brain shape. However, the northern redbelly dace warp grids do show an expansion of the mid- and forebrain (to the left) or hindbrain (to the right) along the PC1 axis, which is seen as relatively larger squares on the grid. Although not detected at the level of significance by the Procrustes analysis, the relatively larger mean optic tecta and olfactory bulb sizes of the HR group are reflected by the preponderance HR morphologies found to left of the y axis on the PCA plot.

Although we cannot directly compare these two experiments due to the methodological differences that we have described, we can report that in both experiments, exposure to a sudden and prolonged exposure to conspecific skin extract resulted in distinct brain morphologies, which are in line with patterns of alteration seen in populations exposed to heightened predation pressure in previous studies. The northern redbelly dace exposed to heightened risk developed larger olfactory bulbs with results similar in magnitude to what was reported by Gonda et al. (2012) in freshwater ninespine sticklebacks exposed to simulated predation risk. These and our other results suggest that brain morphology is strongly influenced by environmental conditions, including predation (Ebbesson and Braithwaite, 2012).

For our Atlantic salmon fry, the transition from the hatchery necessarily entailed a shift in living conditions, including a dramatic decrease in population density, a shift from artificial to natural lighting, and an altered water chemistry. Additionally, cessation of the supplemental feeding upon leaving the hatchery required the fry to feed on and potentially compete for drift fodder (Imre et al., 2005). Beyond the stresses of the transition, the HR fry may have been subject to non-consumptive effects of predation (NCEs), such as reduced foraging time and elevated stress (Elvidge et al., 2014; Elvidge and Brown, 2015). We expected the HR fry to exhibit signs of these NCEs with potentially reduced standard length, mass, condition index, and (or) total brain size. That there was no effect of treatment for these outcomes may indicate that the duration or intensity of risk elevation was insufficient to produce noticeable negative effects (Archard et al., 2012; Elvidge et al., 2014).

In contrast with our Atlantic salmon work, the northern redbelly dace were wild-caught specimens and included the imposition of confinement; thus, preventing their natural diel feeding migrations and creating artificially maintained shoals (Naud and Magnan, 1988). As their pond

was static, we could not rely on sufficient drift fodder entering the northern redbelly dace enclosures and supplemental feeding was employed. Owing to this and the imposition of restricted movement, energy restriction was expected to be less critical than with the Atlantic salmon. Both treatment groups maintained their condition factors and separately exhibited traits indicative of growth and investment in somatic or neural tissue.

The AR group, confined and fed but not exposed to elevated risk, had the largest bodies and the most widely distributed brain morphologies. Within this group, brain shapes spanned the x axis of the PCA plot (Fig. 2.3B), resulting in a significantly greater Procrustes variance. Although effects of confinement (i.e., common garden and hatchery conditions) have been demonstrated in other species, we had no a priori expectations for our northern redbelly dace with regard to shape. As such, the holding conditions themselves may have influenced the final brain shape and further investigation is required to characterize their effects.

One potential consequence of confinement was the establishment of new social hierarchies within the bins. Changes in social status can alter patterns of gene expression in the brain in minutes (Maruska and Fernald, 2010). Furthermore, social status has been shown to regulate growth rate in fish, with social ascent increasing growth rate and social descent slowing and potentially reversing it (Elvidge et al., 2014; Hofmann et al., 1999; Maruska and Fernald, 2010). The wide variance of the AR group may reflect the effects of imposing an inescapable social group, raising the possibility of social rank as an additional variable in future studies.

We relied on the introduction of conspecific chemical alarm cues to simulate a stark increase in predation. The relative concentration of alarm cue used (1.5 cm^2 of skin per exposure) roughly corresponds to the destruction of one individual conspecific in the immediate vicinity of its release. Relative to their previous predation risk (none for Atlantic salmon and presumed to be very little for northern redbelly dace), these concentrations of alarm cue likely represented the introduction of a new and voracious predator into their environment. However, owing to both of our model species having a high degree of olfactory sensitivity, coupled with the proximity of their neighbors and the natural settings of the experiments, our AR groups cannot be said to have been unexposed to predation. Studies with northern redbelly dace and Atlantic salmon suggest that both species are sensitive to degrees of perceived predation risk and exhibit responses proportional to its intensity (Blanchet et al., 2007; Dupuch et al., 2004; Leduc et al., 2010; Wisenden, 2008). Our findings suggest that in both experiments the intensity of risk encountered by the HR groups was sufficiently elevated to result in differentiation.

Under these apparently life or death conditions, changes that reduce the odds of being eaten and their attendant NCEs become worthwhile (Abrahams, 2006; Benard, 2004; Lima and Bednekoff, 1999). Inducible somatic defenses can take weeks or months to become fully effective and their appearance coincides with changes in other traits that can impose a cost for their implementation (Relyea and Auld, 2004). For instance, the greater body depth of crucian carp (*Carassius carassius* (Linnaeus, 1758)) trades reduced swimming efficiency for reduced predation risk (Pettersson and Brönmark, 1999; Vollestad et al., 2004). The rapidity and flexibility of behavioural change in the face of predation is made possible by the brain. There is increasing evidence that this behavioural plasticity is underpinned by concurrent neuroplasticity. As a result, teleosts enjoy a remarkable capacity to cope with a changing world.

These experiments provide a point of reference for anticipating when differences may be detectable. Our results suggest that the teleost brain is more rapidly adaptable than has been previously reported. Further study is needed to determine to what extent these observed differences correlate with specific antipredator behaviour. Presently, our results may inform behavioural research more generally by highlighting how quickly environmental change produces macroscopic changes in morphology.

Table 2.1: Mean (± SE) values for parameters measured for juvenile Atlantic salmon (*Salmo salar,* (Linnaeus, 1758)) in heightened vs. ambient risk conditions. Degrees of freedom = 1 and 38 for all. See text for details.

	Ambient risk	Heightened risk	F[a]	P
Standard length (mm)	32.20 ± 0.86	32.47 ± 0.54	0.08	0.78
Body mass (g)	0.40 ± 0.03	0.40 ± 0.02	0.02	0.80
Condition index	1.18 ± 0.03	1.16 ± 0.03	0.17	0.68
Total brain area (mm^2)	8.55 ± 0.26	8.02 ± 0.24	2.20	0.15

Table 2.2: Mean (± SE) values for parameters measured for dace (*Phoxinus eos, (Cope, 1861)*) in heightened risk, ambient risk, or wild caught conditions. Degrees of freedom = 2 and 71 for all, except total brain area, where df = 2 and 33. See text for details.

	Ambient risk	Heightened risk	Wild caught	F	P
Standard length (mm)	44.60 ± 0.47	43.60 ± 0.46	43.00 ± 0.07	2.07	0.13
Body mass (g)	1.20 ± 0.03	1.12 ± 0.03	1.08 ± 0.03	2.98	0.06
Condition index	1.35 ± 0.02	1.35 ± 0.02	1.36 ± 0.03	0.04	0.97
Total brain area (mm^2)	12.74 ± 0.18	14.00 ± 0.26	12.82 ± 0.47	6.59	0.004

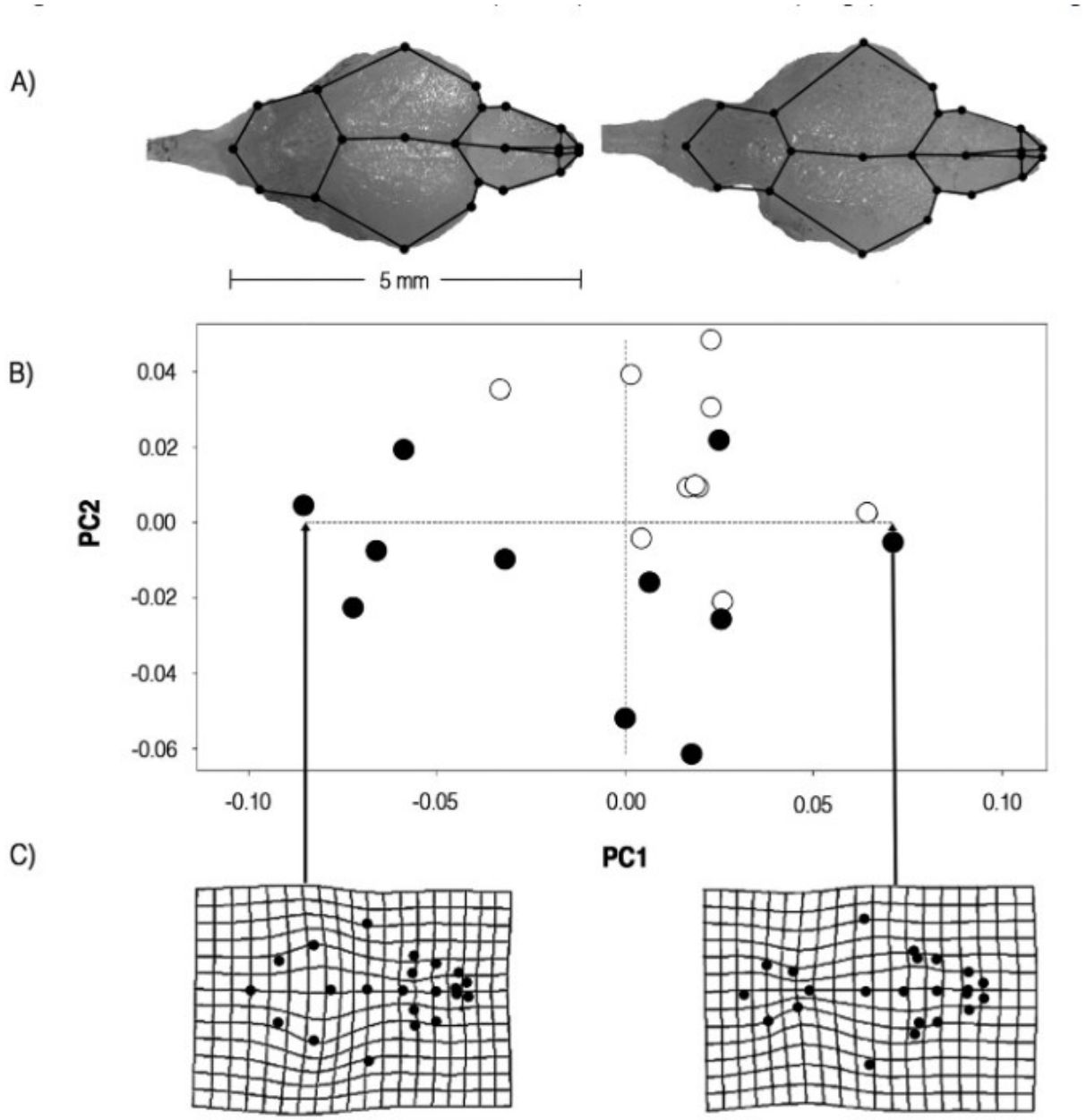

Figure 2.1. Procrustes analysis of the juvenile Atlantic salmon (Salmo salar) showing (A) the configuration of landmarks and polygons used in the analysis overlaid on two example Atlantic salmon brains, which exhibit the sort of variation observed in (B) a principal components (PC) plot of the distribution of brain shapes by treatment (ambient risk (black circles) and heightened risk (white circles)) and (C) wireframe plots representing the shape configurations, at either end of the PC1 axis (arrows), as deformations (warps) of the mean shape for all specimens.

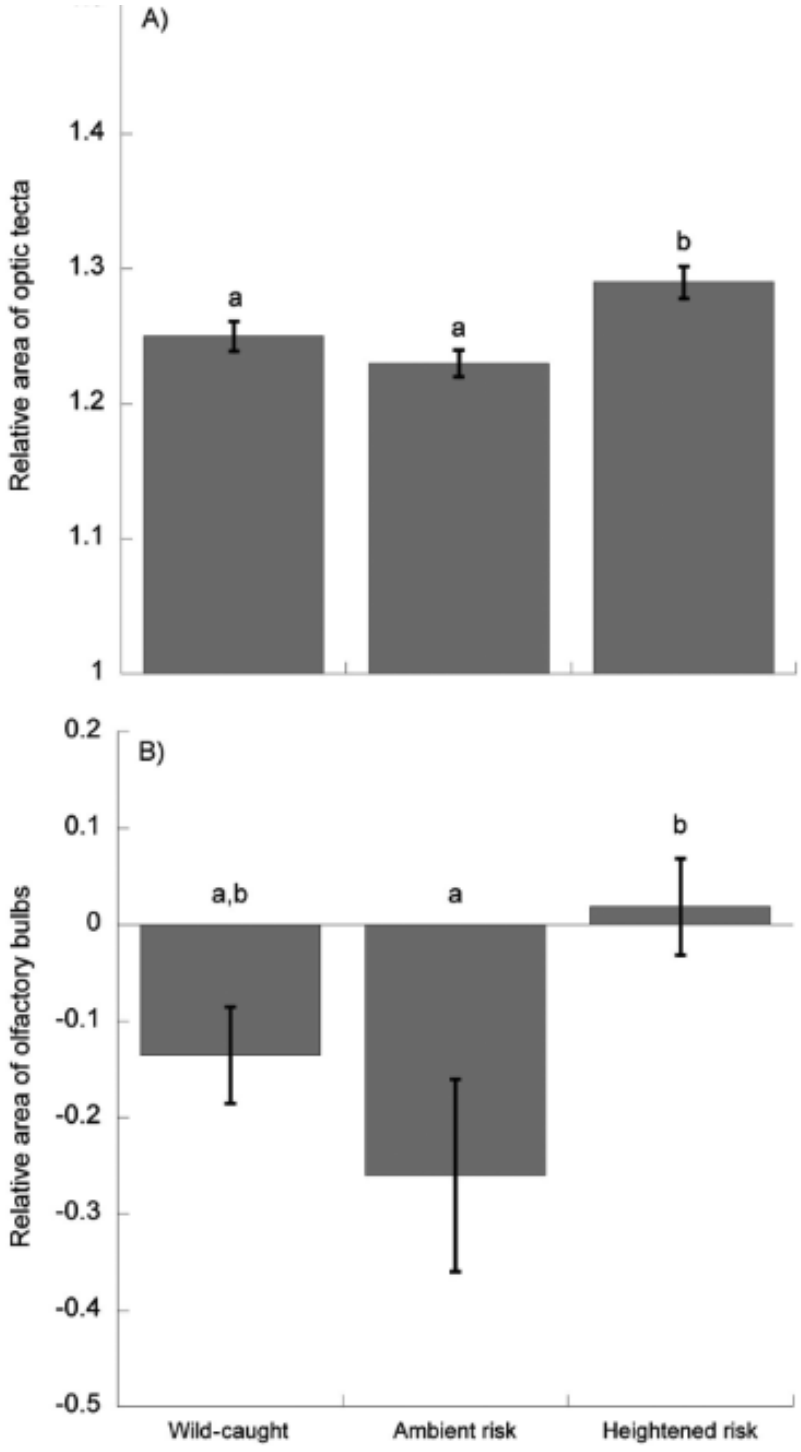

Figure 2.2. The mean (±SE) relative regional areas of the (A) optic tecta and (B) olfactory bulbs by treatment for the northern redbelly dace (Phoxinus eos). Bars with the same letter do not significantly differ ($p > 0.05$).

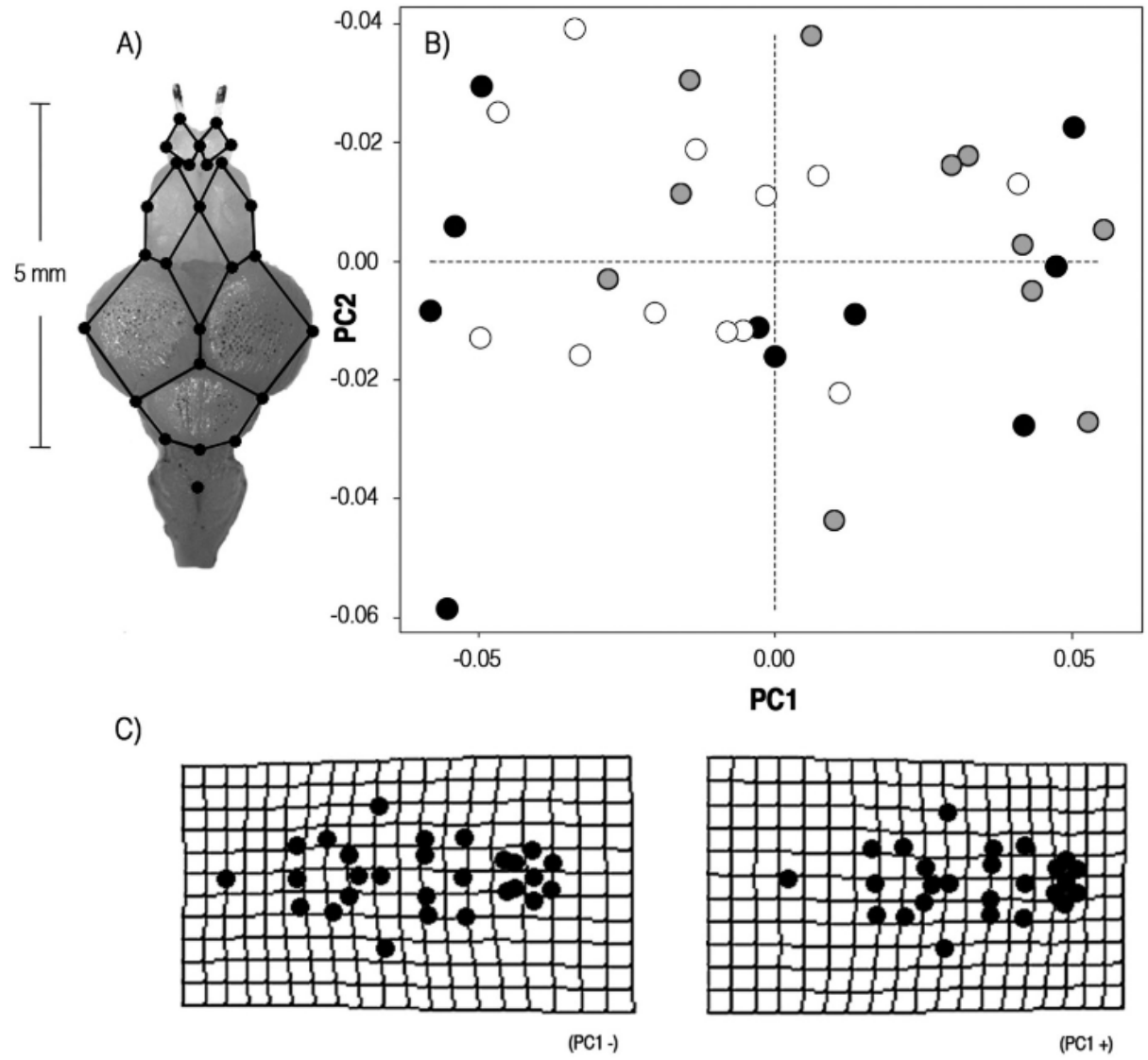

Figure 2.3. Procrustes analysis of the northern redbelly dace (Phoxinus eos) showing (A) the configuration of landmarks and polygons used in the analysis overlaid on an example of a typical northern redbelly dace brain, which exhibits the sort of variation observed in (B) a principal components (PC) plot for brain shape by treatment (ambient risk (black circles), heightened risk (white circles), and wild-caught control (grey circles)) and (C) wireframe plots representing the shape configurations, at either end of the PC1 axis, as deformations (warps) of the mean shape for all specimens.

Chapter 3: Short-term captivity drives hypothalamic plasticity and asymmetry in wild-caught northern red bellied dace (*Chrosomus eos*)

3.1 *Introduction*

Teleosts can undergo active neuroproliferation in adulthood, enabling them to alter their brain morphology in response to changes in their environment within their lifetime (Ebbesson and Braithwaite, 2012). Recently, (Joyce and Brown, 2020b) reported detecting distinct brain morphologies in two freshwater prey fishes, resulting from exposure to simulated predation pressure (SPP). They demonstrated that the morphology of the dorsal brain surface of adult red bellied dace [*Chrosomus eos* Cope, 1861 = *Phoxinus eos* (Cope, 1861)], and juvenile Atlantic salmon *Salmo salar* L. 1758, differed from controls following as little as 14 days of SPP treatment. For C. eos, short-term predation pressure drove the growth of larger optic tecta and olfactory bulbs. This expanded upon previous studies, which looked at differences only after prolonged exposures of a month or more (Gonda et al., 2013, 2012; Näslund et al., 2017; Reddon et al., 2018). This finding suggests that, in response to predation, macroscopic changes in brain morphology can develop rapidly and may occur concurrently with the behavioural changes commonly seen in response to predation risk.

Background predation pressure is also known to shape individual risk-taking tactics and personality. Prey species faced with an increase in predation pressure may become more or less risk adverse, depending on the species and environment (Arnett and Kinnison, 2017). Behavioural differences related to boldness and exploration seen in fish from high predation populations may be linked to an altered hormonal stress response (Archard et al., 2012). The stress response in fish can influence metabolism and gene expression resulting in immune, endocrine, neural and behavioural changes. It is modulated via the hypothalamic–pituitary-interrenal axis (Tort, 2011).

Gonda et al. (2012) reared nine-spined sticklebacks, (*Pungitius pungitius* L. 1758), with SPP to an age of 34 weeks. They found that irrespective of sex or population, both marine and freshwater subjects had smaller hypothalami than controls, suggesting a possible reduction in function as a general response induced by predation. The authors set out to determine if the hypothalami of P. eos responded to SPP similarly, and on a timescale relevant to discussions of short-term behavioural plasticity.

It was hypothesized first that if exposure to SPP or related stressors drives the development of smaller hypothalami relative to controls, changes would be detectable after a period of 2 weeks. Second, after 2 weeks, the observed boldness of the subjects would correlate with hypothalamus size across treatments. Third, it was anticipated that the degree of boldness seen in the C. eos groups would correspond to the intensity of the applied stressor. Finally, the ratio of left and right lobe area may reflect differential investment in, or specialization of, the left or right structures (Schmitz et al., 2019). Based on pronounced differences observed in the size of the hypothalamic lobes (HL) of some of the subjects, it was hypothesized that the degree of hypothalamic asymmetry (HA) may also relate to expressed behaviour.

3.2 *Materials and Methods*

This study was conducted using *C. eos*, a widely distributed bait fish (Stasiak, 2006). The authors used the same methods of fish collection, SPP cue creation (conspecific skin extract), subject preservation and brain extraction as in Joyce and Brown (2020b). Experimental animals were handled and used in accordance with Concordia University Animal Research Ethics protocol 30,000,255. In brief, in the summer of 2017 wild P. eos were caught in minnow traps from a privately owned artificial pond in Ontario, Canada, which is spring fed. The subjects were used either as experimental subjects or for the production of conspecific skin extract (equivalent to 0.15 cm2 of skin per milliliter) for simulating predation pressure (Dupuch et al., 2004). The subjects were held in 32-l bins outdoors, with pea gravel substrate, mesh lids and air-stones, and were fed twice daily with flake food (Nutrafin Max™ Hagen). The bins were flushed with 20–30 l of fresh pond water several times a day; waste was removed using a syphon during daily welfare checks.

Each stressor condition was replicated thrice (n = 12 per bin). The stressors were: (a) 10 ml of SPP cue (equivalent to encountering two badly damaged individuals per day), (b) 1 ml of SPP cue [analogous to more-distant or less-severe predation events (Dupuch et al., 2004)], (c) handling stress, (d) disturbance cues (chemicals released by conspecifics when startled) (Ferrari et al., 2010) and (e) a captive control group. To detect any changes resulting from the imposition of confinement, wild specimens captured from the same area as the others (proximal), and from the opposite side of the pond (distal), were tested and preserved immediately [groups (f) and (g); n = 26 each].

Handling stress involved capturing all subjects with a dip-net, transferring them to a bucket and returning them to their bin twice a day. Bin water (10L) was subsequently collected and used as disturbance cue. SPP, pond water and disturbance cues were introduced into their respective bins twice daily. The exposures occurred between 0600 and 2400 hours (interval: 12.0 ± 3.3 h, mean ± S.D.). The durations of the exposures varied, with a mean of 7.5 ± 1.6 min elapsing prior to having their enclosure flushed with pond water; this took place over 14 days.

Testing took place between 1000 and 1600 hours on day 15. Twelve identical, corrugated white plastic test arenas (90 × 22.5 × 10 cm) were used. Each held 10 l at a depth of 5 cm and had a white plastic (release) box (7.5 × 7.5 × 10 cm) with a 4-cm hole, barred by a removable plastic door. Individuals were placed in the release boxes and allowed to acclimate for 10 min before release box doors were removed. The arenas were recorded by high-definition security cameras for 10 min, mounted 1 m above the water to capture the subject's latency to emerge. Immediately after behavioural testing, the subjects were euthanized using an anaesthetic overdose of clove oil followed by preservation in 4% paraformaldehyde.

The subjects were weighed and measured for standard length. Their brains were excised and placed beside a millimetric grid such that all measured structures lay within the focal plane of the microscope camera. They were photographed at 15×. Cross-sections of regional areas are a good proxy for lobe volume (Park and Bell, 2010); regional areas were estimated as n-sided polygons outlining the region of interest. The outlines of the whole dorsal brain surface (BD) and the HL were defined by placing points around their perimeter in TpsDig2 (Rohlf, 2018): 32 and 18 points, respectively. The measures of the BD and HL were combined total brain area (BT). All images were coded by one individual. A sub-set of brains (n = 4) were re-photographed at a

later time. The areas of the HL and pituitary were measured separately, and together as a whole, thrice per photo. Repeatability of measurement was estimated by interclass correlation coefficients for measures made within and between photographs of the same brain.

Of the initial 232 individuals, 157 were used in this analysis (Table 3.1). During the exposure period, there were 17 mortalities, putatively attributed to enteric red-mouth disease (*Yersinia ruckeri*). During testing, nine behavioural tests were invalidated by individuals that jumped either out of their box prematurely or into an adjacent occupied lane. In addition, 49 brains damaged during extraction were excluded from analysis. Finally, three hypothalamic area measurements were rejected, because of incorrect positioning of the scale during photography; the calculation of hypothalamic asymmetry for these subjects was unaffected by this error.

All data were analyzed using IBM SPSS Statistics for Windows, version 25.0 (IBM Corp., Armonk, NY, USA). Intra-rater repeatability was good between different photos of the same brain, and excellent when measures were from the same photograph. The single measures intraclass correlation coefficients were 0.83 between, and 0.92 within photos of the same brain (95% C.I. 0.75–0.88, $F_{(123,123)} = 5.775$ and 0.86–0.96, $F_{(31,62)} = 35.82$, $P < 0.01$ for both). Standard length, mass and emergence time were log10 transformed. The residuals for all variables were assessed for normality graphically (histogram, Q-Q plot), and by calculation of Z test statistics for skew and kurtosis. Relative hypothalamic investment (RHI) was determined as the log of total hypothalamic area divided by log of BT.HA was calculated as the area of the subject's right lobe divided by the area of the left. Not all subjects emerged within the recording period; their emergence time was coded as 600 s, but they were excluded from the subsequent generalized linear mixed model (GLMM) analysis. The proportion of non-emergers by treatment was assessed with a GLMM with a binomial response variable.

The relationship between emergence time and RHI was explored using a linear GLMM. Only those subjects that emerged were included in the analysis. The initial GLMM was run factorially with the standardized residuals for RHI and BD as covariates, and stressor and replicate number as factors, including all interaction terms. Interaction terms were excluded from subsequent analyses, in order of non-significance (Bolker et al., 2009). The final model retained RHI and HA as covariates and stressor as a factor; it included RHI * stressor, HA * stressor and RHI * HA * stressor interaction terms. One-way ANOVA was used for comparisons of RHI and asymmetry, between stressors and across holding conditions.

3.3 *Results*

The overall ANOVA found that in captive subjects the total hypothalamic area was reduced by 4% (1.62 ± 0.16 vs. 1.69 ± 0.25 mm^2, $F_{(1, 152)} = 3.91$, $P = 0.05$, $\eta p^2 = 0.03$) and their hypothalami were 5% less symmetric (1.06 ± 0.07 vs. 1.01 ± 0.1, right: left, $F_{(1,155)} = 10.00$, $P < 0.01$, $\eta p^2 = 0.06$). These differences were not apparent among different stressors (Table 3.1). The proportion of those that did not emerge was 0.30 ± 0.08 (mean ± S.D.) and did not significantly differ by treatment (GLMM $\chi^2_{(6, N = 157)} = 4.04$, $P > 0.1$). Emergence times between groups were not significantly different, though notably, and contrary to the authors' expectations, the 10-ml SPP group had the highest mean emergence time, 83.5 s.

The GLMM (Omnibus test $\chi^2_{(20, N = 104)} = 33.1$, $P < 0.05$; Table 3.2) had significant model effects of RHI and HA*stressor ($\chi^2_{(1, N = 104)} = 12.082$, $P < 0.05$, $\chi^2_{(6, N = 104)} = 19.85$, and $P <$

0.05). The effects of HA and RHI*stressor were not significant ($\chi^2_{(1, N = 104)} = 0.66$ and $\chi^2_{(6, N = 104)} = 12.50$. $P > 0.5$ for both). Plots of emergence time vs. relative hypothalamic size and vs. asymmetry were generated to highlight the findings of the GLMM. RHI correlated with emergence time across all treatments (Pearson $r = 0.29$, $N = 104$, $P < 0.01$), especially among those exposed to SPP (Pearson $r = 0.42$, $N = 28$, $P < 0.05$) (Figure 3.1a). In addition, hypothalamic asymmetry in SPP subjects was also significantly correlated with emergence time, whereas the other treatments had contrasting but insignificant slopes [Figure 3.1b, Pearson $r = -0.42$, $N = 28$, $P < 0.05$ (SPP) and $r = 0.17$, $N = 76$, $P > 0.05$ (other treatments overall)]. RHI and HA were uncorrelated in the wild and SPP groups (Pearson $r = 0.08$, $N = 56$, $P > 0.5$) and was positively correlated in captive subjects not exposed to SPP (Pearson $r = 0.29$, $N = 48$, $P < 0.05$).

3.4 *Discussion*

The results confirm that the hypothalami of C. eos are plastic and capable of undergoing measurable, macroscopic changes in morphology, over short time scales. Notably, the imposition of captivity resulted in this decrease in size and increase in asymmetry, irrespective of the type of stressor used. In this experiment, the holding conditions were relatively barren, a condition which is less conducive to neural plasticity and may have constrained growth and differentiation between stressors (Salvanes et al., 2013).

The correlation between relative hypothalamus size and emergence time may reflect the importance of the hypothalamus in governing the inclination to emerge from shelter (i.e., shy vs. bold phenotypes), with their reduced volume corresponding to a less-intense stress response. This trend was exhibited similarly by all treatments and may represent a fundamental relationship between hypothalamic investment and risk-taking decisions under stress. Further study is needed to determine if the relationship holds for other behaviours relating to the shy–bold axis of behaviour. The elevated mean emergence time of the 10-ml SPP group as compared with the captive control subjects was contrary to the authors' expectation of increased boldness and may suggest the role of an induced neophobic response to the novel environment (Brown et al., 2016; Crane et al., 2015).

The asymmetry in size and function in the brains of fish, including the hypothalamus, has been the subject of much study from genetic, morphological and behavioural perspectives (Schmitz et al., 2019). Notably, captivity resulted in greater asymmetry; nonetheless, the relationship between hypothalamic asymmetry and emergence time appears to be dependent on prior experience with predation pressure. The difference in slopes may result from recent predation pressure or possibly reflect the expression of acute neophobia. This is the first observation of a relationship between hypothalamic asymmetry observed macroscopically, and a behavioural measure of personality.

3.5 *Conclusions*

The findings show that there is a great deal more to be understood about the relationship between brain morphology and behaviour, especially as it relates to the role of predation risk driving morphological plasticity. It is becoming increasingly evident that teleost neuroplasticity must be considered when examining individual subjects' behaviour over time. The potential for rapid hypothalamic plasticity may have implications for any future work which involves wild-caught fish being tested or held captive for any length of time. The potential for plastic changes

in brain morphology, stress responses and behaviour should be a consideration when assessing coping styles or personality. Furthermore, in light of the very high rate of predation experienced by fish stocked for conservation purposes (Brown and Day, 2002), exploiting brain plasticity may enable conservationists to boost post-stocking survival, by "pre-adapting" fish to their intended habitat via the application of SPP.

Table 3.1 - Mean (± SD) values for parameters measured for *Chrosomus eos* (Cope 1861) exposed for 14 days to either water, conspecific disturbance cues, repeated handling, skin extract simulating the injury (1 ml) or death (10 ml) of a conspecific, and wild subjects caught at two locations. One-way ANOVA; degrees of freedom = 6 and 150 for all except hypothalamic size (df = 6 and 146) and emergence time (df = 6 and 100). **, P < 0.01.

Metric	Captive Control	Disturbance Cue	Handling Stress	1ml SPP	10ml SPP	Wild Proximal	Wild Distal	F
SL (cm)	3.89 (0.18)	3.90 (0.16)	3.94 (0.11)	3.93 (0.18)	3.97 (0.11)	3.85 (0.25)	3.92 (0.20)	1.015
Mass (g)	0.95 (0.15)	0.97 (0.11)	0.91 (0.06)	0.93 (0.12)	0.93 (0.09)	1.02 (0.14)	1.04 (0.12)	4.072**
Brain Size (mm^2)	8.74 (1.26)	8.82 (0.95)	8.61 (1.38)	8.77 (1.35)	8.31 (1.41)	9.41 (0.78)	8.90 (0.99)	2.122
Hypothalamic Size (mm^2)	1.605 (0.153)	1.581 (0.174)	1.626 (15)	1.683 (0.164)	1.585 (0.174)	1.659 (0.273)	1.719 (0.230)	1.595
Hypothalamic Asymmetry (R/L)	1.06 (0.07)	1.07 (0.08)	1.03 (0.08)	1.07 (0.09)	1.06 (0.06)	1.02 (0.10)	1.01 (0.10)	1.985
Emergence Time (sec)	41.98 (48.28)	52.55 (33.18)	63.33 (51.89)	54.62 (25.22)	83.49 (45.16)	46.44 (79.10)	63.64 (93.80)	1.217
N	27	17	15	29	19	26	24	

Table 3.2 - Parameters Estimates for the generalized linear mixed models (GLMM) of Emergence Time, Hypothalamic Asymmetry (ASYM) and Relative Hypothalamic Investment (RHI). The seventh, distally caught wild controls served as the reference category. The scale (0.631 ± 0.0875, B ± SE) was based on a maximum likelihood estimate. *, $P < 0.05$, **, $P < 0.01$

	B	Std. Error	df	Z Score	Exp(B)	95% C.I. Lower	95% C.I. Upper
Intercept	0.445	0.297	1	1.499	1.560	0.872	2.790
RHI	0.393	0.164	1	2.401*	1.481	1.075	2.041
ASYM	0.555	0.204	1	2.724**	1.742	1.168	2.598
Captive Control	-0.877	0.388	1	-2.260*	0.416	0.195	0.890
Captive Control x RHI	-0.911	0.331	1	-2.750**	0.402	0.210	0.770
Captive Control x ASYM	-0.237	0.338	1	-0.700	0.789	0.407	1.530
Disturbance Cue	-0.492	0.323	1	-1.523	0.611	0.325	1.152
Disturbance Cue x RHI	-0.222	0.237	1	-0.933	0.801	0.503	1.276
Disturbance Cue x ASYM	-0.441	0.258	1	-1.714	0.643	0.388	1.065
Handling Stress	-0.389	0.322	1	-1.209	0.678	0.361	1.274
Handling Stress x RHI	0.185	0.229	1	0.807	1.203	0.768	1.885
Handling Stress x ASYM	-0.401	0.231	1	-1.739	0.669	0.426	1.052
10ml SPP	-0.074	0.326	1	-0.227	0.929	0.490	1.761
10ml SPP x RHI	-0.121	0.179	1	-0.672	0.886	0.624	1.260
10ml SPP x ASYM	-0.901	0.269	1	-3.345**	0.406	0.240	0.689
1ml SPP	-0.441	0.308	1	-1.431	0.643	0.351	1.177
1ml SPP x RHI	-0.183	0.198	1	-0.927	0.833	0.565	1.226
1ml SPP x ASYM	-0.788	0.234	1	-3.367**	0.455	0.288	0.719
Wild Caught Proximal	-0.468	0.471	1	-0.993	0.626	0.249	1.577
Wild Caught Proximal x RHI	-0.032	0.291	1	-0.109	0.969	0.548	1.714
Wild Caught Proximal x ASYM	-0.719	0.297	1	-2.420*	0.487	0.272	0.872

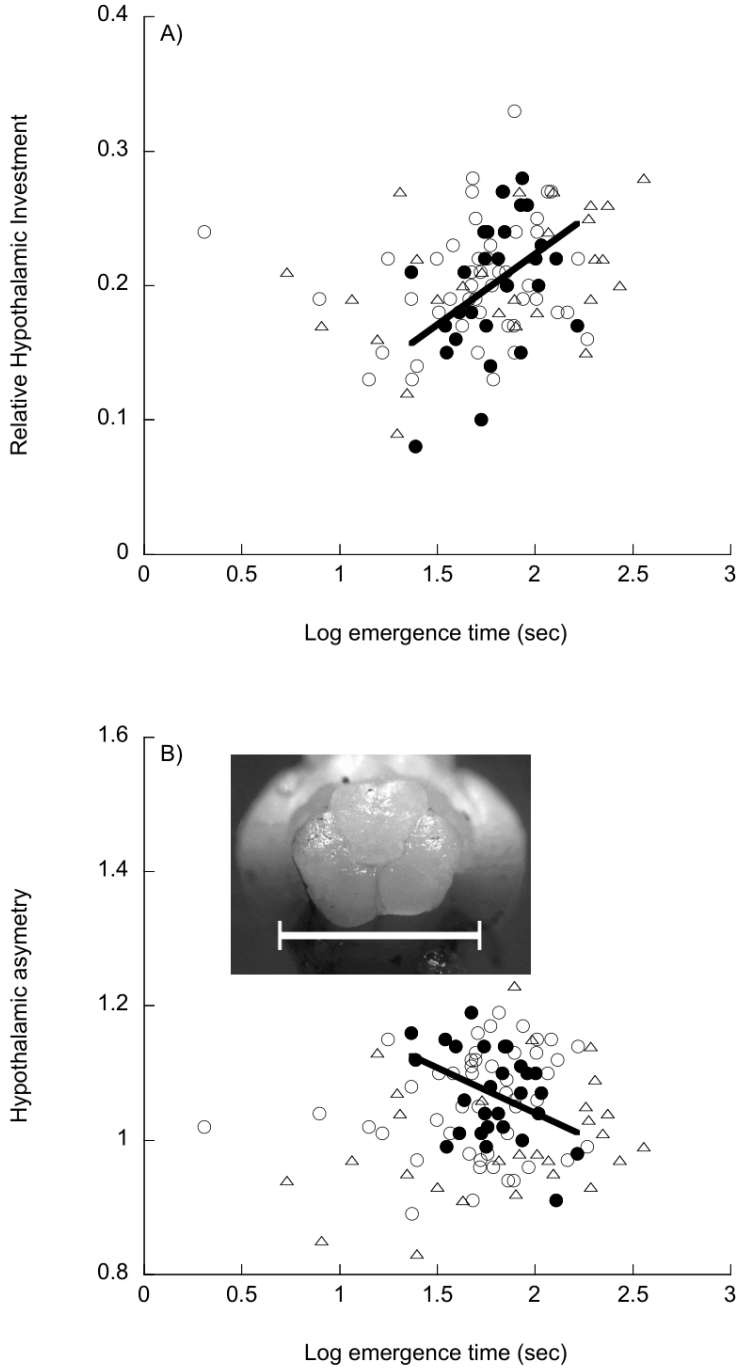

Figure 3.1 – Scatterplots of $\log_{10}$ transformed latency to emerge from shelter versus, (Panel A) hypothalamic area, controlling for body size and (Panel B) the ratio of right and left inferior hypothalamic lobe areas; in *Chrosomus eos* (Cope 1861). Both show the subjects exposed to simulated predation pressure (closed circles), those in the other captive conditions (open circles) and the wild caught group (triangles). The relationships between emergence behaviour and hypothalamic investment and with the degree of asymmetry were significant in subjects exposed to simulated predation pressure ($N = 28$; $R = 0.42$, $P < 0.05$, $y = 1.705x + 1.448$, and $R = -0.42$, $P < 0.05$, $y = -0.14 + 1.32$ respectively). Insert: ventral image of a *C. eos* brain, showing the pituitary and asymmetric inferior hypothalamic lobes (1.08 R:L, 2mm scale bar).

Chapter 4: Olfaction and Reaction: The Role of Olfactory and Hypothalamic Investment in the Antipredator Response of Northern Redbelly Dace (*Chrosomus eos*) to Chemical Alarm Cues

4.1 *Introduction*

Numerous fish species have been found to exhibit divergent brain morphologies between high and low predation populations (Kotrschal et al., 2017). These morphologies likely contribute to various behavioural and physiological adaptations exhibited by populations subject to high predation (Dunlap et al., 2019). However, the influence of predation on patterns of neural investment within teleost brains is not easily generalized and is often sex, ecotype, and/or context-specific (Axelrod et al., 2018; Gonda et al., 2011; Herczeg et al., 2015). For instance, female guppies from populations that are sympatric with wolf fish (*Hoplias malabaricus*, an ambush predator), invest in their vision centers (optic tecta), while those sympatric with blue acaras (*Andinoacara pulcher*, a pursuit predator), reduced investment in their olfactory bulbs and hypothalamic lobes (Kotrschal et al., 2017). Interpreting the significance of this predation-driven regional investment typically relies on the principle that a region's relative size reflects its utility to the individual (Iglesias et al., 2018; Kaslin et al., 2008).

Generally, the utility of a brain region is presumed to offset the high energetic cost of investing in the growth and maintenance of neural tissue (Tsuboi et al., 2016). This principle - that investment reflects utility - is seen in the optic tectum size of cave-dwelling shortfin molly (*Poecilia sphenops*) (Eifert et al., 2015), and nine-spine sticklebacks (*Pungitius pungitius*), raised in water with black dye (Pike et al., 2018); both of which, in the absence of useful visual information, had reduced reliance on visual processing. Similarly, both freshwater and marine nine-spine sticklebacks, exposed to predation risk, developed larger olfactory bulbs, but only the freshwater populations exhibited smaller hypothalami (Gonda et al., 2012). While this principle has been found to apply to sensory regions (Lee et al., 2017), the significance of changes in the size of the hypothalamus, an integrational center (Delgado et al., 2017), is less clear.

The hypothalamic-pituitary-interrenal (HPI) axis in fish influences most of their endocrine systems, playing an important role in feeding and reproductive behaviors (Blanco, 2020; Trudeau and Somoza, 2020). Importantly, the HPI axis governs the intensity of physiological stress responses which, in turn, can influence behaviour (Thomson et al., 2016). In redbelly dace, having larger hypothalami correlated with the latency to explore a novel arena (shyness) (Joyce and Brown, 2020b); this experiment also observed significant hypothalamic plasticity in response to captivity. Consequently, we looked at hypothalamic investment as an additional variable that might influence risk taking behaviour. However, this approach required an additional consideration; owing to the observation that some aspects of hypothalamic function have been found to vary with stress coping style (Wong et al., 2019).

Reactive and proactive fish handle stress differently; proactive fish have lower post-stress cortisol, reduced behavioural flexibility, and a higher proportion of cortisol receptors which provide negative feedback for the stress response (Vindas et al., 2017a,b). Butler et al. (2018) found that, in the African cichlid (*Astatotilapia burtoni*), patterns of neuronal activation across much of the brain, including the hypothalamus, varied by stress coping style. Their results suggested that the hypothalami are more active during exploration amongst proactive individuals and more active amongst reactive fish when freezing (an antipredator response). Based on this

we opted to examine morphological correlates of behaviour by background risk and behavioural phenotype.

The morphological and behavioral plasticity previously observed in redbelly dace in response to short-term changes in predation pressure and captivity were significant but subtle, and the actual impact of such changes on antipredator behavior remains to be seen. Here, we used predation cues to generate a greater range of brain morphologies and behavioral responses than might be found in the source population (Bell and Sih, 2007), to explore we test several predictions (Table 4.1) regarding the potential links between exposure to predation risk, gross brain morphology and risk-taking tactics in redbelly dace. First, we compared relative hypothalamic and olfactory investment with shyness and with the intensity of their antipredator response (reactivity) (Dingemanse et al., 2010; Toms et al., 2010), expecting it to positively correlate with both. Then, we predicted that per the investment-utility principle, within groups exposed to the same background risk and cue concentration, relative olfactory bulb size would correlate with antipredator response intensity.

4.2 *Materials and Methods*

4.2.1 Fish collection and holding

In the summer of 2018, redbelly dace were captured and sorted following the methods described in (Joyce and Brown, 2020a). In brief, redbelly dace were caught in minnow traps from an isolated spring-fed artificially dug pond (≈0.25 ha) in Ontario, Canada. The pond was initially stocked with brown bullhead catfish (*Ameiurus nebulosus*); redbelly and finescale dace (*Chrosomus neogaeus*) appeared later, possibly introduced as eggs by predatory waterfowl (Lovas-Kiss et al., 2020). Experimental animals were handled and used per Concordia University Animal Research Ethics protocol #30000255. Following capture and sorting, the bycatch, including any finescale or reproductively active redbelly dace, was returned to the pond. Healthy adults were used for conspecific skin extract (alarm cue) production or retained as experimental subjects and held under semi-natural conditions.

The large semi-natural enclosures used in this experiment were meant to avoid the imposition of barren conditions used in previous experiments (Joyce and Brown 2020a,b), which had limited space and restricted sightlines which may constrain plasticity (Fong et al., 2019; Mes et al., 2020). The enclosures consisted of mesh bags, approximately (0.6 x 0.8m) attached to weighted baskets (Fig 4.1a). The holes in the mesh (3mm) were small enough to prevent escape but large enough to permit the entrance of drift fodder. Airline tubing was strung to each of the enclosures for the delivery of cues and supplementary food and the tops were covered with netting to prevent jump-outs. To ensure adequate nutrition, each occupied enclosure received 2-3 g of brine shrimp flakes once a day. Enclosures were suspended in the water column off the sides of square rafts and had a volume of approximately 110L. The rafts were tethered approximately 9m from shore to ensure a constant water depth and they were kept a minimum of 6m apart. Each raft received 20 ml per enclosure of either pond water (ambient risk) or alarm cue (heightened risk) twice a day, at haphazard times between 06:00 and 21:00.The heightened and ambient risk groups were kept approximately 24m apart. Light exposure and water temperature were the same for both groups.

4.2.2 Alarm Cue Production

The conspecific skin extract used for the alarm cue was prepared from healthy redbelly dace euthanized by a sharp blow to the head. Skin fillets were removed, and their dimensions recorded, before homogenization with distilled water. The solution was filtered through polyester floss and diluted to produce a stock solution of approximately 0.15 cm2 ml^{-1} which was frozen in 20 ml aliquots until needed. The alarm cue for the behavioral assay was prepared as needed by serial dilution of the stock cue to concentrations of 10%, 1%, 0.01%, and 0.001%, with distilled water (0%) as the control (as in Dupuch et al., 2004).

4.2.3 Experimental Setup

The dace were evaluated individually in 20L tanks fitted with equal lengths of 3mm tubing to deliver air and olfactory cues. The tanks were filled with well water and held around 20ºC. Behavior was recorded using high-definition digital cameras, each facing an array of 5 tanks that occupied equal portions of the field of view; opaque plastic dividers between the tanks prevented fish from seeing one another (Fig 4.1b). The tanks were marked with lines dividing the front of the tank space into a 3 x 3 grid (Fig 4.1c). A floor-length curtain hung behind the camera which screened the experimenters from view during testing. To control for the impact of water temperature on expressed behavior (Biro et al., 2010), water from the test tanks was gradually introduced to the transfer buckets until they were within 2ºC of the experimental tanks. After 30 minutes of acclimation, subjects were individually transferred to refuge boxes for individual emergence time testing. The refuges (Fig 4.1d) were square PVC tubes 10 cm on a side and 15cm long, with plastic mesh fixed across one end and as a sliding mesh gate at the other.

4.2.4 Emergence Time Assay

Individual dace were tested for latency to emerge from their shelter and explore a novel environment (emergence time) in the face of unknown risk, a proxy for boldness (Burns, 2008). Emergence time into a novel arena correlates with measures of exploration, and when associated with a perceived threat, also with measures of fear and escape (Toms et al., 2010). In terms of stress, the process of being captured by dip-net and later released into the refuge was analogous to escaping a predator (Donaldson et al., 2010). After a further 10-minute acclimation period in the refuges, the gates were lifted and the time until more than half of the subject's body crossed the threshold (emergence time) was recorded. This relatively short time ensured that the free choice to emerge was first presented before the dissipation of the secondary stress response (Barton, 2002; Wong et al., 2019) and may increase repeatability (O'Neill et al., 2018). Any trials where an obvious external stimulus that may have influenced the results, e.g., a door slammed shut, were excluded. After 18 minutes the refuges were removed and subjects who never emerged were coded as taking the maximum time of 1080 seconds.

4.2.5 Antipredator Response Assay

Following an additional post-emergence acclimation period of at least 60 minutes, 10 minutes of pre-stimulus behavior was recorded. After the initial observation, a syringe was used to withdraw and discard two 60 ml aliquots of water, which cleared the injection line and primed it with clean water. Subsequently, 5 ml of the stimulus was introduced, followed by 60 ml of well water. The moment of injection for each tank was recorded and the tanks were filmed for 10

minutes post-stimulus. Between tests, the tanks were thoroughly drained, repeatedly rinsed, then refilled with oxygenated well water held at room temperature (20-22ºC). Following the behavioral assays, subjects were individually euthanized with an overdose of clove oil (0.03% v/v) and transferred to 15ml centrifuge tubes containing 4% paraformaldehyde in phosphate-buffered saline and refrigerated until dissection.

4.2.6 Video Coding

Videos were coded by recording the position of the subject within the tank as well as its swimming speed at regular intervals. The videos were coded twice, the 10-minute pre/post video was coded at 20-second intervals. The horizontal and vertical positions were expressed as their 2D grid coordinates as seen from the camera's position (X: 1 to 3, Y: 0 to 3, Activity 0 to 3). The vertical position of zero refers to an additional area comprising the very bottom of the tank, from 0 - 2.5cm. Activity level was defined by swimming speed. Subject unmoving/hovering in position within the water column (0), directed movement 0.5-1 body lengths per second (1), 1.5-2.5 per second (2), and dashing (3) at 2.5+. The combination of being at the very bottom and not moving (Y:0, A:0) was considered a special condition that may reflect a strong antipredator response.

4.2.7 Dissection and Photography

The subjects' weight and standard lengths were recorded. Their brains were extracted and photographed, dorsally and ventrally, in the same manner, described in (Joyce and Brown 2020a). In brief, the skull was split open, the olfactory nerves were severed at the nares, and the spinal cord was cut where it exits the base of the skull. Finally, the optic nerves were severed as the brain was lifted out. The brains were kept moist until photographed at a fixed 10X magnification and full illumination using a Leica EZ4W dissection scope. The focal plane of the scope was used as a gauge for positioning. Correct positioning required that all the regions to be examined were visible within the focal plane.

The apparent cross-sectional area of each region served as a proxy for volume (Joyce and Brown, 2022). It was found by tracing its outline in ImageJ (Fig 4.2) (Schneider et al., 2012) using series of discrete anatomical points (landmarks) and points delineating the perimeter between them (semi-landmarks). They were placed using tpsDig2 (Rohlf, 2018); see Park and Bell (2010) and Fig 4.2a. Brain areas were log-transformed and expressed as a proportion of the whole brain; regional symmetry ratios are all left/right.

4.2.8 Statistical Analysis

All linear models, correlations, regressions, cluster analysis, and standard analysis of variance (ANOVA), were computed using SPSS v.27 (SPSS Statistics for Windows 2020). Overall brain shape was analyzed using MorphoJ v1.07a (Klingenberg, 2011). A multivariate general linear model (GLM) was used to assess the relationship between the regional area values and symmetry rations by treatment and body size; significant results were reexamined with a univariate GLM. We compared regional investment and symmetries between heightened and ambient risk subjects using one-way ANOVA. Linear models were performed factorially using standardized values, with replicate number as a factor, and with all interaction terms. In

subsequent runs, terms were excluded from the model in order of non-significance (Bolker et al., 2009).

The two-step cluster analyses for grouping behavioural phenotypes into early/late emergers and strong/weak antipredation responders used log-likelihood as the distance measure and Schwarz's Bayesian criterion for clustering; it was performed on the standardized residuals for emergence time and on changes in vertical area use, activity level, and time spent stationary on the substrate post-stimulus. In both cases, the number of clusters (two) was determined automatically. Chi-square analysis was used to determine if the proportion of subjects in each category differed by treatment. Antipredator response intensity in the dace was quantified using their activity level, proximity to the substrate, and time spent stationary at the bottom of the tank (Geffroy et al., 2020; Wisenden et al., 2009). Later, a single principal component, Antipredator Response Intensity, was extracted which encompassed all three variables.

4.3 *Results*

4.3.1 Behavior

The latency to emerge was shorter in heightened risk subjects, 165 ± 173 vs 308 ± 338 sec ($F_{(1,116)} = 4.053$, P = 0.046, $\eta p^2 = 0.03$). Additionally, 6 ambient risk subjects failed to emerge in the allotted time. Emergence time in both groups was uncorrelated with weight and only correlated with body length in ambient risk fish (Pearson r = -0.312, N = 65, P = 0.011). Multivariate GLM of the antipredator response variables found a significant effect of treatment (Pillai's trace = 0.065, $F_{(3,126)} = 3.172$, P = 0.038) and treatment by concentration level (Pillai's trace = 0.228, $F_{(12,384)} = 3.172$, P = 0.002). Post hoc LSD analysis found that minimum concentration of AC which produced an overt response, with significant reductions in vertical position and activity levels relative to the controls, was 0.001% for heightened risk (MD = -0.189, SE = 0.086 (position), MD = -0.180, SE = 0.080, P = 0.028 (activity)), and 0.01% for ambient risk fish; heightened risk (MD = -0.219, SE = 0.069, P = 0.002 (position), MD = -0.140, SE = 0.077, P = 0.072 (activity)). A GLMM found that the change in the number of time intervals spent stationary and at the bottom (Position: 0, Activity: 0) was lower in heightened risk fish (M = 2.59, SD = 8.20 (heightened) vs M = 4.42, SD = 8.52 (ambient) GLMM $\chi^2_{(3, N = 141)} = 7.721$, P = 0.005). Time stationary on the substrate decreased with body length and olfactory investment (Exp(β) =0.119, GLMM $\chi^2_{(3, N = 141)} = 6.754$, P = 0.009 (length) and Exp(β) = 1.042 , $\chi^2_{(3, N = 141)} = 4.794$, P = 0.029 (investment). A total of 17 fish across the 8 replicates were excluded due to external interference while testing.

4.3.2 Risk-taking Phenotypes

The two-step cluster analysis for the bolder early emerging and shyer late emerging fish groupings was based on the latency to emerge from the refuge box. Individuals were classified as either early emerging (bolder) (35.5%, mean Z-score = -1.12) or late-emerging (shyer) (64.5%, mean Z-score = 0.61). The proportions of shyer and bolder individuals were not significantly different within the heightened risk subjects (32 vs 27, $\chi^2_{(1, N = 59)} = 0.424$, P = 0.515) while in ambient risk fish, shy fish were significantly more common (48 vs 17, $\chi^2_{(1, N = 65)} = 14.785$, P <0.001). Individuals were identified as having a weak (more proactive) or strong (more reactive) antipredator response (APR) based on the proportional change in their vertical position, activity level, and time spent stationary on the substrate; variable importance = 1 (position), 0.94

(activity), and 0.5 (time stationary). The strong APR (reactive) group represented 45.4% of individuals, while 55.6% were proactive (weak APR); (mean Z-scores = -0.71 vs 0.59 (vertical position), -0.69 vs 0.59 (activity), 0.5 vs -0.42 (time stationary)); (mean Z-scores = 0.59 (vertical position), 0.57 (activity), -0.42 (time stationary)). Heightened risk fish were marginally more likely to have a weaker APR (42 vs 27, $\chi^2_{(1, N = 69)} = 3.261$, P = 0.071), while for ambient risk fish the proportions of weak APR and strong APR fish were comparable (35 vs 37, $\chi^2_{(1, N = 72)} = 3.261$, P = 0.814).

Within the ambient risk treatment, the proportion of individuals found in each of the four phenotypic combinations of early/late emergence time and strong/weak APR (Fig 4.3a), was significantly different ($\chi^2_{(3, N = 65)} = 2.627$, P = <0.001), while the distribution amongst the heightened risk fish was roughly equal ($\chi^2_{(3, N = 59)} = 2.627$, P = 0.453). Between treatments, the number of early emerging/weak APR individuals was significantly higher in the heightened risk group (N = 17 vs N = 5, $\chi^2_{(1, N = 22)} = 0.6545$, P = 0.011) (EW, Fig 4.3a). The proportions of the remaining combinations were not significantly different (χ^2, p > 0.1 for all).

4.3.3 *Brain Shape and Regional Areas*

Between treatments ambient risk fish had a greater overall left side bias versus heightened risk fish; 5.95% ± 0.06 versus 3.43% ± 0.06 ($F_{(1,139)} = 5.849$, P = 0.017, $\eta p^2 = 0.04$) for their telencephalons and 8.89% ± 0.05 versus 6.59% ± 0.06 ($F_{(1,139)} = 5.744$, P = 0.018, $\eta p^2 = 0.04$) for their optic tecta. We found that individuals from the heightened risk treatment had proportionally larger optic tecta (0.51 ± 0.02 vs 0.50 ± 0.02, $F_{(1,139)} = 6.385$, P = 0.013, $\eta p^2 = 0.04$), smaller hypothalami (0.14 ± 0.009 vs 0.15 ± 0.01, $F_{(1,139)} = 4.413$, P = 0.037, $\eta p^2 = 0.03$) and, controlling for standard length, larger olfactory bulbs ($F_{(1,139)} = 4.293$, P = 0.04, $\eta p^2 = 0.03$) (Fig 4.3b).

One-way ANOVA found that individuals with a stronger antipredator response (APR) invested proportionally less in their olfactory bulbs, 5.28% of total brain area vs 5.49% ($F_{(1,139)} = 4.629$, P = 0.033, $\eta p^2 = 0.03$) and their brains on average were 3.61% smaller than those of the weak APR (Fig 4.3c). The size of other regions did not differ significantly between treatments, nor did body length, weight, or condition. The brains of weak APR individuals were more symmetric than those of strong APR fish (5.6% vs 7.4%, $F_{(1,139)} = 5.530$, P = 0.020, $\eta p^2 = 0.04$). Strong APR fish had more left side lateralization of their optic tecta, 6.34% ± 4.72 versus 9.47% ± 6.53 ($F_{(1,139)} = 10.837$, P = 0.001, $\eta p^2 = 0.07$). Their hypothalamic lobes that had significantly more right-side bias, 4.89% ± 6.69 vs 2.44% ± 6.43 ($F_{(1,139)} = 4.880$, P = 0.029, $\eta p^2 = 0.03$) and were marginally larger relative to the total brain area (14.7 vs 14.4%, P=0.086). Regional sizes within the brain were highly correlated in the shy group; suggesting concerted growth (Table 4.2).

4.3.4 Brain Morphology and Behavioral Correlates

After controlling for body size, the latency to emerge from shelter correlated positively with hypothalamus size for ambient and negatively for heightened risk fish (Fig 4.4a, Pearson r = 0.274, $F_{(1,63)} = 5.131$, N = 65, P = 0.027 (ambient risk) vs -0.407, $F_{(1,57)} = 11.317$, N = 59, P = 0.001 (heightened risk)). Linear regression found a significant effect for hypothalamic ratio in heightened risk only (Pearson R = 0.487, $F_{(2, 56)} = 8.692$, P = 0.001, $\beta_{(\text{hypothalamus})} = -0.447$, P = 0.001, $\beta_{(\text{hypothalamic ratio})} = -0.270$, $p_{(\text{hypothalamic ratio})} = 0.026$). When the water only controls relative were excluded, olfactory bulb size was found to correlate positively with positively with vertical

displacement; especially in the heightened risk fish (Pearson r = 0.203, $F_{(1,112)} = 4.810$, P = 0.030, Pearson r = 0.273, $F_{(1,52)} = 4.202$, P = 0.045).). A GLMM ($\chi^2_{(19, N = 141)} = 31.114$, P = 0.039), looking at antipredator response intensity versus olfactory investment found significant [alarm cue] by [risk level] ($\chi^2_{(4, N = 141)} = 17.218$, P = 0.002) and [alarm cue] by [risk] by [olfactory investment] ($\chi^2_{(9, N = 141)} = 38.624$, P < 0.001) differences between heightened and ambient risk for the 0.001% and 0.1% levels. Spearman correlations were used to detect any monotonic relationships between olfactory and hypothalamic measures with antipredator response intensity by treatment and cue concentration (Table 4.3).

A follow-up univariate GLM revealed that the relationship between olfactory investment and response intensity varied significantly by antipredator response phenotype (P < 0.001); with olfactory investment only correlating with APR intensity in the weak response (proactive) grouping. The number of intervals spent stationary on the substrate (an overt antipredator response) and olfactory investment were significantly correlated for only the weak APR fish (weak APR: Pearson r = 0.319, N=77, P = 0.005, versus strong APR: Pearson r = 0.089, P = 0.483).

4.4 *Discussion*

We found that in redbelly dace, exposure to perceived predation led to increased olfactory investment and led to a response reflective of proportional response intensities from the heightened risk fish at alarm cue concentrations above and below the response thresholds of the ambient risk group. This may imply that relatively larger olfactory bulbs may facilitate behavioral decision-making when navigating alarm cue concentration gradients at the extremes of their detection range (Holmes and McCormick, 2011). However, confidence in this conclusion is tempered by the observation that the relationship between regional size, symmetry, and behavioral outcomes may be dependent on recent experience with predation, as with the hypothalamus size and emergence time.

The proportionally larger olfactory and optic sensory regions seen in the heightened risk dace suggest a generalized response to a perceived increase in predation risk; both sensory modalities may facilitate their detection of predators (Fischer et al., 2017). Correspondingly, the decreased investment in the hypothalamic lobes of the heightened risk dace may suggest a reduction in the reactivity of their hypothalamic-pituitary-interrenal axis; as seen in proactive fish, and those from high predation environments, which tend to have lower basal and post-stress cortisol levels (Fürtbauer et al., 2015; Vindas et al., 2017a).

Contrary to previous findings (Joyce and Brown, 2020b), the heightened-risk subjects reduced their hypothalamic investment and investment was negatively correlated with the latency to emerge from a shelter when controlling for body size. An analogous effect has been seen in fathead minnows, where elevating perceived predation not only promoted boldness (propensity for risk-taking) but disrupted the correlation between boldness and body size (Meuthen et al., 2019). This may suggest a reduced role of the hypothalamus in the decision to emerge from shelter or a decrease in cortisol output amongst the heightened-risk fish, which were bolder overall (do Carmo Silva et al., 2018; Magnhagen and Borcherding, 2008). Conversely, it may suggest a heightened stress response in the ambient risk fish to the handling associated with the emergence test; influencing their subsequent behavior (Fürtbauer et al., 2015).

Antipredator response intensity (APR) was used as a second behavioral axis a proxy for a proactive/reactive response to risk (Mesquita et al., 2015); defined by the relative change in vertical position and activity level in response to a stimulus. The heightened risk fish measurably reacted at the lowest cue concentration (0.001%), and significant correlations between olfactory bulb size and response intensity in the heightened-risk fish were seen only at the highest (10%) and lowest (0.001%) concentrations. Whereas in the ambient risk group olfactory investment only correlated with response intensity significantly at the 1% concentration. This contrasts with the observation that fish from higher predation populations tend to exhibit a more graded response to perceived threats, while individuals from lower predation populations tend to react in a more hypersensitive or "all or nothing" manner (Brown et al., 2006). An explanation for this increased responsiveness from the heightened risk group may be that repeated exposure to perceived predation pressure broadened the sensitivity range for olfaction in the heightened risk group.

A corresponding result, also contrary to expectation, was that the correlations between the change in their vertical position and activity level with olfactory bulb size, were positive. The weak APR (proactive) responders were found to invest more in their olfactory bulbs and exhibited the expected positive graded between response intensity and olfactory bulb size (Fig 4.4b); this graded response to olfactory cues is more consistent with a proactive stress coping style and/or bolder personalities. These results suggest that, for the proactive individuals, increased olfactory investment may provide more nuanced olfactory information upon which to base decisions (Kermen et al., 2013); possibly owing to larger or more diverse populations of olfactory receptors (Bazáes et al., 2013).

Looking at both behavioural axes together, the heightened risk group had an even distribution of behavioural phenotypes, while the ambient risk group had remarkably few early emerging / weak APR fish. The threat of predation has previously been found to strengthen the association (behavioural syndrome) between boldness and aggressiveness (Bell and Sih, 2007). Similarly, here the association between boldness and proactivity appears to have increased in response to predation risk (Fig 4.3a).

Our findings illustrate the potential power and pitfalls of relating gross brain morphology to complex behavior. The interactions between stress coping style, predation pressure, and neuroplastic responses within individual brains have the potential to impact outcomes behavioural in ways that are difficult to predict. Future investigations examining the relationship between the gross morphology and behavioral responses of the teleost brain should consider how concurrent changes in sensory capacity and stress coping style may contextualize behavioural variation.

Table 4.1 – Predictions and outcomes for a) predation-induced morphological and behavioral changes and b) correlations between brain morphology and behavior; HR – heightened risk, AR – ambient risk, PR – proactive individuals

	Prediction	Result	
a) Pre-exposed to Heightened risk			
	(1) Increased investment in optic tecta/ olfactory bulbs	True	
	(2) Decreased hypothalamic investment	True	
	(3) Reduced anti-predator response (more proactive individuals)	True	
b) Overall Correlations			
	(4) Latency to emerge correlates positively with hypothalamus size	Mixed	(AR+/HR-)
	(5) Antipredator response correlated with hypothalamus size	False	
	(6) Antipredator response intensity correlates with olfactory investment	Mixed	(PR only)

Table 4.2 – Spearman's Rho correlations between the $\log_{10}$ transformed size of brain regions for dace in the ambient risk (N = 72) vs. heightened risk (N = 69) treatments (table 5.2a), classified as having a strong (N = 77) or weak (N = 64) antipredator response phenotypes (table 5.2b), or classified as early emergers (N = 44) or late emergers (N = 80). OB – olfactory bulbs, TE – telencephalon, OP – optic tecta, CE – cerebellum, HY – hypothalami. *P<0.05, **P<0.01

(a) Predation Pressure		TE	OP	CE	HY
Ambient risk					
	OB	0.219	-0.256*	0.061	-0.18
	TE		-0.448**	-0.075	-0.225
	OP			-0.478**	-0.198
	CE				-0.167
Heightened risk					
	OB	-0.059	-0.072	-0.301*	-0.082
	TE		-0.516**	-0.312**	0.152
	OP			-0.088	-0.558**
	CE				-0.209

(b) Antipredator Response		TE	OP	CE	HY
Strong (reactive)					
	OB	0.184	-0.185	-0.157	-0.087
	TE		-0.434**	-0.177	-0.208
	OP			-0.312*	-0.220
	CE				-0.307*
Weak (proactive)					
	OB	-0.036	-0.135	-0.155	-0.117
	TE		-0.486**	-0.200	0.084
	OP			-0.302**	-0.458**
	CE				-0.099

(c) Emergence Time		TE	OP	CE	HY
Early (bolder)					
	OB	0.187	0.200	0.226	0.113
	TE		0.512**	0.419**	0.513**
	OP			0.351*	0.547**
	CE				0.228
Late (shyer)					
	OB	0.586**	0.565**	0.334**	0.384**
	TE		0.710**	0.507**	0.623**
	OP			0.575**	0.547**
	CE				0.444**

Table 4.3 - Spearman Rho correlations between relative olfactory or hypothalamic investment vs. the change in vertical area use (VAU), activity level (ACT), and time spent stationary (TS). Pearson r correlations with antipredator response intensity (ARI), in dace exposed to a) ambient risk or b) heightened risk treatments. *P<0.05, **P<0.01.

Risk treatment	Stimulus	N	ΔVAU	ΔACT	ΔTS	ARI
(a) Ambient risk						
Olfactory bulbs	DW	12	0.049	0.294	0.182	0.148
	0.001%	16	-0.224	0.041	0.08	-0.181
	0.01%	14	0.367	-0.134	0.262	-0.89
	1%	15	0.664**	0.656**	-0.056	0.500*
	10%	15	-0.175	-0.286	0.324	-0.290
Hypothalami	DW	12	-0.273	0.049	00.211	-0.063
	0.001%	16	0.379	0.065	-0.058	0.105
	0.01%	14	0.367	-0.134	0.262	-0.193
	1%	15	-0.374	-0.411	0.375	-0.511*
	10%	15	0.068	-0.339	0.159	-0.101
(b) High risk						
Olfactory bulbs	DW	15	-0.143	-0.079	0.023	-0.091
	0.001%	15	0.546*	0.543*	0.115	0.658**
	0.01%	13	-0.154	-0.429	0.469	-0.382
	1%	13	-0.311	-0.313	0.111	-0.342
	10%	13	0.615*	0.385	0.152	0.554*
Hypothalami	DW	15	-0.236	-0.129	0.05	0.126
	0.001%	15	0.225	0.068	0.116	0.150
	0.01%	13	0.066	-0.176	0.017	-0.189
	1%	13	0.028	-0.143	-0.108	0.025
	10%	13	-0.203	0.137	-0.380	0.148

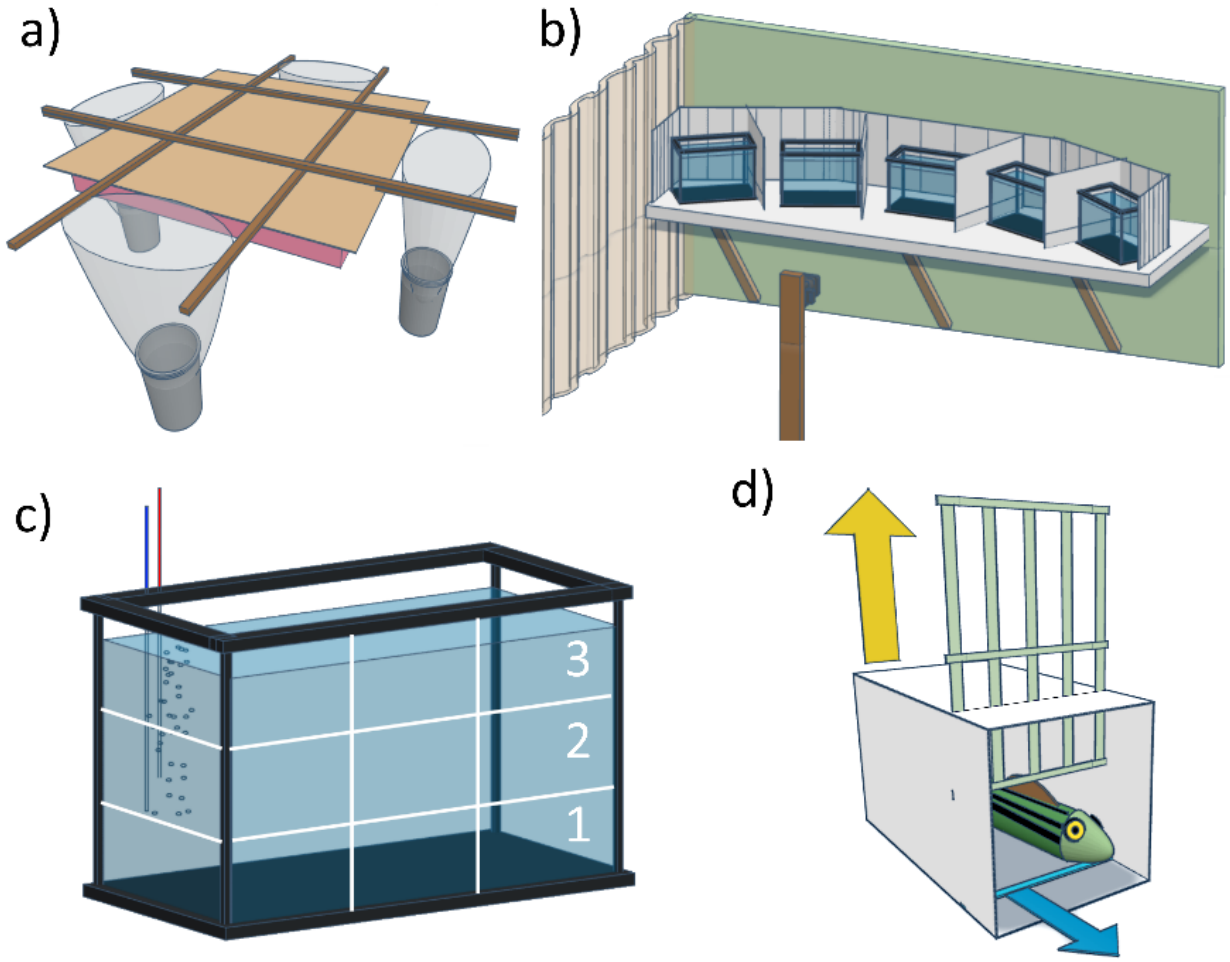

Figure 4.1 – Diagrams of a) the rafts used to suspend the mesh enclosures, b) the single camera setup for recording multiple tanks for behavioural testing, c) an experimental test tank with 3x3 grid, and d) a refuge used for emergence time testing; (see text for dimensions).

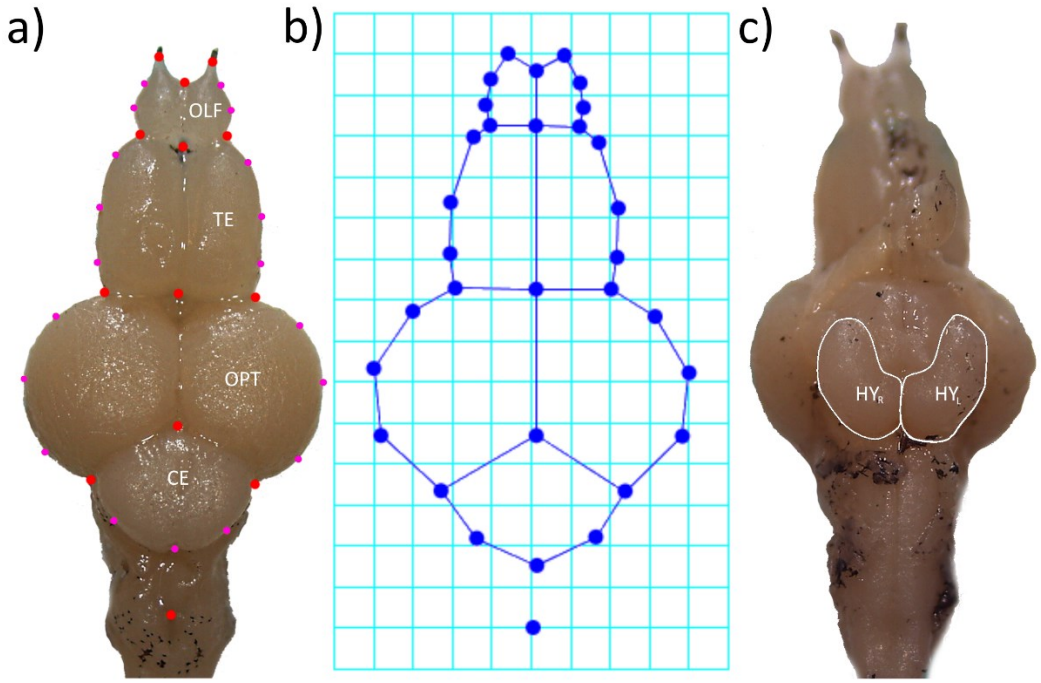

Figure 4.2 - a) The dorsal surface of a dace brain, showing the positions of the landmarks (red) and semi-landmarks (magenta) used for morphometrics; b) a wireframe showing the mean configuration of landmark points for all specimens following Procrustes alignment; c) The ventral surface of a dace brain showing the left and right inferior lobes of the hypothalamus. Grid: approximately 0.25mm; scale bar: 4mm.

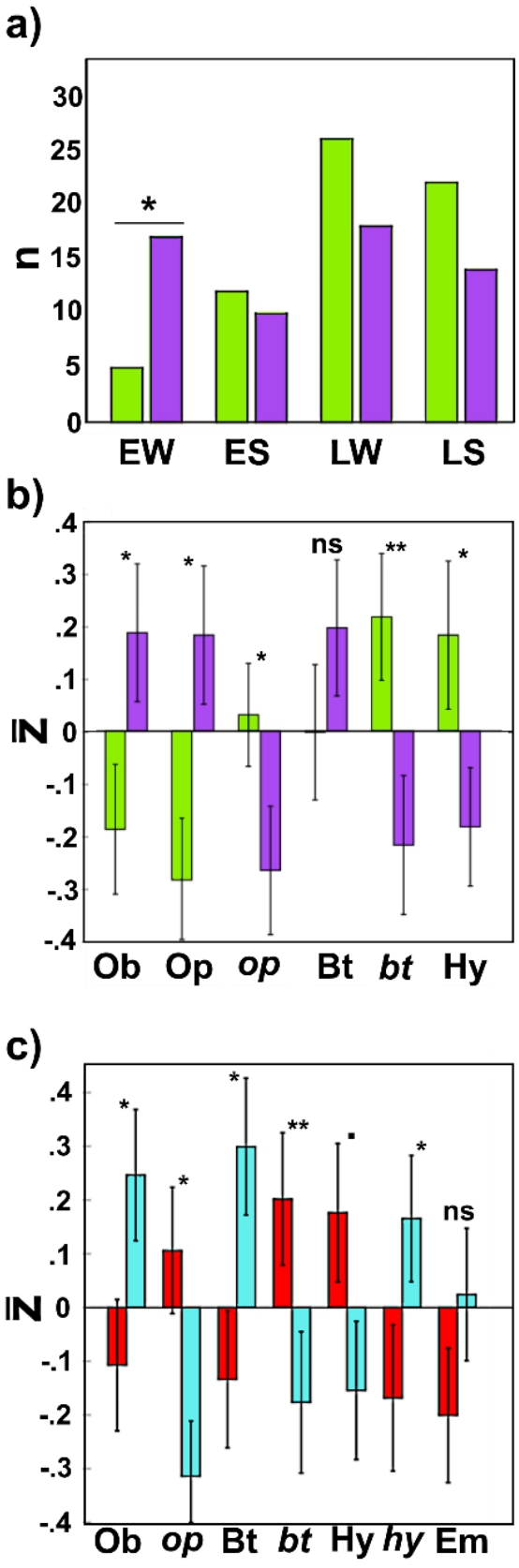

Figure 4.3 – a) Bar chart showing the number of individuals (n) in each combination of early (E) and late (L) emergers and weak (W) and strong (S) antipredator responders for ambient risk (green) and heightened risk (purple); notable differences in mean brain morphology and symmetry ($\bar{z}$, standardized variables) by b) background risk– ambient risk (green) and heightened risk (purple), and c) by antipredator response – strong response (reactive, red) group (red) and weak (proactive) responders (cyan); Ob – olfactory bulb size, Op – optic tecta size, op –optic tecta ratio, Bt – total brain area, bt – brain laterization ratio, Hy – hypothalamus, hy - hypothalamic ratio, Em – emergence time; ns ($P > 0.05$), *$P < 0.05$, **$P < 0.01$.

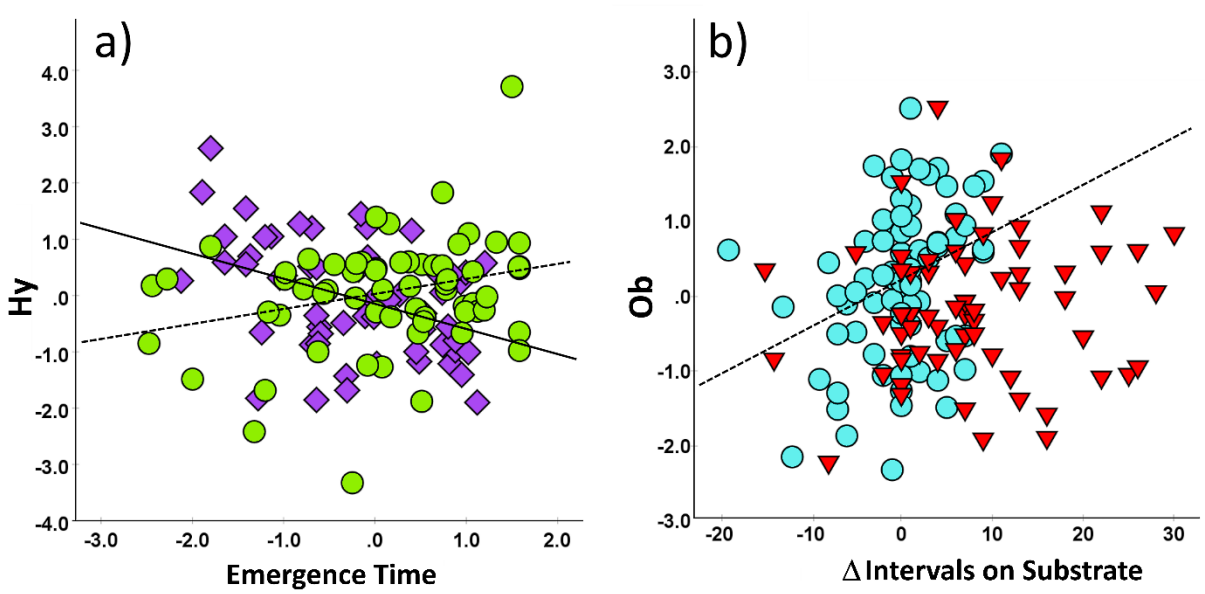

Figure 4.4 – The standardized values for a) relative hypothalamic investment controlling for body size (Hy) versus log10 transformed latency to emerge from shelter - HR (purple diamonds, solid line) and AR (green circles, dashed line) subjects; and b) relative olfactory investment (Ob) the change in the number of intervals spent stationary on the substrate, weakly responding (proactive) fish (cyan circles, dashed line) and strongly responding (reactive) fish (red triangles).

Chapter 5: Estimating the Volume of Biological Structures from a Single 2D Image: Considering Apparent Cross-Sectional Area as an Alternative to the Ellipsoid Method

5.1 *Introduction*

In ecological research, the volume of biological structures is frequently estimated from photographs, including brains (Liao et al., 2015), craniums (Logan and Palmstrom, 2015), fruit (Koc, 2007), and trees (Miranda-Fuentes et al., 2015). Despite their simplicity, photographic volume estimation (PVE) can produce satisfactory results which broadly align with values derived from more advanced approaches (Dehais et al., 2017; Foong and Lim, 2010; Forbes, 2000; Meise et al., 2014; Monkman et al., 2020).

PVE is especially useful as a cost-effective alternative to more advanced imaging tools, such as MRI or CT scanning. CT and MRI are more precise and can visualize regions and voids found within a structure (Camilieri-Asch et al., 2020a; Udagawa et al., 2019; Ullmann et al., 2010). However, typically as the sophistication of the method increases so do the attendant costs. For this reason, PVE remains popular in the study of gross brain morphology of fish and anurans (Liao et al., 2015; Pollen et al., 2007). A study comparing PVE to other methods for estimating the volume of brain regions in fish found that all methods produced comparable results and supported the same general conclusions (White and Brown, 2015). Despite its lack of sophistication, approximately 70% of studies concerning the gross brain morphology of lower vertebrates, published in the past two years, used some form of PVE (Table E.1).

Amongst the forms of PVE, the most common is the ellipsoid method (EM), which treats an object as an ellipsoid ($V = \pi/6$ x Length x Width x Height, equation 1). An object's dimensions for EM are measured from a pair of images taken from orthogonal viewpoints. There exists an alternative measure, which, unlike EM, can provide quantifiable measures of size and shape from a single photograph. The apparent cross-sectional area (ACA) of an object is measured from its planar projection, (i.e., its two-dimensional silhouette). ACA is found by tracing or placing points around the perimeter of the object's silhouette and can provide a reasonable proxy for the object's volume (Fig 5.1a). Approaches to volume estimation using simple planar projection are used to measure produce (Wulfsohn et al., 2004), whole fish (Tran et al., 2017), corals (House et al., 2018; Lavy et al., 2015), and nutritional portion sizes (Xu et al., 2013).

Methodologically, ACA's advantage lies in its ability to provide satisfactory PVE and additional morphological insights for effort comparable to EM. PVE is advantageous for live subjects in the field, where extensive handling should be avoided (Logan and Palmstrom, 2015) or is prohibited (House et al., 2018), or in cases where collecting volumetric data is otherwise cost-prohibitive. By eliminating the need for multiple additional photographs (Fig 5.1b), ACA permits volume estimation when the third dimension is not accessible, i.e., photographing from a distance or imaging an anatomical structure in situ. For instance, in species with semi-transparent heads, a recently introduced method of ACA (Näslund, 2014b), permits a rough estimation of the whole brain size in vivo by transillumination. This approach, by eliminating the dissection step, allows for repeated measures over time (Mitchell et al., 2020), and the time saved may also facilitate higher throughput (Jenkins et al., 2021).

In fishes, the use of ACA for measuring brain regions was first described by Burns & Rodd (2008), who showed that regional area traced from a dorsal photograph (Fig 5.1a), was highly correlated with the volume estimated by EM (Fig 5.1). The use of ACA for brains was further refined by Park & Bell (2010), who used landmarks to capture morphometric data regarding shape and centroid size (Fig 5.1a,b). Park and Bell found that the 2D centroid size of regional areas correlated well with volume as estimated from histological sections. Thus far, however, the ACA approach, represented in 17% of the recent studies we identified, has failed to gain much traction relative to EM at 53% (Table E.1).

This may in part be due to the seemingly counterintuitive assertion that information from two dimensions is sufficient to estimate volume. However, this intuition may not consider the extent to which other methods rely on two-dimensional estimations. For instance, methods like histology, CT, and MRI routinely use the cross-sectional areas of individual "slices" multiplied by a uniform thickness and summed together for volume estimation (Shen et al., 2003). In this sense, for solid objects, ACA is analogous to using the area of the largest cross slice from those methods as a proxy for volume. By comparison, EM relies on three lengths derived from 6 points, discarding potentially relevant shape data.

Simply put, two objects may possess the same elliptical dimensions while being otherwise dissimilar (Fig 5.2a). Figure 5.2 shows how the accuracy of ACA at estimating the cross-sectional area and volume of a rotationally symmetric pear increases with the number of perimeter points to where ACA can rival or surpass EM's performance. Both methods employ points placed on photographs to extract volumetric data; we argue that in some cases, ACA has the potential to use more points on fewer photographs to better effect.

Comparisons of the results of 2D and 3D morphometric analyses suggest that, despite the distortions ACA necessarily introduces, 2D shape data when properly collected, can serve as a good proxy for 3D morphology (Cardini, 2014; McWhinnie and Parsons, 2019). It should be noted, however, that this is not universally true; for comparisons using 2D methods to be effective, the plane used to image the object should include the axes with the greatest shape variation (Buser et al., 2018). Cardini (2014) proposed a test for evaluating the goodness of fit of 2D versus 3D data using software such as MorphoJ (Klingenberg, 2011).

When applied to a sphere and its corresponding shadow, EM and ACA produce equivalent estimates of volume. As described, they also perform comparably well when applied to the approximate ellipsoids formed by brain regions. However, how ACA handles deviations from an ellipsoidal shape versus EM in other contexts is not well established. Given the adoption of EM by fields as disparate as endocrinology (Fujita et al., 2021), ornithology (Logan and Palmstrom, 2015), and dendrology (Miranda-Fuentes et al., 2015), a generalized and interdisciplinary examination of ACA's performance in other contexts is warranted.

Here we provide a brief introduction to the general methodology of ACA as applied to physical objects. Furthermore, we contextualize ACA's performance relative to EM, with data collected under idealized conditions, across a broad range of shapes with two *in-silico* experiments. First, using an assortment of 3d object files, we evaluated the accuracy of both methods relative to the objects' similarity to a regular ellipsoid. Then, as a follow-up, using 3D scans of real-world echinoderm specimens compare the performance of top-down and side-on

ACA estimates to EM using full and half-ellipsoids. In doing so we illustrate under what circumstances ACA may be considered a viable or potentially preferable alternative to EM, for estimating the volume of biological structures.

5.1.2 *General Methodology of ACA*

ACA requires only basic equipment; tools for handling the specimens, a camera, and a computer are all that are needed. The key principle of ACA is that subjects must be carefully and consistently photographed. The primary concerns are those of reducing error, which may be imparted by variance in the preparation, positioning, or measurement of the subjects (Fruciano, 2016). The lens of the camera must be orthogonal to the plane of the structure's surface and, to be meaningful, that plane should include the longest axis of the object. Also, the type of camera/lens, lighting, magnification, and related settings should be consistent across specimens.

To minimize distortion introduced by the camera lens, each specimen should occupy approximately the same proportion of the field of view when centered under the camera lens. This is best achieved by using a lens with a fixed focal length and adjusting the distance between the lens and object, rather than adjusting the zoom. Photographing on a grid can help detect optical distortions (Zelditch et al., 2012). For smaller specimens, the use of a dissecting scope with an integrated camera is helpful, and for large objects, a fixed tripod/camera is recommended. See Muir et al., (2012) for more on minimizing distortions introduced during photography for shape analysis.

ACA requires that the positioning of specimens be kept consistent for all photographs; live subjects be kept as still as possible. For top-down photography, the object needs to be supported to present a planar imaging surface (Muir et al., 2012). This can be done by eye, by ensuring neither side of the object appears closer through the camera. For smaller specimens, the camera's depth of field at high magnification may be useful as a guide to ensure all regions of interest appear within the focal plane. Objects can be outlined in ImageJ (Schneider et al., 2012) or any image editing software which supports measuring the area of a selection; traced freehand, as a polygon, or identified through automated color identification, as applicable (Fig 5.1a).

If placed judiciously, the same points used for ACA (Figs 5.1&5.2) may also be suitable for concurrent or subsequent morphometric analysis. Geomorphic morphometrics relies on landmarks, which are discrete anatomical loci whose position can be described by cartesian coordinates, and semi-landmarks, which are points located along a curve whose position is defined relative to other features (Zelditch et al., 2012). Landmarks and semi-landmarks for geomorphic morphometrics can be applied as outlined in Park & Bell (2010) using software such as TPSDig (Rohlf, 2018). For additional guidance see the practical introduction on the topic by Webster & Sheets (2010). Landmark data can be analyzed in R using the Geomorph package (Adams and Otárola-Castillo, 2013; "Geomorph: Software for geometric morphometric analyses. R package version 4.0," 2021) or with software such as MorphoJ (Klingenberg, 2011). For additional guidance, see the resources listed in Table E.2

5.1.3 *ACA for Brains and Other Fixed Soft Tissues*

Special considerations may be necessary for capturing the morphology of preserved soft tissues. Foremost, during photography fixed tissue should be kept moist to prevent shrinkage.

There are various means of achieving this, including positioning the object on an agarose gel or submerging it in phosphate-buffered saline (Kotrschal et al., 2012; White and Brown, 2015). For soft specimens, deformation due to gravity may be a concern even when supported (Yokoyama et al., 2021); submersion may help mitigate this as well.

When fixatives are used to preserve tissue there exists the possibility of introducing preservation effects; potentially skewing results (Martinez et al., 2013). Fixatives containing formalin are popular choices owing to their ability to preserve tissue architecture with minimal deformation, however, they may still introduce volumetric artifacts; both initially and over time (Fox et al., 1985; Weisbecker, 2012). Combining or directly comparing data from specimens preserved in different ways or stored for different durations is contraindicated for this reason (Fruciano, 2016).

5.2 *Methods - ACA Validation in Silico*

To validate ACA as an alternative to EM across a range of object shapes, twenty-one 3D object (.obj) files depicting an array of common items were obtained from online repositories (Table 5.1). Unlike previous validations, our method used a variety of common objects with shapes of varying complexity. The advantage of using virtual objects is that their volumes are known, they have predefined axes, and they can be visualized with high-contrast backgrounds, allowing for reliable automated tracing; all of which help to minimize human error in measurement.

Images depicting two orthogonal views of each object were exported using 3D Viewer (v7.2107 Microsoft) at a resolution of 640 x 480 pixels; irregular objects were rotated around the longest axis and had it appear in both images. Objects with a high degree of rotational symmetry e.g., the red blood cell, were imaged parallel and perpendicular to the axis of symmetry. These 'photographs' were measured with ImageJ (Schneider et al., 2012), where the objects were isolated from the contrasting neutral background with the automatic color selection tool in legacy mode with the threshold adjusted downwards until the object was outlined. ImageJ was used to record the area (A) within the selection for ACA, and the maximum apparent length and width of the object for EM.

Ellipsoidal volume was based on the length and width of one image, with the remaining dimension (height), measured from the orthogonal view and perpendicular to the plane of the first image; it was estimated using equation 1. Measurements were first converted from pixels to 'arbitrary units' for each image based on the dimensions and volume specified in the object files. Two estimates of ACA and EM were produced for each object, one pair from each image. Linear regression of the estimates versus known volume (V) was performed using their log-transformed values (Fig 5.3a) in SPSS ("SPSS Statistics for Windows," 2020).

Percent error was calculated after converting the EM and ACA estimates to common units by treating volume and area values as those of spheres and circles respectively and calculating their radii. The spherical radius (SR) of an object was $SR = (3V/4\pi)^{(1/3)}$ (equation 2) based on volume and $SR = (A/\pi)^{(1/2)}$ (equation 3) based on ACA. In the case of a perfect sphere, the radius of the object and the radius of its cross-section are equal and thus EM and ACA are expected to yield the same result with percent error (PE) = 0. The PE between the estimated and actual SR values was calculated for each photograph and compared by a paired sample t-test.

To characterize shape variation, ImageJ calculated the circularity (4π Area/Perimeter^2, equation 4) and solidity (Area/Convex area, equation 5), for each object image. Both metrics range from 0 to 1, for circularity, this corresponds to a maximally elongated shape versus a perfect circle. Solidity is the ratio of an object's apparent area to the maximum area enclosed by points around its perimeter. The one object for which both circularity and solidity should be at a maximum, regardless of vantage point, is a sphere. An object's apparent circularity and solidity decrease as its shape deviates from sphericity.

Finally, the regression was repeated with the SR values. To assess the impact of object shape on the accuracy of the estimates, Spearman correlations of the PE values for each method with the circularity and solidity for each primary image were computed. The average values for each image were calculated and are presented in Table 5.1; a one-sample nonparametric binomial test was used to evaluate the frequency of over and underestimation.

We repeated our protocol using nine phenotypically disparate echinoderm species; whose models were scanned from dried or fossilized echinoderm specimens (Fig 5.4, Table 5.2). Across genera, echinoderms exhibit high variability in morphology in the planes perpendicular and parallel to their axis of rotational symmetry. EM volume was estimated twice, as full and half ellipsoid; the latter using half of the volume found using equation 1 after doubling height. Owing to the rotational symmetry of echinoderms the mean ellipsoidal volume estimate for each specimen was used; whichever model (half or full) produced the lowest PE estimate was considered optimal for that specimen.

Images of each specimen, classified as top-down or side-on, had their ACA values examined separately and averaged together. Finally, Wulfsohn et al. (2004) suggest that volumes estimated from averaging two or more planar projections may be more accurate than that from a single projection. Correspondingly we tested to determine how estimates from EM compared to those from pairs of ACA values for both sets of data (Table E.3).

For Fig 5.2b, the area of the symmetrical pear (right) was measured as a polygon in ImageJ for 8, 16, 24, 32, 34, and 36 points, spaced around the perimeter, and with the automatic color selection (wand) tool. Actual and elliptical volumes were calculated assuming rotational symmetry about the long axis, i.e., the short axis value was used for width and height. Area and volume estimated were converted to radii and the PE the object's polygonal ACA and volume based on point estimates.

The models from the echinoderm set (Table 5.2, Fig 5.4), were selected to provide a spectrum of circularity and solidity values. The models for *Patiria pectinifera* (Muller & Troschel, 1842), *Ophioplocus japonicus* (H.L. Clark, 1911), and *Astropecten scoparius* (Müller & Troschel, 1842), are from FiMSEA (FFish.asia, Kano et al., 2013). Models of fossilized *Conulus albogalerus* (Leske, 1778) and *Oreaster reticulatus* (Linnaeus, 1758), plus a dried *Strongylocentrotus purpuratus* (Stimpson, 1857) were found in the Digital Atlas for Ancient Life (Allmon et al., 2018). The dried *Pycnopodia Helianthoides* (Brandt, 1835) was uploaded by the RISD Nature Lab (naturelab.risd.edu), and the fossilized *Eupatagus antillarum* (Agassiz & Desor 1847), and *Culcita schmideliana* (Retzius, 1805), were made available online by S. Luallin (sketchfab.com/paleogirl) and J. Merck (sketchfab.com/jmerck) respectively. The paired silhouettes are representative of the models used in this study and illustrate the shape variation of

each specimen in two measured planes; models from the Digital Atlas of Ancient Life are in public domain (CC0 1.0), all other models are CC BY 4.0 of their respective creators (Table 5.2).

5.3 *Results*

For the set of 3D objects, ACA and EM estimation methods produced comparable results, while ACA was more accurate for elongated objects. Linear regression found that both EM and ACA were closely correlated with object volume (Fig 5.3a, Pearson $R^2 = 0.915$ and 0.943 respectively). Paired sample t-tests found that the PE was not significantly lower with ACA than with EM, for both orientations (ACA: M=0.20, SD = 0.19, EM: M=0.25, SD = 0.33, $t_{(41)} = 1.247$, p=0.220). The means of two ACA values, as seen in Table 5.1, produced significantly lower PEs than for a single ACA value (Two-sample t-test, $P < 0.001$) and were lower than the mean EM estimates for 17 of the 21 objects.

The slopes for EM and ACA versus volume were close to those expected for log transformed values ($\beta = 0.933$ vs 1 and $\beta = 0.653$ vs 0.67 respectively, $F_{(1,40)} = 428.51$ (EM) and 678.02 (ACA), $p<0.001$ for both). The standardized β coefficients for the regression the SR values were 0.977 for EM and, 0.975 for ACA ($F_{(1,40)} = 826.39$ (EM) and 768.83 (ACA), $p<0.001$ for both).

The PE of EM was weakly correlated with circularity (Spearman $\rho = -0.269$, $P = 0.085$ and controlling for volume Spearman $\rho = -0.334$, $P = 0.031$; Fig 5.3b). The PE of EM was also significantly correlated with solidity (Spearman $\rho = -0.385$, $P = 0.012$; Fig 5.3c) and volume (Spearman $\rho = -0.335$, $P = 0.03$). Overall, the PE of ACA was uncorrelated with circularity, solidity, and volume ($P > 0.3$ for all) and was negatively correlated with volume (Spearman $\rho = -0.446$, $P = 0.043$) only for the image subset which used an object's narrower or end-on silhouette. ACA estimates ignoring the longest axis, e.g., the side view of the red blood cell (a bi-concave disk) and the end on view of the thika seed pod (a rough cylinder), had especially high PE relative to those which included it (PE of 0.44 vs 0.2 and 0.52 vs 0.04 respectively).

For EM PE varied most between orientations for the coffee bean (an irregular half ellipsoid, PE 0.22 vs 0.06) and the starfruit (PE 0.26 vs 0.07). A one-sample binomial test determined that, for these objects, the difference in frequency of over versus underestimation was not statistically significant ($P = 0.165$ (ACA) and 0.877 (EM)). ACA overestimated 61.9% of cases and EM 52.4%. The mean ACA PE values (Table 5.1) were also lower than the mean EM PE (Paired samples t-test, $P = 0.011$).

The results of the echinoderm set resembled those of the object set (Fig 5.4, Table E.3). Both half/full-EM and ACA top/side values correlated with object volume (Pearson $R^2 \geq 0.979$ for all). Across all estimations, PE was not significantly lower with ACA than with EM. However, performance did vary between approaches (Fig 5.4b). Overall, the PE for top-down/side-on ACA and full/half-ellipsoid models for each species were not significantly different; the PEs of top-down ACA and the mean ACA were both significantly lower than for the half-ellipsoid model (Fig 5.4). Circularity correlated with PE for all methods similarly (Spearman $\rho = -0.673$ (top), -0.712 (side), -0.650 (optimal EM) $p = 0.03$, 0.047 and 0.058 respectively). While only EM and side-on ACA correlated with solidity (Spearman $\rho = -0.879$ (side) and -0.945 (optimal EM), $p < 0.002$ (both). The PE of the averaged ACA values was lower than for the optimal EM model for 6 of the 9 specimens.

5.4 *Discussion*

There have been several species-specific validations of ACA showing its suitability for specific applications. Our validation differs in that it evaluated the performance of ACA across a wide array of object shapes and sizes, and in more than one orientation. This revealed that, when applied to a diverse collection of objects with complex silhouettes, ACA performed comparably well to EM for estimating volume, and that their relative performance varies with the target object's shape and orientation.

Despite its relative simplicity and using half as many images, ACA tended to produce estimates that were as or more accurate than EM values estimated from the same image. Furthermore, an ACA approach facilitates morphometric measurement, permitting the examination of shape and symmetry in addition to size. Given its comparable performance, while simplifying the positioning and photography steps, ACA is an attractive option when trying to minimize the handling time of live/delicate specimens.

In our diversified set of objects, we found that ACA was not significantly affected by deviations from circularity or solidity, whereas the accuracy of EM was partially tied to an object's ellipticity. In both sets of images, ACA was more sensitive to object orientation and depends upon the image capturing as much meaningful shape variation in the plane of the image as possible. This information may inform future decisions regarding what, if any, PVE approach a project might use. Our echinoderm set serves to illustrate the broad applicability of ACA for comparisons between disparate species/shapes and underscores how accuracy can vary between orientations for ACA and half and full ellipsoid models for EM.

The notable drop in PE for the mean ACA values seen in both sets is consistent with Wulfsohn et al. (2004), who found that averaging two or more planar projections may produce superior estimates. These results suggest that, for some shapes, using an ACA approach in two planes may provide an advantage over EM. While this application would forgo many of the benefits of ACA concerning time savings, dual-ACA may be worth considering in cases where EM is applied to extant image sets, MRI/CT data, or comparisons between museum specimens.

As shown in our pear example, two objects may have the same volume according to the ellipsoid model but have distinct shapes. In circumstances such as these, ACA and/or morphometrics may differentiate between objects whose volume is deemed equivalent by EM, such as detecting instances where overall investment in tissue is the same. This is especially relevant when considering heterogeneous structures, such as a brain region, whose shape reflects variation in cellular composition, or a limb whose form is influenced by underlying musculature (Ye et al., 2020; Zaaf et al., 1999). Consequently, we argue that there exists a great deal of potentially relevant morphological variation in size and shape; within individuals, between populations, and across species, which ACA may facilitate exploring.

Its relative ease of adoption means that ACA lends itself well to student projects, pilot studies, and follow-up investigations, providing an onramp towards new insights. Thus, making the inclusion of morphology metrics for size and/or shape in experimental designs more accessible with a minimal investment in time and equipment. As we have shown, be it a brain region, a bird's skull, or a starfish, for the basic estimation of the volume of biological structures, ACA can be a versatile and inexpensive alternative tool for PVE.

Table 5.1- 3D model metrics and mean estimates

Object	Circularity	Solidity	Volume[a]	$R^{b,c}$	$R_{EM}^{b,d}$	$R_{ACA}^{b,e}$	$PE_{EM}^{d,f}$	$PE_{ACA}^{e,f}$	Source
Apple Segment	0.91	0.98	5.22	34.15	44.61	40.61	30.63	18.92	(AmazingDesign, 2015)
Brain Coral	0.79	0.99	3.30	7.83	7.28	8.05	7.02	2.75	(printable_models, 2018a)
Coffee Bean	0.75	0.99	5.30	36.38	41.56	38.15	14.22	4.87	(3Dpowdersgroup, 2019)
Heart	0.76	0.98	3.29	7.74	7.91	8.42	2.13	8.72	(printable_models, 2018b)
Humpback	0.21	0.59	1.70	2.29	5.31	3.87	131.66	69.00	(umar6419, 2011)
Kiwi	0.81	0.99	4.73	23.41	20.99	22.92	10.34	2.09	(Iphei97, 2012)
Lightbulb	0.72	0.96	3.04	6.41	7.29	6.63	13.73	3.35	(printable_models, 2018c)
Peach	0.80	0.99	2.24	3.46	3.51	3.50	1.30	1.16	(printable_models, 2018d)
Pear	0.58	0.93	2.48	4.15	5.07	4.71	22.05	13.37	(printable_models, 2018e)
Personal Watercraft	0.51	0.91	4.85	25.72	24.71	28.74	3.93	11.72	(printable_models, 2018f)
Pufferfish	0.31	0.72	2.54	4.35	8.55	5.81	96.55	33.45	(printable_models, 2018g)
Red Blood Cell	0.72	0.99	3.29	7.78	7.15	8.71	8.10	11.89	(Guidoo, 2015)
Rock	0.86	0.98	0.48	0.89	0.80	0.80	10.67	10.11	(michaelbolton, 2015)
Rugby Ball	0.86	0.99	3.57	9.61	7.71	9.66	19.82	0.47	(printable_models, 2018h)
Sausage in Bun	0.73	0.99	2.61	4.59	3.82	4.57	16.78	0.44	(printable_models, 2018i)
Sea Cucumber	0.27	0.79	2.39	3.89	6.08	4.52	56.17	16.07	(printable_models, 2018j)
Squash	0.53	0.91	2.99	6.14	4.05	4.39	34.04	28.58	(printable_models, 2018k)
Starfruit	0.68	0.99	2.76	5.17	5.67	5.65	9.67	9.19	(printable_models, 2018l)
Submarine	0.21	0.67	6.05	64.48	60.04	63.39	6.89	1.70	(Simonpk, 2019)
Thika Seed Pod	0.82	0.99	4.48	19.32	16.22	20.47	16.05	5.93	(RISD Nature Lab, 2020)
Turkey (cooked)	0.51	0.91	4.31	16.99	18.64	19.34	9.71	13.83	(printable_models, 2018m)
Mean	0.63	0.91	3.41	14.04	14.62	14.9	24.83	12.74	
Standard deviation	0.22	0.12	1.35	15.58	15.84	16.02	32.68	15.65	

a) $\log_{10}$ transformed; b) radius corresponding to a sphere of the same c) known volume, d) ellipsoidal volume, e) apparent cross-sectional area; f) percent error

Table 5.2 - The percent differences by echinoderm specimen between full / half ellipsoid estimates (F/H), top-down / side-on (T/S) orientations for ACA, and between the optimal choice between methods (ACA/EM); Min PE – the method producing the lowest PE.

Species	F/H	T/S	ACA/EM		Min PE	Model Source
O. japonicus	89.31	107.43	113.79	(T/H)	ACA	(ffish.asia, 2021a)
A. scoparius	110.44	169.60	104.50	(T/F)	ACA	(ffish.asia, 2021b)
P. helianthoides	16.22	11.97	20.32	(S/F)	EM	(RISD Naturelab, 2021)
P. pectinifera	80.81	115.32	85.95	(S/H)	ACA	(ffish.asia, 2021c)
O. reticulatus	94.46	116.23	60.16	(S/H)	ACA	(DigitalAtlasofLife, 2018a)
C. schmideliana	123.61	185.05	168.62	(T/F)	ACA	(Merck, 2020)
E. antillarum	181.25	29.04	133.42	(T/F)	EM	(Luallin, 2020)
C. albogalerus	189.67	150.18	5.51	(T/F)	ACA/EM	(DigitalAtlasofLife, 2018b)
S. purpuratus	140.65	118.56	93.30	(T/F)	ACA	(DigitalAtlasofLife, 2019)

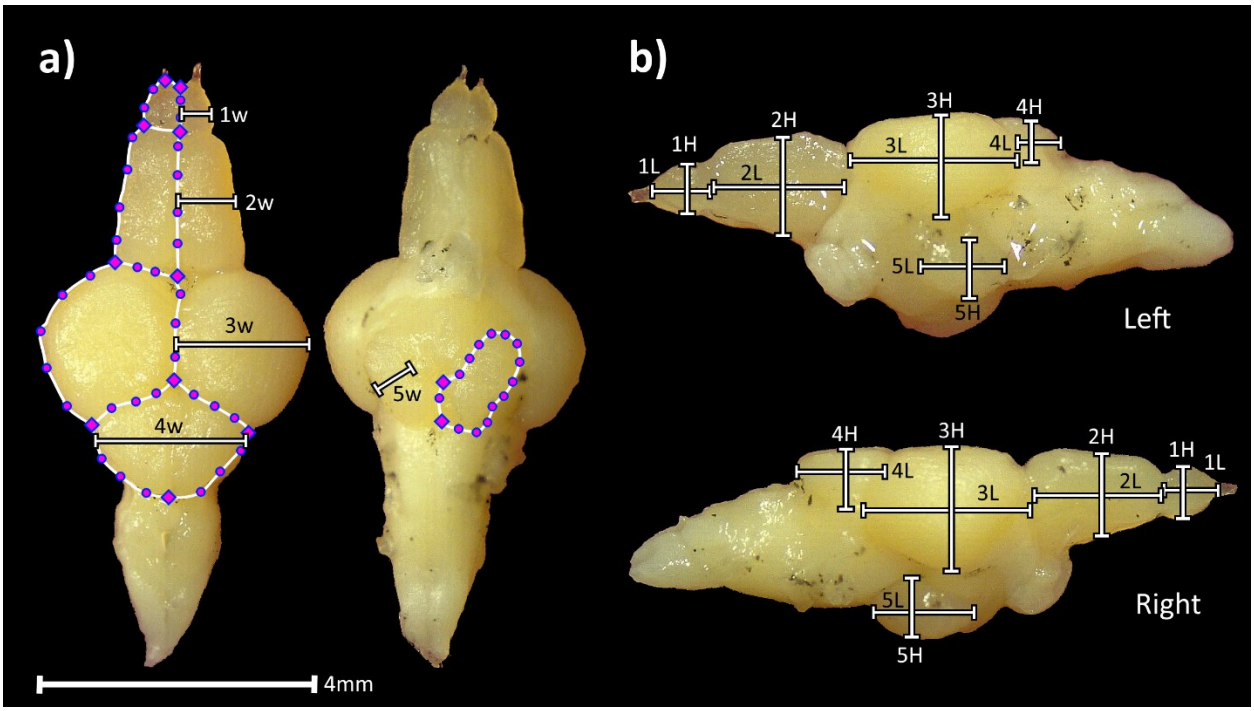

Figure 5.1 – The brain of an adult northern redbelly dace (*Chrosomus eos,* Cope, 1861); showing the subregions of the brain – the olfactory bulbs (1), the telencephalic pallium (2), the optic tectum (3), the cerebrum (4) and hypothalamus (5) as measured by ACA and EM. Bars are dimensions (L x H x W) used for EM. a) Dorsal and ventral views where subregions on the subject's left side are outlined. Dots are semi-landmarks and diamond landmarks suitable for morphometrics. b) The additional left and right lateral photographs are necessary for EM measurement of length (L), and height (H). Scale bar: 4mm.

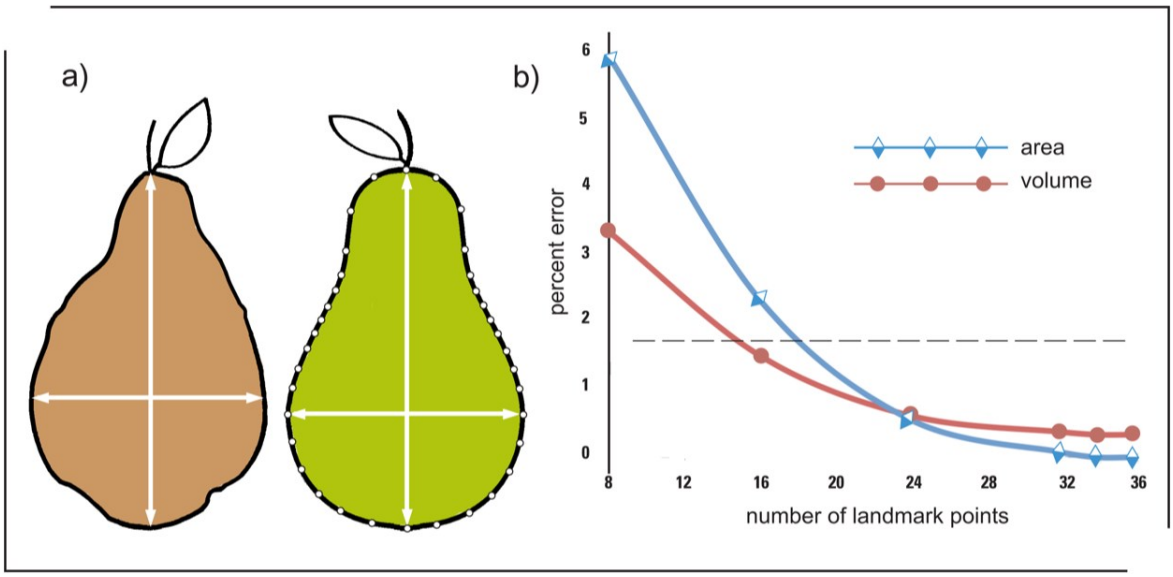

Figure 5.2 - a) Two distinctly different pears with identical lengths and widths. The pear on the right shows the placement of measurement points spaced around the perimeter. b) Percent error for estimates comparing volume and area values for the center pear using polygons with 8, 16, 24, 32, 34, and 36 points. The dashed line represents the PE for volume estimated by EM.

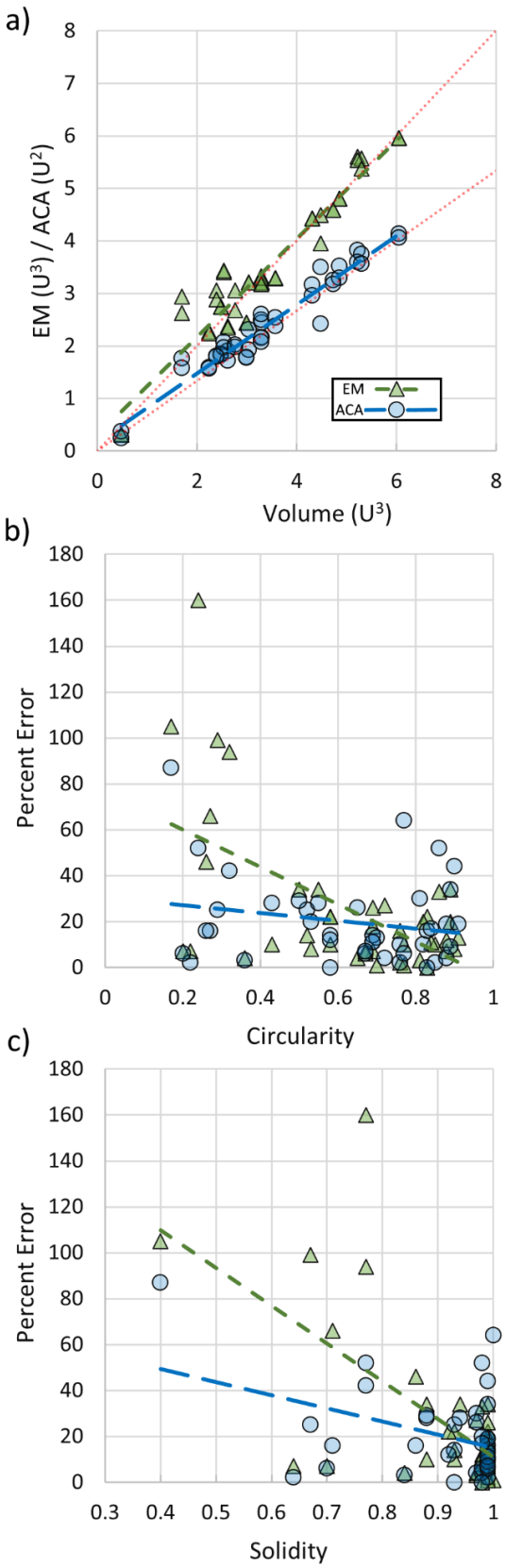

Figure 5.3 a) Log_{10} transformed volume estimates versus known volume; red dotted reference lines show the expected 1:1 and 2:3 slopes. Percent error of ACA and EM estimates versus apparent b) circularity and c) solidity.

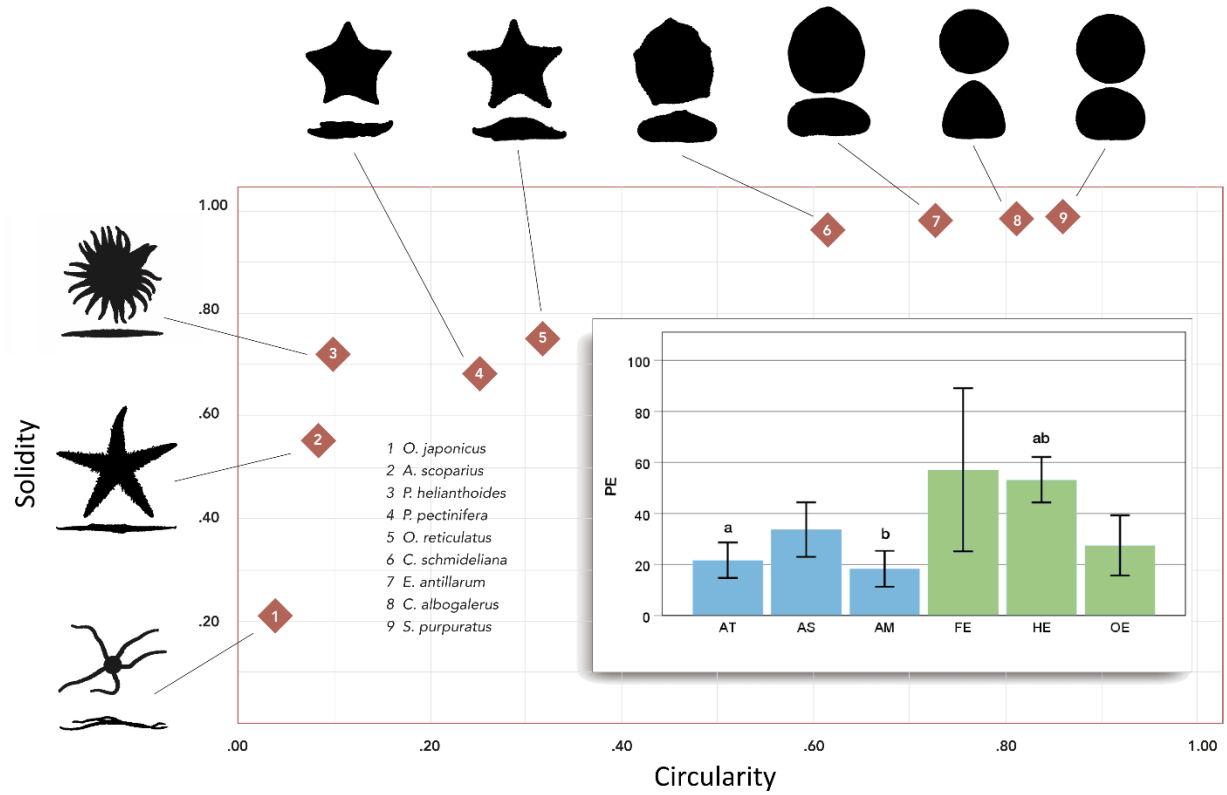

Figure 5.4 – Scatterplot showing the average circularity and solidity of nine echinoderm specimens, with their silhouettes shown. Inset: bar chart showing the mean percent error (PE) for top-down (AT), side-on (AS), and mean ACA estimates (AM), full/half-ellipsoids (FE/HE), and for EM when the optimal model is selected for each specimen (OE).

General Discussion

Aquatic environments are highly variable, and their structure and function can change rapidly as a result of a disturbance in the biotic or abiotic environment (Wilkinson et al., 2020). Correspondingly, the brains of teleosts remain phenotypically plastic in adulthood, which helps them to adapt to and thrive in a changing world. However, it also means that environmental stimuli can trigger rapid neuroplastic changes in brain morphology, resulting in the emergence of new morphological and behavioural phenotypes. The neuroplastic capacity of teleosts makes them good candidates for exploring questions regarding the interplay of genes and the environment in shaping brains and behaviour. However, if unaccounted for, their phenotypic plasticity also has the potential to confound experimental results. This thesis explored the potential ramifications of plastic brain morphology in fish for brain and behavioural research.

We began with a preliminary literature review (Chapter 1) to identify the variables which are likely to produce a rapid morphological response. Predation was identified as a likely candidate as the fitness costs associated with failing to adapt to predation can be absolute. The review showed that predation pressure is known to influence brain morphology in ninespine sticklebacks (*Pungitius pungitius*) (Gonda et al., 2012) and in guppies (*Poecilia reticulata)* (Burns and Rodd, 2008). Also, from previous work, we know that elevated predation risk can produce rapid shifts in behavioural phenotype (Brown et al., 2016). In our experiments, we used conspecific chemical alarm cues (conspecific skin extract) as an olfactory cue which serves as a reliable indicator of risk in fish (Dupuch et al., 2004; Wisenden et al., 2009). We also reviewed the literature for a suitable method for measuring brain morphology. At the time a method using the apparent cross-sectional areas of brain regions, recently introduced by Burns and Rodd (2008) and further refined by Park & Bell (2010), was well represented in the literature and was selected as an acceptable means of collecting morphological data.

Having established a methodology for inducing and quantifying brain morphology, we set out to test if the brain morphology would be significantly changed following short-term exposure to predation (Chapter 2). Our initial hypothesis was based on the results of neurology where substantial lesions to the brain were repaired on time-scales measured in weeks (Kishimoto et al., 2012; Kroehne et al., 2011). We expected that changes in brain morphology could occur more rapidly than previously supposed. Two experiments were conducted, using juvenile Atlantic salmon (*Salmo salar*) and adult northern redbelly dace (*Chrosomus eos*) in semi-natural enclosures. Both were exposed to alarm cues for two weeks, simulating a stark increase in predation. The brain morphology of the treatment group diverged from controls in both species. The similar rate and degree of morphological divergence seen in the distantly related juvenile salmon and adult dace illustrate how neuroplasticity is widely conserved in teleosts across species and into adulthood (Kaslin et al., 2008; Zupanc, 2006).

From this point on, we focused on experiments with adult redbelly dace as a model species. Redbelly dace is an abundant and widely distributed bait fish (Goertz and Phoenix, 2015; Stasiak, 2006). In addition to availability, redbelly dace were selected for their high sensitivity to alarm cue and their well-characterized, concentration-dependent behavioural

responses (Dupuch et al., 2004; Wisenden et al., 2009). Finally, the brains of redbelly dace closely resemble those of their fellow cyprinid, the well-characterized zebrafish (*Danio rerio*) (Marquart et al., 2017). Armed with a workable methodology and a suitable model organism we proceeded to explore the connection between morphology and behaviour.

Previous work has shown that ninespine stickleback exposed to alarm cue developed smaller hypothalami (Gonda et al., 2012). The hypothalamus plays an integral part in the teleost stress response, which is regulated by the hypothalamic-pituitary-interrenal (HPI) axis (Oswald et al., 2012), and a reduction in hypothalamic investment would be consistent with the downregulated stress response seen in some predation exposed populations (Archard et al., 2012). In turn, a downregulation of the physiological stress response is associated with bolder behavioral phenotypes (Raoult et al., 2012). Additionally, exposure to predation risk is known to induce bold phenotypes in three-spine sticklebacks (Bell and Sih, 2007).

Based on this, in Chapter 3, we hypothesized that exposure to conspecific alarm cues or disturbance cues (Vavrek et al., 2008), or handling stress, would show reduced hypothalamic investment and that the treatment groups would become bolder (less risk-averse). We tested this and, contrary to expectation, the treatment groups did not differ from each other or the captive controls. Captive subjects overall had smaller hypothalami, and shorter emergence times (i.e., bolder phenotypes) compared to contemporaneously caught wild controls. We also found that risk-aversion (shyness) correlated with hypothalamus size for all fish. Although we found no treatment effects for the stressors on captive dace. However, it has been shown that environmental enrichment and swimming exercise promote plasticity in the teleost brain (Mes et al., 2020; Näslund and Johnsson, 2016), and both of these were drastically reduced when the dace were moved to aquaria. As a result, we inadvertently tested the effect of short-term captivity in relatively barren conditions and showed that holding conditions can have a profound effect on experimental outcomes, potentially overshadowing other experimental interventions.

In our final plasticity experiment (Chapter 4), we sought to correlate the behaviour of our dace with their brain morphology. In Chapter 2 we found that alarm cue treatment promoted increased investment in the olfactory bulb, while in Chapter 3 it led to reduced investment in the hypothalamus. Taken together these results suggest the possibility of an individual fish becoming simultaneously better able to detect alarm cues and less inclined to react to it. We used wild caught dace and treated with alarm cue or water, to generate a range of brain morphologies, with varying degrees of olfactory and hypothalamic investment. We hypothesized that olfactory bulb size would correspond to olfactory sensitivity, such that antipredator responses would intensify with increasing concentrations of alarm cues, also, we hypothesized that response intensity would correlate with hypothalamus size.

A study using an African cichlid (*Astatotilapia burtoni*) looked at patterns of neuronal activation in the brain across varying contexts (Butler et al., 2018); they found that regional activation differed between fish with proactive verses reactive stress coping styles. In proactive individuals, the hypothalamus was activated during exploration, while in reactive fish it activated when defensively freezing. This suggests that the significance of hypothalamic investment may

vary with stress coping style, and we tested for this using an assay for boldness (latency to explore a novel arena) and for stress-coping style (response to simulated predation event). First, we found that exposure to predation led to a shift towards bolder and more proactive phenotypes compared to controls. Unlike our previous results in Chapter 3, the morphological and personality shifts in Chapter 4 are more in line with what was seen previously in ninespine (smaller hypothalami) and three-spine sticklebacks (bolder personality) exposed to predation (Bell and Sih, 2007; Gonda et al., 2012). We attribute the change to improvements where the dace were held in large mesh enclosures suspended in the pond where they originated; thereby reducing the impact of captivity and promoting neural plasticity (Salvanes et al., 2013).

Additionally, we found that olfactory investment correlated with antipredator response intensity, but only in proactive individuals, whereas the reactive individuals responded with similar intensity regardless of alarm cue concentration. This implies that an individual's stress-coping phenotype may extend to how it uses information from the environment, leading to a graded or hypersensitive response (Brown et al., 2006). These results are consistent with what is known about the physiological and genetic differences between proactive and reactive individuals; whose behavioural differences are underpinned by physiological differences within their brains. Proactive individuals tend to have lower levels of the stress hormone cortisol (Vindas et al., 2017b) and their HPI axis is less reactive (Vindas et al., 2017a). The increased stress tolerance and performance of proactive individuals (Wong et al., 2019), may have facilitated the decision-making which produced the graded response we observed. Our results suggest that individual variation in stress coping should be considered as a variable with the potential to confound or contextualize experimental findings.

Chapter 5 departed from the preceding chapters and examined the validity of our method for estimating the size of brain regions (cross-sectional area). When our literature review was updated for inclusion as Chapter 1, it became apparent that an alternative approach, the ellipsoid estimation, had since become the most common. To confirm how comparable those methods were we performed two *in-silico* experiments, which rather than assessing the agreement between the methods, compared the absolute performance of both approaches, using virtual objects of known volume. Estimates of volume from both methods were found to broadly align for most structures, suggesting that a 2D approach to volume estimation can, in some cases, be more expedient without being less effective. We found this approach to be broadly applicable for estimating the volume of biological structures and we employed it for the morphology experiments in Chapters 2-4.

The results of our experiments suggest that teleost brain morphology, being highly responsive to the environment, can provide valuable context for the interpretation of individual and group behaviour. Furthermore, they suggest that changes in brain morphology are inducible and relatively simple to quantify. The myriad of factors known to influence brain morphology, including water temperature (Závorka et al., 2020), social environment (Abigél Gonda et al., 2009; Sørensen et al., 2007), and habitat complexity (Näslund and Johnsson, 2016), must be accounted for potential confounds, but also present a broad range of possible experimental interventions. Notably, we were only able to induce brain morphology with alarm cues under

semi-natural conditions (Chapters 2 and 4). When we attempted to house wild-caught individuals in aquaria (Chapter 3), the imposition of captivity overrode any signal our treatments produced. The profound effect captivity had on the brains and behaviour of our wild dace highlights both the importance of environmental enrichment, and the potential for short periods in captivity to skew experimental results.

This work was the first to detect macroscopic changes in the brain morphology of a teleost in response to short-term exposure to an environmental stimulus. Our findings illustrate how neuroplasticity allows fish to rapidly respond to changes in the environment. In our experiments, we found that elevated predation risk resulted in a characteristic pattern of investment favouring olfaction and vision while reducing the hypothalamus. Their morphological response to alarm cues in Chapters 2 and 4, suggested a plastic response to generalized non-specific predation risk, future experiments might look at whether the 'default' response to predation confers a fitness benefit using a selection experiment with live predators. Our results from Chapter 4 also suggested that correlations between brain morphology and behaviour can vary by behavioural phenotype. Future studies seeking to correlate brain morphology and behaviour should consider including individual stress coping styles in their models; this may help to account for an interaction between a fish's response to stress and patterns of morphological investment within the brain.

Additional potential avenues of research in this area include exploring the lower limits of treatment durations which produce detectable macroscopic morphological differentiation, as well as charting how morphological changes correspond with changes in behaviour over time. Both lines of inquiry might elucidate the nature of the transition between phenotypes. More generally, the plasticity of the brain might be better understood in the context of the whole individual, for instance, the plasticity and morphology of the optic tectum (Howell et al., 2021) might be examined relative to the plasticity of the eye (Vinterstare et al., 2020). Connecting the plasticity of sensory regions with the plasticity of sensory organs could enhance our understanding of both.

Conceptually, the brain morphology of teleosts can be viewed as dynamic and reactionary; influenced by various aspects of the biotic, abiotic, and social environment. Correspondingly, a fish's brain morphology can be viewed as an indicator of its current capacities and a reflection of its evolutionary history and recent experiences. In this sense, morphology metrics resemble body mass, both are variable, but nevertheless, represent variables with considerable explanatory and predictive power. Fortunately, as discussed in Chapters 1 and 5, the tools necessary for quantifying brain morphology have become increasingly accessible, which may encourage the inclusion of brain morphology in future investigations.

References

3Dpowdersgroup, 2019. Coffee bean 3D model. URL https://www.thingiverse.com/thing:3684171 (accessed 2.2.22).

Abrahams, M., 2006. The Physiology Of Antipredator Behaviour: What You Do With What You've Got, In: Fish Physiology. p. 30.

Adams, D., 2018. morphol.disparity function: Morphological disparity for one or more groups of specimens . URL https://www.rdocumentation.org/packages/geomorph/versions/3.0.7/topics/morphol.disparity (accessed 7.10.18).

Adams, D., Collyer, M., Kaliontzopoulou, A., Baken, E., 2017. geomorph: Geometric Morphometric Analyses of 2D/3D Landmark Data.

Adams, D.C., Anthony, C.D., 1996. Using randomization techniques to analyse behavioural data. Animal Behaviour 51, 733–738. https://doi.org/10.1006/anbe.1996.0077

Adams, D.C., Otárola-Castillo, E., 2013. geomorph: an R package for the collection and analysis of geometric morphometric shape data. Methods Ecol Evol 4, 393–399. https://doi.org/10.1111/2041-210X.12035

Adams, D.C., Rohlf, F.J., Slice, D.E., 2013. A field comes of age: geometric morphometrics in the 21st century. Hystrix, the Italian Journal of Mammalogy 24. https://doi.org/10.4404/hystrix-24.1-6283

Ahmed, N.I., Thompson, C., Bolnick, D.I., Stuart, Y.E., 2017. Brain morphology of the threespine stickleback (*Gasterosteus aculeatus*) varies inconsistently with respect to habitat complexity: A test of the Clever Foraging Hypothesis. Ecology and Evolution. 3372–3380. https://doi.org/10.1002/ece3.2918

Aiello, L.C., Wheeler, P., 1995. The Expensive-Tissue Hypothesis: The Brain and the Digestive System in Human and Primate Evolution. Current Anthropology 36, 199–221. https://doi.org/10.1086/204350

Allmon, W.D., Dietl, G.P., Hendricks, J.R., Ross, R.M., 2018. Bridging the two fossil records: Paleontology's "big data" future resides in museum collections. https://doi.org/10.1130/2018.2535(03)

AmazingDesign, 2015. Apple-3-Half 3D model . URL https://www.thingiverse.com/thing:509379 (accessed 2.2.22).

Amelia, T.S.M., Khalik, W.M.A.W.M., Ong, M.C., Shao, Y.T., Pan, H.-J., Bhubalan, K., 2021. Marine microplastics as vectors of major ocean pollutants and its hazards to the marine ecosystem and humans. Prog Earth Planet Sci 8, 12. https://doi.org/10.1186/s40645-020-00405-4

Ampatzis, K., Dermon, C.R., 2007. Sex differences in adult cell proliferation within the zebrafish (*Danio rerio*) cerebellum. European Journal of Neuroscience 11.

Ampatzis, K., Makantasi, P., Dermon, C.R., 2012. Cell proliferation pattern in adult zebrafish forebrain is sexually dimorphic. Neuroscience 226, 367–381. https://doi.org/10.1016/j.neuroscience.2012.09.022

Archard, G.A., Braithwaite, V.A., 2011. Increased exposure to predators increases both exploration and activity level in Brachyrhaphis episcopi. Journal of Fish Biology 78, 593–601. https://doi.org/10.1111/j.1095-8649.2010.02880.x

Archard, G.A., Earley, R.L., Hanninen, A.F., Braithwaite, V.A., 2012. Correlated behaviour and stress physiology in fish exposed to different levels of predation pressure: Stress

hormones, behaviour and predation. Functional Ecology 26, 637–645. https://doi.org/10.1111/j.1365-2435.2012.01968.x
Arnett, H.A., Kinnison, M.T., 2017. Predator-induced phenotypic plasticity of shape and behavior: parallel and unique patterns across sexes and species. Curr Zool zow072. https://doi.org/10.1093/cz/zow072
Axelrod, C.J., Laberge, F., Robinson, B.W., 2021. Interspecific and intraspecific comparisons reveal the importance of evolutionary context in sunfish brain form divergence. J Evol Biol 34, 639–652. https://doi.org/10.1111/jeb.13763
Axelrod, C.J., Laberge, F., Robinson, B.W., 2020. Isolating the effects of ontogenetic niche shift on brain size development using pumpkinseed sunfish ecotypes. Evolution & Development 22, 312–322. https://doi.org/10.1111/ede.12333
Axelrod, C.J., Laberge, F., Robinson, B.W., 2018. Intraspecific brain size variation between coexisting sunfish ecotypes. Proc. R. Soc. B. 285, 20181971. https://doi.org/10.1098/rspb.2018.1971
Bacon, P.J., Malcolm, I.A., Fryer, R.J., Glover, R.S., Millar, C.P., Youngson, A.F., 2015. Can Conservation Stocking Enhance Juvenile Emigrant Production in Wild Atlantic Salmon? Transactions of the American Fisheries Society 144, 642–654. https://doi.org/10.1080/00028487.2015.1017655
Barton, B.A., 2002. Stress in Fishes: A Diversity of Responses with Particular Reference to Changes in Circulating Corticosteroids. Integrative and Comparative Biology 42, 517–525. https://doi.org/10.1093/icb/42.3.517
Bazáes, A., Olivares, J., Schmachtenberg, O., 2013. Properties, Projections, and Tuning of Teleost Olfactory Receptor Neurons. J Chem Ecol 39, 451–464. https://doi.org/10.1007/s10886-013-0268-1
Beckmann, F., Heise, K., Kölsch, B., Bonse, U., Rajewsky, M.F., Bartscher, M., Biermann, T., 1999. Three-Dimensional Imaging of Nerve Tissue by X-Ray Phase-Contrast Microtomography. Biophysical Journal 76, 98–102. https://doi.org/10.1016/S0006-3495(99)77181-X
Bell, A.M., Sih, A., 2007. Exposure to predation generates personality in threespined sticklebacks (*Gasterosteus aculeatus*). Ecol Letters 10, 828–834. https://doi.org/10.1111/j.1461-0248.2007.01081.x
Benard, M.F., 2004. Predator-Induced Phenotypic Plasticity in Organisms with Complex Life Histories. Annu. Rev. Ecol. Evol. Syst. 35, 651–673. https://doi.org/10.1146/annurev.ecolsys.35.021004.112426
Beston, S.M., Broyles, W., Walsh, M.R., 2017. Increased juvenile predation is not associated with evolved differences in adult brain size in Trinidadian killifish (*Rivulus hartii*). Ecol Evol 7, 884–894. https://doi.org/10.1002/ece3.2668
Biro, P.A., Beckmann, C., Stamps, J.A., 2010. Small within-day increases in temperature affects boldness and alters personality in coral reef fish. Proc. R. Soc. B. 277, 71–77. https://doi.org/10.1098/rspb.2009.1346
Blanchet, S., Bernatchez, L., Dodson, J.J., 2007. Behavioural and Growth Responses of a Territorial Fish (Atlantic Salmon, *Salmo salar*, L.) to Multiple Predatory Cues. Ethology 113, 1061–1072. https://doi.org/10.1111/j.1439-0310.2007.01410.x

Blanco, A.M., 2020. Hypothalamic- and pituitary-derived growth and reproductive hormones and the control of energy balance in fish. General and Comparative Endocrinology 287, 113322. https://doi.org/10.1016/j.ygcen.2019.113322

Blanco, A.M., Sundarrajan, L., Bertucci, J.I., Unniappan, S., 2018. Why goldfish? Merits and challenges in employing goldfish as a model organism in comparative endocrinology research. General and Comparative Endocrinology 257, 13–28. https://doi.org/10.1016/j.ygcen.2017.02.001

Bolker, B.M., Brooks, M.E., Clark, C.J., Geange, S.W., Poulsen, J.R., Stevens, M.H.H., White, J.-S.S., 2009. Generalized linear mixed models: a practical guide for ecology and evolution. Trends in Ecology & Evolution 24, 127–135. https://doi.org/10.1016/j.tree.2008.10.008

Boulanger-Weill, J., Sumbre, G., 2019. Functional Integration of Newborn Neurons in the Zebrafish Optic Tectum. Front. Cell Dev. Biol. 7, 57. https://doi.org/10.3389/fcell.2019.00057

Brignon, W.R., Pike, M.M., Ebbesson, L.O.E., Schaller, H.A., Peterson, J.T., Schreck, C.B., 2018. Rearing environment influences boldness and prey acquisition behavior, and brain and lens development of bull trout. Environ Biol Fish 101, 383–401. https://doi.org/10.1007/s10641-017-0705-z

Brown, C., Day, R.L., 2002. The future of stock enhancements: lessons for hatchery practice from conservation biology. Fish Fisheries 3, 79–94. https://doi.org/10.1046/j.1467-2979.2002.00077.x

Brown, C., Gardner, C., Braithwaite, V.A., 2005. Differential stress responses in fish from areas of high- and low-predation pressure. J Comp Physiol B 175, 305–312. https://doi.org/10.1007/s00360-005-0486-0

Brown, C., Gardner, C., Braithwaite, V.A., 2004. Population variation in lateralized eye use in the poeciliid *Brachyraphis episcopi*. Proc. R. Soc. Lond. B 271. https://doi.org/10.1098/rsbl.2004.0222

Brown, C., Krause, J., Laland, K.N. (Eds.), 2011. Fish cognition and behavior, 2nd ed. ed, Fish and aquatic resources series. Wiley-Blackwell, Chichester, West Sussex, UK ; Ames, Iowa.

Brown, G.E., Demers, E.E., Joyce, B.J., Ferrari, M.C.O., Chivers, D.P., 2015. Retention of neophobic predator recognition in juvenile convict cichlids: effects of background risk and recent experience. Anim Cogn 18, 1331–1338. https://doi.org/10.1007/s10071-015-0902-0

Brown, G.E., Jackson, C.D., Joyce, B.J., Chivers, D.P., Ferrari, M.C.O., 2016. Risk-induced neophobia: does sensory modality matter? Anim Cogn 19, 1143–1150. https://doi.org/10.1007/s10071-016-1021-2

Brown, G.E., Rive, A.C., Ferrari, M.C.O., Chivers, D.P., 2006. The dynamic nature of antipredator behavior: prey fish integrate threat-sensitive antipredator responses within background levels of predation risk. Behav Ecol Sociobiol 61, 9–16. https://doi.org/10.1007/s00265-006-0232-y

Buechel, S.D., Noreikiene, K., DeFaveri, J., Toli, E., Kolm, N., Merilä, J., 2019. Variation in sexual brain size dimorphism over the breeding cycle in the three-spined stickleback. Journal of Experimental Biology 222, jeb194464. https://doi.org/10.1242/jeb.194464

Burns, J.G., 2008. The validity of three tests of temperament in guppies (*Poecilia reticulata*). Journal of Comparative Psychology 122, 344–356. https://doi.org/10.1037/0735-7036.122.4.344
Burns, J.G., Rodd, F.H., 2008. Hastiness, brain size and predation regime affect the performance of wild guppies in a spatial memory task. Animal Behaviour 76, 911–922. https://doi.org/10.1016/j.anbehav.2008.02.017
Burns, J.G., Saravanan, A., Helen Rodd, F., 2009. Rearing Environment Affects the Brain Size of Guppies: Lab-Reared Guppies have Smaller Brains than Wild-Caught Guppies. Ethology 115, 122–133. https://doi.org/10.1111/j.1439-0310.2008.01585.x
Buser, T.J., Sidlauskas, B.L., Summers, A.P., 2018. 2D or Not 2D? Testing the Utility of 2D Vs. 3D Landmark Data in Geometric Morphometrics of the Sculpin Subfamily Oligocottinae (Pisces; Cottoidea). Anat. Rec. 301, 806–818. https://doi.org/10.1002/ar.23752
Butler, J.M., Whitlow, S.M., Roberts, D.A., Maruska, K.P., 2018. Neural and behavioural correlates of repeated social defeat. Sci Rep 8, 6818. https://doi.org/10.1038/s41598-018-25160-x
Cadwallader, P.L., 1975. Relationship between brain morphology and ecology in New Zealand Galaxiidae, particularly *Galaxias vulgaris* (Pisces: Salmoniformes). New Zealand Journal of Zoology 2, 35–43. https://doi.org/10.1080/03014223.1975.9517860
Camilieri-Asch, V., Shaw, J.A., Mehnert, A., Yopak, K.E., Partridge, J.C., Collin, S.P., 2020a. diceCT: A Valuable Technique to Study the Nervous System of Fish. eNeuro 7, ENEURO.0076-20.2020. https://doi.org/10.1523/ENEURO.0076-20.2020
Camilieri-Asch, V., Shaw, J.A., Yopak, K.E., Chapuis, L., Partridge, J.C., Collin, S.P., 2020b. Volumetric analysis and morphological assessment of the ascending olfactory pathway in an elasmobranch and a teleost using diceCT. Brain Struct Funct 225, 2347–2375. https://doi.org/10.1007/s00429-020-02127-1
Campbell, J.M., Carter, P.A., Wheeler, P.A., Thorgaard, G.H., 2015. Aggressive Behavior, Brain Size and Domestication in Clonal Rainbow Trout Lines. Behav Genet 45, 245–254. https://doi.org/10.1007/s10519-014-9696-0
Cardini, A., 2014. Missing the third dimension in geometric morphometrics: how to assess if 2D images really are a good proxy for 3D structures? Hystrix, the Italian Journal of Mammalogy 25. https://doi.org/10.4404/hystrix-25.2-10993
Chapman, L., Albert, J., Galis, F., 2008. Developmental Plasticity, Genetic Differentiation, and Hypoxia-induced Trade-offs in an African Cichlid Fish. TOEVOLJ 2, 75–88. https://doi.org/10.2174/1874404400802010075
Chapman, L.J., Hulen, K.G., 2001. Implications of hypoxia for the brain size and gill morphometry of mormyrid fishes. J. Zoology 254, 461–472. https://doi.org/10.1017/S0952836901000966
Cigliola, V., Becker, C.J., Poss, K.D., 2020. Building bridges, not walls: spinal cord regeneration in zebrafish. Disease Models & Mechanisms 13, dmm044131. https://doi.org/10.1242/dmm.044131
Clark, J.R., Camus, A.C., Comolli, J., Divers, S.J., Gendron, K.P., 2022. MRI of the live fish brain at 3 Tesla: Feasibility, technique and interspecies anatomic variations. Vet Radiology Ultrasound vru.13128. https://doi.org/10.1111/vru.13128
Conte, F.S., 2004. Stress and the welfare of cultured fish. Applied Animal Behaviour Science 86, 205–223. https://doi.org/10.1016/j.applanim.2004.02.003

Costa, S.S., Andrade, R., Carneiro, L.A., Gonçalves, E.J., Kotrschal, K., Oliveira, R.F., 2011. Sex Differences in the Dorsolateral Telencephalon Correlate with Home Range Size in Blenniid Fish. Brain Behav Evol 77, 55–64. https://doi.org/10.1159/000323668

Crane, A.L., Mathiron, A.G.E., Ferrari, M.C.O., 2015. Social learning in a high-risk environment: incomplete disregard for the 'minnow that cried pike' results in culturally transmitted neophobia. Proc. R. Soc. B. 282, 20150934. https://doi.org/10.1098/rspb.2015.0934

Crispo, E., Chapman, L.J., 2010. Geographic variation in phenotypic plasticity in response to dissolved oxygen in an African cichlid fish: Variation in plasticity in an African cichlid. Journal of Evolutionary Biology 23, 2091–2103. https://doi.org/10.1111/j.1420-9101.2010.02069.x

Dahm, R., Geisler, R., 2006. Learning from Small Fry: The Zebrafish as a Genetic Model Organism for Aquaculture Fish Species. Mar Biotechnol 8, 329–345. https://doi.org/10.1007/s10126-006-5139-0

Dehais, J., Anthimopoulos, M., Shevchik, S., Mougiakakou, S., 2017. Two-View 3D Reconstruction for Food Volume Estimation. IEEE Trans. Multimedia 19, 1090–1099. https://doi.org/10.1109/TMM.2016.2642792

Delgado, M.J., Cerdá-Reverter, J.M., Soengas, J.L., 2017. Hypothalamic Integration of Metabolic, Endocrine, and Circadian Signals in Fish: Involvement in the Control of Food Intake. Front. Neurosci. 11, 354. https://doi.org/10.3389/fnins.2017.00354

DePasquale, C., Neuberger, T., Hirrlinger, A.M., Braithwaite, V.A., 2016. The influence of complex and threatening environments in early life on brain size and behaviour. Proc. R. Soc. B. 283, 20152564. https://doi.org/10.1098/rspb.2015.2564

DigitalAtlasofLife, 2019. Echinoid: *Strongylocentrotus* (PRI 78783) . URL https://sketchfab.com/models/ff7eca213f1b4afcb22ec5457f244c1b/embed?autostart=1 (accessed 8.6.22).

DigitalAtlasofLife, 2018a. Asteroid: *Oreaster reticulatus* . URL https://sketchfab.com/models/32de6a92ad104e20aaa841c8e3eef93f/embed?autostart=1 (accessed 8.6.22).

DigitalAtlasofLife, 2018b. Echinoid: *Conulus albogalerus* (PRI 44594) . URL https://sketchfab.com/models/507aa6970a534a4f95b1d15e14fff147/embed?autostart=1 (accessed 8.6.22).

Dingemanse, N.J., Kazem, A.J.N., Réale, D., Wright, J., 2010. Behavioural reaction norms: animal personality meets individual plasticity. Trends in Ecology & Evolution 25, 81–89. https://doi.org/10.1016/j.tree.2009.07.013

Diniz, D.G., de Siqueira, L.S., Henrique, E.P., Pereira, P.D.C., Diniz, C.G., de Abreu, C.C., de Morais Magalhães, N.G., da Silva Soares, G.L., Paixão, P.E.G., Meneses, J.O., do Couto, M.V.S., da Costa Sousa, N., dos Santos Cunha, F., Diniz, C.W.P., Fujimoto, R.Y., 2020. Environmental enrichment increases the number of telencephalic but not tectal cells of angelfish (*Pterophyllum scalare*): an exploratory investigation using optical fractionator. Environ Biol Fish 103, 847–857. https://doi.org/10.1007/s10641-020-00986-5

do Carmo Silva, R.X., Lima-Maximino, M.G., Maximino, C., 2018. The aversive brain system of teleosts: Implications for neuroscience and biological psychiatry. Neuroscience & Biobehavioral Reviews 95, 123–135. https://doi.org/10.1016/j.neubiorev.2018.10.001

Donaldson, B.P., Brown, G.E., 2022. Predation Cues Lead to Rapid Changes in Brain Morphology of Juvenile Convict Cichlids (*Amitatlania nigrofasciata*). Proc Zool Soc. https://doi.org/10.1007/s12595-022-00450-5

Donaldson, M.R., Clark, T.D., Hinch, S.G., Cooke, S.J., Patterson, D.A., Gale, M.K., Frappell, P.B., Farrell, A.P., 2010. Physiological Responses of Free-Swimming Adult Coho Salmon to Simulated Predator and Fisheries Encounters. Physiological and Biochemical Zoology 83, 973–983. https://doi.org/10.1086/656336

Dunlap, K.D., Corbo, J.H., Vergara, M.M., Beston, S.M., Walsh, M.R., 2019. Predation drives the evolution of brain cell proliferation and brain allometry in male Trinidadian killifish, *Rivulus hartii*. Proc. R. Soc. B. 286, 20191485. https://doi.org/10.1098/rspb.2019.1485

Dupuch, A., Magnan, P., Dill, L.M., 2004. Sensitivity of northern redbelly dace, *Phoxinus eos* , to chemical alarm cues. Can. J. Zool. 82, 407–415. https://doi.org/10.1139/z04-003

Ebbesson, L.O.E., Braithwaite, V.A., 2012. Environmental effects on fish neural plasticity and cognition. Journal of Fish Biology 81, 2151–2174. https://doi.org/10.1111/j.1095-8649.2012.03486.x

Eifert, C., Farnworth, M., Schulz-Mirbach, T., Riesch, R., Bierbach, D., Klaus, S., Wurster, A., Tobler, M., Streit, B., Indy, J.R., Arias-Rodriguez, L., Plath, M., 2015. Brain size variation in extremophile fish: local adaptation versus phenotypic plasticity: Brain size variation in extremophile fish. J Zool 295, 143–153. https://doi.org/10.1111/jzo.12190

Elvidge, C.K., Brown, G.E., 2015. Nonconsumptive Effects of Predation and Impaired Chemosensory Risk Assessment on an Aquatic Prey Species. International Journal of Ecology 2015, 1–9. https://doi.org/10.1155/2015/894579

Elvidge, C.K., Ramnarine, I., Brown, G.E., 2014. Compensatory foraging in Trinidadian guppies: Effects of acute and chronic predation threats. Current Zoology 60, 323–332. https://doi.org/10.1093/czoolo/60.3.323

Evans, M.L., Chapman, L.J., Mitrofanov, I., Bernatchez, L., 2013. Variable extent of parallelism in respiratory, circulatory, and neurological traits across lake whitefish species pairs. Ecol Evol 3, 546–557. https://doi.org/10.1002/ece3.469

Ferrari, M.C.O., 2014. Short-term environmental variation in predation risk leads to differential performance in predation-related cognitive function. Animal Behaviour 95, 9–14. https://doi.org/10.1016/j.anbehav.2014.06.001

Ferrari, M.C.O., Wisenden, B.D., Chivers, D.P., 2010. Chemical ecology of predator–prey interactions in aquatic ecosystems: a review and prospectus Can. J. Zool. 88, 698–724. https://doi.org/10.1139/Z10-029

ffish.asia, 2021a. Brittle Star: *Ophioplocus japonicus* . URL https://sketchfab.com/models/da1968d4e0434afd9fc0abb37b9c050d/embed?autostart=1 (accessed 8.6.22).

ffish.asia, 2021b. Toxic Starfish: *Astropecten scoparius* . URL https://sketchfab.com/models/0a9e1faf6a024323991cdcd3f04ed1c6/embed?autostart=1 (accessed 8.6.22).

ffish.asia, 2021c. Starfish: *Patiria pectinifera* . URL https://sketchfab.com/models/14319712a5f445fe8a1eb461eadf6527/embed?autostart=1 (accessed 8.6.22).

Fischer, S., Bessert-Nettelbeck, M., Kotrschal, A., Taborsky, B., 2015. Rearing-Group Size Determines Social Competence and Brain Structure in a Cooperatively Breeding Cichlid. The American Naturalist 186, 123–140. https://doi.org/10.1086/681636
Fischer, S., Oberhummer, E., Cunha-Saraiva, F., Gerber, N., Taborsky, B., 2017. Smell or vision? The use of different sensory modalities in predator discrimination. Behav Ecol Sociobiol 71, 143. https://doi.org/10.1007/s00265-017-2371-8
Fluet-Chouinard, E., Funge-Smith, S., McIntyre, P.B., 2018. Global hidden harvest of freshwater fish revealed by household surveys. Proc. Natl. Acad. Sci. U.S.A. 115, 7623–7628. https://doi.org/10.1073/pnas.1721097115
Fong, S., Buechel, S.D., Boussard, A., Kotrschal, A., Kolm, N., 2019. Plastic changes in brain morphology in relation to learning and environmental enrichment in the guppy (*Poecilia reticulata*). Journal of Experimental Biology jeb.200402. https://doi.org/10.1242/jeb.200402
Foong, S.K., Lim, C.C., 2010. Can you tell the density of the watermelon from this photograph? Phys. Educ. 45, 352–355. https://doi.org/10.1088/0031-9120/45/4/004
Forbes, K., 2000. Volume Estimation of Fruit from Digital Profile Images. University of Cape Town.
Fox, C.H., Johnson, F.B., Whiting, J., Roller, P.P., 1985. Formaldehyde fixation. J Histochem Cytochem. 33, 845–853. https://doi.org/10.1177/33.8.3894502
Fraser, D.F., Gilliam, J.F., 1987. Feeding under predation hazard: response of the guppy and Hart's rivulus from sites with contrasting predation hazard. Behav Ecol Sociobiol 21, 203–209. https://doi.org/10.1007/BF00292500
Fraser, T.W.K., Fjelldal, P.G., Skjaeraasen, J.E., Hansen, T., Mayer, I., 2012. Triploidy alters brain morphology in pre-smolt Atlantic salmon ***Salmo salar*** : possible implications for behaviour. Journal of Fish Biology 81, 2199–2212. https://doi.org/10.1111/j.1095-8649.2012.03479.x
Froese, R, Pauly, D., 2018. Fish Identification - Genus Chrosomus . URL https://www.fishbase.ca/identification/SpeciesList.php?class=&order=&famcode=&subfamily=&genus=Chrosomus&areacode=&c_code=&depth=&spines=&fins=&TL=&BD=&resultPage=1&sortby=species (accessed 3.26.18).
Fruciano, C., 2016. Measurement error in geometric morphometrics. Dev Genes Evol 226, 139–158. https://doi.org/10.1007/s00427-016-0537-4
Fuchs, E., Flügge, G., 2014. Adult Neuroplasticity: More Than 40 Years of Research. Neural Plasticity 2014, 1–10. https://doi.org/10.1155/2014/541870
Fujita, N., Kato, K., Abe, S., Naganawa, S., 2021. Variation in thyroid volumes due to differences in the measured length or area of the cross-sectional plane: A validation study of the ellipsoid approximation method using CT images. J Appl Clin Med Phys 22, 15–25. https://doi.org/10.1002/acm2.13125
Fürtbauer, I., Pond, A., Heistermann, M., King, A.J., 2015. Personality, plasticity and predation: linking endocrine and behavioural reaction norms in stickleback fish. Funct Ecol 29, 931–940. https://doi.org/10.1111/1365-2435.12400
Geffroy, B., Alfonso, S., Sadoul, B., Blumstein, D.T., 2020. A World for Reactive Phenotypes. Front. Conserv. Sci. 1, 611919. https://doi.org/10.3389/fcosc.2020.611919
Geomorph: Software for geometric morphometric analyses. R package version 4.0, 2021.

Goertz, D.E., Phoenix, R.D., 2015. Range extensions for Northern Redbelly Dace (*Chrosomus eos*), Fathead Minnow (*Pimephales promelas*), and Iowa Darter (*Etheostoma exile*) in Ontario, Canada. Can Field Nat 129, 237. https://doi.org/10.22621/cfn.v129i3.1722

Gonda, A., Herczeg, G., Merilä, J., 2013. Evolutionary ecology of intraspecific brain size variation: a review. Ecol Evol 3, 2751–2764. https://doi.org/10.1002/ece3.627

Gonda, A., Herczeg, G., Merilä, J., 2011. Population variation in brain size of nine-spined sticklebacks (*Pungitius pungitius*) - local adaptation or environmentally induced variation? BMC Evol Biol 11, 75. https://doi.org/10.1186/1471-2148-11-75

Gonda, Abigél, Herczeg, G., Merilä, J., 2009. Habitat-dependent and -independent plastic responses to social environment in the nine-spined stickleback (*Pungitius pungitius*) brain. Proc. R. Soc. B. 276, 2085–2092. https://doi.org/10.1098/rspb.2009.0026

Gonda, A., Herczeg, G., Merilä, J., 2009. Adaptive brain size divergence in nine-spined sticklebacks (*Pungitius pungitius*)? Journal of Evolutionary Biology 22, 1721–1726. https://doi.org/10.1111/j.1420-9101.2009.01782.x

Gonda, A., Välimäki, K., Herczeg, G., Merilä, J., 2012. Brain development and predation: plastic responses depend on evolutionary history. Biol. Lett. 8, 249–252. https://doi.org/10.1098/rsbl.2011.0837

Guidoo, 2015. Red Blood Cell . URL https://www.thingiverse.com/thing:1137317 (accessed 2.2.22).

Guillen, J., Natale, F., Carvalho, N., Casey, J., Hofherr, J., Druon, J.-N., Fiore, G., Gibin, M., Zanzi, A., Martinsohn, J.Th., 2019. Global seafood consumption footprint. Ambio 48, 111–122. https://doi.org/10.1007/s13280-018-1060-9

Hall, D.G., 1998. Continuity and the Persistence of Objects: When the Whole Is Greater Than the Sum of the Parts. Cognitive Psychology 37, 28–59. https://doi.org/10.1006/cogp.1998.0688

Hall, Z.J., Tropepe, V., 2020. Using Teleost Fish to Discern Developmental Signatures of Evolutionary Adaptation From Phenotypic Plasticity in Brain Structure. Front. Neuroanat. 14, 10. https://doi.org/10.3389/fnana.2020.00010

Handelsman, C.A., Broder, E.D., Dalton, C.M., Ruell, E.W., Myrick, C.A., Reznick, D.N., Ghalambor, C.K., 2013. Predator-Induced Phenotypic Plasticity in Metabolism and Rate of Growth: Rapid Adaptation to a Novel Environment. Integrative and Comparative Biology 53, 975–988. https://doi.org/10.1093/icb/ict057

Herczeg, G., Gonda, A., Balázs, G., Noreikiene, K., Merilä, J., 2015. Experimental evidence for sex-specific plasticity in adult brain. Front Zool 12, 38. https://doi.org/10.1186/s12983-015-0130-0

Hinsch, K., Zupanc, G.K.H., 2007. Generation and long-term persistence of new neurons in the adult zebrafish brain: A quantitative analysis. Neuroscience 146, 679–696. https://doi.org/10.1016/j.neuroscience.2007.01.071

Hofmann, H.A., Benson, M.E., Fernald, R.D., 1999. Social status regulates growth rate: Consequences for life-history strategies. Proc. Natl. Acad. Sci. U.S.A. 96, 14171–14176. https://doi.org/10.1073/pnas.96.24.14171

Holmes, T.H., McCormick, M.I., 2011. Response across a gradient: behavioural reactions of newly settled fish to predation cues. Animal Behaviour 81, 543–550. https://doi.org/10.1016/j.anbehav.2010.11.019

House, J.E., Brambilla, V., Bidaut, L.M., Christie, A.P., Pizarro, O., Madin, J.S., Dornelas, M., 2018. Moving to 3D: relationships between coral planar area, surface area and volume. PeerJ 6, e4280. https://doi.org/10.7717/peerj.4280

Howell, K.J., Beston, S.M., Stearns, S., Walsh, M.R., 2021. Coordinated evolution of brain size, structure, and eye size in Trinidadian killifish. Ecol. Evol. 11, 365–375. https://doi.org/10.1002/ece3.7051

Iglesias, T.L., Dornburg, A., Warren, D.L., Wainwright, P.C., Schmitz, L., Economo, E.P., 2018. Eyes Wide Shut: the impact of dim-light vision on neural investment in marine teleosts. J. Evol. Biol. 31, 1082–1092. https://doi.org/10.1111/jeb.13299

Imre, I., Grant, J.W.A., Cunjak, R.A., 2005. Density-dependent growth of young-of-the-year Atlantic salmon *Salmo salar* in Catamaran Brook, New Brunswick: Density-dependent growth of young-of-the-year Atlantic salmon. Journal of Animal Ecology 74, 508–516. https://doi.org/10.1111/j.1365-2656.2005.00949.x

Iphei97, 2012. Kiwi Free 3D model . URL https://free3d.com/3d-model/kiwi-67347.html (accessed 2.2.22).

Irvine, J.R., Gross, M.R., Wood, C.C., Holtby, L.B., Schubert, N.D., Amiro, P.G., 2005. Canada's Species at Risk Act: An Opportunity to Protect Endangered Salmon. Fisheries 30, 11–19. https://doi.org/10.1577/1548-8446(2005)30[11:CSARA]2.0.CO;2

Ishikawa, Y., Yoshimoto, M., Yamamoto, N., Ito, H., Yasuda, T., Tokunaga, F., Iigo, M., Wakamatsu, Y., Ozato, K., 2001. Brain Structures of a Medaka Mutant, *el(eyeless)*, in Which Eye Vesicles Do Not Evaginate. Brain, Behavior and Evolution 58, 173–184. https://doi.org/10.1159/000047271

Ishizaki, Y., Masuda, R., Uematsu, K., Shimizu, K., Arimoto, M., Takeuchi, T., 2001. The effect of dietary docosahexaenoic acid on schooling behaviour and brain development in larval yellowtail. Journal of Fish Biology 58, 1691–1703. https://doi.org/10.1111/j.1095-8649.2001.tb02323.x

Ito, H., Ishikawa, Y., Yoshimoto, M., Yamamoto, N., 2007. Diversity of Brain Morphology in Teleosts: Brain and Ecological Niche. Brain Behav Evol 69, 76–86. https://doi.org/10.1159/000095196

Ito, H., Yamamoto, N., 2009. Non-laminar cerebral cortex in teleost fishes? Biol. Lett. 5, 117–121. https://doi.org/10.1098/rsbl.2008.0397

Jadhao, A.G., D'Aniello, B., Malz, C.R., Pinelli, C., Meyer, D.L., 2001. Intrasexual and intersexual dimorphisms of the red salmon prosencephalon. Cell and Tissue Research 304, 121–140. https://doi.org/10.1007/s004410000335

Jenkins, M.R., Cummings, J.M., Cabe, A.R., Hulthén, K., Peterson, M.N., Langerhans, R.B., 2021. Natural and anthropogenic sources of habitat variation influence exploration behaviour, stress response, and brain morphology in a coastal fish. J Anim Ecol 90, 2446–2461. https://doi.org/10.1111/1365-2656.13557

Jolles, J.W., Boogert, N.J., Sridhar, V.H., Couzin, I.D., Manica, A., 2017. Consistent Individual Differences Drive Collective Behavior and Group Functioning of Schooling Fish. Current Biology 27, 2862-2868.e7. https://doi.org/10.1016/j.cub.2017.08.004

Jones, N.A.R., Webster, M.M., Salvanes, A.G.V., 2021. Physical enrichment research for captive fish: Time to focus on the DETAILS. J Fish Biol 99, 704–725. https://doi.org/10.1111/jfb.14773

Joyce, B.J., Brown, G.E., 2022. Estimating the volume of biological structures from a single 2D image: considering apparent cross-sectional area as an alternative to the ellipsoid method. Evol Ecol. https://doi.org/10.1007/s10682-022-10211-7

Joyce, B.J., Brown, G.E., 2020a. Short-term captivity drives hypothalamic plasticity and asymmetry in wild-caught northern red bellied dace (*Chrosomus eos*). J Fish Biol 97, 577–582. https://doi.org/10.1111/jfb.14408

Joyce, B.J., Brown, G.E., 2020b. Rapid plastic changes in brain morphology in response to acute changes in predation pressure in juvenile Atlantic salmon (*Salmo salar*) and northern redbelly dace (*Phoxinus eos*). Can. J. Zool. 98, 186–194. https://doi.org/10.1139/cjz-2019-0131

Joyce, B.J., Demers, E.E., Ferrari, M.C.O., Chivers, D.P., Brown, G.E., 2016. Background Predation Risk and Learned Predator Recognition in Convict Cichlids: Does Risk Allocation Constrain Learning? Ethology 122, 841–849. https://doi.org/10.1111/eth.12532

Kalueff, A.V., Echevarria, D.J., Stewart, A.M., 2014. Gaining translational momentum: More zebrafish models for neuroscience research. Progress in Neuro-Psychopharmacology and Biological Psychiatry 55, 1–6. https://doi.org/10.1016/j.pnpbp.2014.01.022

Kano, Y., Adnan, M.S., Grudpan, C., Grudpan, J., Magtoon, W., Musikasinthorn, P., Natori, Y., Ottomanski, S., Praxaysonbath, B., Phongsa, K., Rangsiruji, A., Shibukawa, K., Shimatani, Y., So, N., Suvarnaraksha, A., Thach, P., Thanh, P.N., Tran, D.D., Utsugi, K., Yamashita, T., 2013. An online database on freshwater fish diversity and distribution in Mainland Southeast Asia. Ichthyol Res 60, 293–295. https://doi.org/10.1007/s10228-013-0349-8

Kaslin, J., Ganz, J., Brand, M., 2008. Proliferation, neurogenesis and regeneration in the non-mammalian vertebrate brain 22.

Keagy, J., Braithwaite, V.A., Boughman, J.W., 2018. Brain differences in ecologically differentiated sticklebacks. Current Zoology 64, 243–250. https://doi.org/10.1093/cz/zox074

Kermen, F., Franco, L.M., Wyatt, C., Yaksi, E., 2013. Neural circuits mediating olfactory-driven behavior in fish. Front. Neural Circuits 7. https://doi.org/10.3389/fncir.2013.00062

Kihslinger, R.L., Lema, S.C., Nevitt, G.A., 2006. Environmental rearing conditions produce forebrain differences in wild Chinook salmon *Oncorhynchus tshawytscha*. Comparative Biochemistry and Physiology Part A: Molecular & Integrative Physiology 145, 145–151. https://doi.org/10.1016/j.cbpa.2006.06.041

Kihslinger, R.L., Nevitt, G.A., 2006. Early rearing environment impacts cerebellar growth in juvenile salmon. Journal of Experimental Biology 209, 504–509. https://doi.org/10.1242/jeb.02019

Kishimoto, N., Shimizu, K., Sawamoto, K., 2012. Neuronal regeneration in a zebrafish model of adult brain injury. Disease Models & Mechanisms 5, 200–209. https://doi.org/10.1242/dmm.007336

Klingenberg, C.P., 2011. MorphoJ: an integrated software package for geometric morphometrics: computer program note. Molecular Ecology Resources 11, 353–357. https://doi.org/10.1111/j.1755-0998.2010.02924.x

Koc, A.B., 2007. Determination of watermelon volume using ellipsoid approximation and image processing. Postharvest Biology and Technology 45, 366–371. https://doi.org/10.1016/j.postharvbio.2007.03.010
Kolm, N., Gonzalez-Voyer, A., Brelin, D., Winberg, S., 2009. Evidence for small scale variation in the vertebrate brain: mating strategy and sex affect brain size and structure in wild brown trout (*Salmo trutta*). Journal of Evolutionary Biology 22, 2524–2531. https://doi.org/10.1111/j.1420-9101.2009.01875.x
Kotrschal, A., Corral-Lopez, A., Szidat, S., Kolm, N., 2015. The effect of brain size evolution on feeding propensity, digestive efficiency, and juvenile growth: Brief Communication. Evolution 69, 3013–3020. https://doi.org/10.1111/evo.12784
Kotrschal, A., Deacon, A.E., Magurran, A.E., Kolm, N., 2017. Predation pressure shapes brain anatomy in the wild. Evol Ecol 31, 619–633. https://doi.org/10.1007/s10682-017-9901-8
Kotrschal, Alexander, Räsänen, K., Kristjánsson, B.K., Senn, M., Kolm, N., 2012a. Extreme Sexual Brain Size Dimorphism in Sticklebacks: A Consequence of the Cognitive Challenges of Sex and Parenting? PLoS ONE 7, e30055. https://doi.org/10.1371/journal.pone.0030055
Kotrschal, Alexander, Rogell, B., Maklakov, A.A., Kolm, N., 2012b. Sex-specific plasticity in brain morphology depends on social environment of the guppy, *Poecilia reticulata*. Behav Ecol Sociobiol 66, 1485–1492. https://doi.org/10.1007/s00265-012-1403-7
Kotrschal, A., Sundström, L.F., Brelin, D., Devlin, R.H., Kolm, N., 2012. Inside the heads of David and Goliath: environmental effects on brain morphology among wild and growth-enhanced coho salmon *Oncorhynchus kisutch*. Journal of Fish Biology 81, 987–1002. https://doi.org/10.1111/j.1095-8649.2012.03348.x
Kotrschal, A., Trombley, S., Rogell, B., Brannström, I., Foconi, E., Schmitz, M., Kolm, N., 2014. The mating brain: early maturing sneaker males maintain investment into the brain also under fast body growth in Atlantic salmon (*Salmo salar*). Evol Ecol 28, 1043–1055. https://doi.org/10.1007/s10682-014-9715-x
Kotrschal, K., Van Staaden, M.J., Huber, R., 1998. Fish brains: evolution and environmental relationships. Reviews in Fish Biology and Fisheries 8, 373–408. https://doi.org/10.1023/A:1008839605380
Krauzlis, R.J., Bogadhi, A.R., Herman, J.P., Bollimunta, A., 2018. Selective attention without a neocortex. Cortex 102, 161–175. https://doi.org/10.1016/j.cortex.2017.08.026
Kristiansen, T.S., Fernö, A., Pavlidis, M.A., van de Vis, H. (Eds.), 2020. The Welfare of Fish, Animal Welfare. Springer International Publishing, Cham. https://doi.org/10.1007/978-3-030-41675-1
Kroehne, V., Freudenreich, D., Hans, S., Kaslin, J., Brand, M., 2011. Regeneration of the adult zebrafish brain from neurogenic radial glia-type progenitors. Development 138, 4831–4841. https://doi.org/10.1242/dev.072587
Lavy, A., Eyal, G., Neal, B., Keren, R., Loya, Y., Ilan, M., 2015. A quick, easy and non-intrusive method for underwater volume and surface area evaluation of benthic organisms by 3D computer modelling. Methods Ecol Evol 6, 521–531. https://doi.org/10.1111/2041-210X.12331
Leduc, A.O.H.C., Roh, E., Macnaughton, C.J., Benz, F., Rosenfeld, J., Brown, G.E., 2010. Ambient pH and the Response to Chemical Alarm Cues in Juvenile Atlantic Salmon:

Mechanisms of Reduced Behavioral Responses. Transactions of the American Fisheries Society 139, 117–128. https://doi.org/10.1577/T09-024.1
Lee, H.J., Schneider, R.F., Manousaki, T., Kang, J.H., Lein, E., Franchini, P., Meyer, A., 2017. Lateralized Feeding Behavior is Associated with Asymmetrical Neuroanatomy and Lateralized Gene Expressions in the Brain in Scale-Eating Cichlid Fish. Genome Biology and Evolution 9, 3122–3136. https://doi.org/10.1093/gbe/evx218
Lema, S.C., Hodges, M.J., Marchetti, M.P., Nevitt, G.A., 2005. Proliferation zones in the salmon telencephalon and evidence for environmental influence on proliferation rate. Comp Biochem Physiol A Mol Integr Physio 141, 327–335. https://doi.org/10.1016/j.cbpb.2005.06.003
Liao, W.B., Lou, S.L., Zeng, Y., Merilä, J., 2015. Evolution of anuran brains: disentangling ecological and phylogenetic sources of variation. J. Evol. Biol. 28, 1986–1996. https://doi.org/10.1111/jeb.12714
Lima, S.L., Bednekoff, P.A., 1999. Temporal Variation in Danger Drives Antipredator Behavior: The Predation Risk Allocation Hypothesis. The American Naturalist 153, 11. https://doi.org/10.1086/303202
Lima, S.L., Dill, L.M., 1990. Behavioral decisions made under the risk of predation: a review and prospectus. Can. J. Zool. 68, 619–640. https://doi.org/10.1139/z90-092
Liu, M., Liu, Y., Wang, X., Wang, H., 2021. Brain morphological adaptations of *Gambusia affinis* along climatic gradients in China. J Zool Syst Evol Res 59, 2150–2160. https://doi.org/10.1111/jzs.12544
Logan, C.J., Palmstrom, C.R., 2015. Can endocranial volume be estimated accurately from external skull measurements in great-tailed grackles (*Quiscalus mexicanus*)? PeerJ 3, e1000. https://doi.org/10.7717/peerj.1000
Lovas-Kiss, Á., Vincze, O., Löki, V., Pallér-Kapusi, F., Halasi-Kovács, B., Kovács, G., Green, A.J., Lukács, B.A., 2020. Experimental evidence of dispersal of invasive cyprinid eggs inside migratory waterfowl. Proc. Natl. Acad. Sci. U.S.A. 117, 15397–15399. https://doi.org/10.1073/pnas.2004805117
Luallin, S., 2020. Eupatagus antillarum . URL https://sketchfab.com/models/d188cfba30b8444788802b3830321e46/embed?autostart=1 (accessed 8.6.22).
Lyons, J, 2018. Fish details - Finescale dace . URL https://www.seagrant.wisc.edu/fish-id/ (accessed 3.26.18).
Magnhagen, C., Borcherding, J., 2008. Risk-taking behaviour in foraging perch: does predation pressure influence age-specific boldness? Animal Behaviour 75, 509–517. https://doi.org/10.1016/j.anbehav.2007.06.007
Marchetti, M.P., Nevitt, G.A., 2003. Effects of Hatchery Rearing on Brain Structures of Rainbow Trout, *Oncorhynchus mykiss*. Environmental Biology of Fishes 66, 9–14. https://doi.org/10.1023/A:1023269221678
Marquart, G.D., Tabor, K.M., Horstick, E.J., Brown, M., Geoca, A.K., Polys, N.F., Nogare, D.D., Burgess, H.A., 2017. High-precision registration between zebrafish brain atlases using symmetric diffeomorphic normalization. GigaScience 6. https://doi.org/10.1093/gigascience/gix056

Martinez, P.A., Berbel-Filho, W.M., Jacobina, U.P., 2013. Is formalin fixation and ethanol preservation able to influence in geometric morphometric analysis? Fishes as a case study. Zoomorphology 132, 87–93. https://doi.org/10.1007/s00435-012-0176-x

Martín-Martín, A., Thelwall, M., Orduna-Malea, E., Delgado López-Cózar, E., 2021. Google Scholar, Microsoft Academic, Scopus, Dimensions, Web of Science, and OpenCitations' COCI: a multidisciplinary comparison of coverage via citations. Scientometrics 126, 871–906. https://doi.org/10.1007/s11192-020-03690-4

Maruska, K.P., Fernald, R.D., 2010. Behavioral and physiological plasticity: Rapid changes during social ascent in an African cichlid fish. Hormones and Behavior 58, 230–240. https://doi.org/10.1016/j.yhbeh.2010.03.011

Mayer, I., Meager, J., Skjæraasen, J.E., Rodewald, P., Sverdrup, G., Fernö, A., 2011. Domestication causes rapid changes in heart and brain morphology in Atlantic cod (*Gadus morhua*). Environ Biol Fish 92, 181–186. https://doi.org/10.1007/s10641-011-9831-1

McCallum, E.S., Capelle, P.M., Balshine, S., 2014. Seasonal plasticity in telencephalon mass of a benthic fish: seasonal plasticity in telencephalon mass. J Fish Biol 85, 1785–1792. https://doi.org/10.1111/jfb.12507

McWhinnie, K.C., Parsons, K.J., 2019. Shaping up? A direct comparison between 2D and low-cost 3D shape analysis using African cichlid mandibles. Environ Biol Fish 102, 927–938. https://doi.org/10.1007/s10641-019-00879-2

Meise, K., Mueller, B., Zein, B., Trillmich, F., 2014. Applicability of Single-Camera Photogrammetry to Determine Body Dimensions of Pinnipeds: Galapagos Sea Lions as an Example. PLoS ONE 9, e101197. https://doi.org/10.1371/journal.pone.0101197

Merck, J., 2020. Enchinoderm: Culcita schmideliana (@jmerck) . URL https://sketchfab.com/models/5e0d5fea32ad4394b7c53f72e6a46aab/embed?autostart=1 (accessed 8.6.22).

Merilä, J., 2013. Nine-spined stickleback (*Pungitius pungitius*): an emerging model for evolutionary biology research: Nine-spined stickleback evolution. Ann. N.Y. Acad. Sci. 1289, 18–35. https://doi.org/10.1111/nyas.12089

Mes, D., Palstra, A.P., Henkel, C.V., Mayer, I., Vindas, M.A., 2020. Swimming exercise enhances brain plasticity in fish. R. Soc. open sci. 7, 191640. https://doi.org/10.1098/rsos.191640

Mesquita, F.O., Borcato, F.L., Huntingford, F.A., 2015. Cue-based and algorithmic learning in common carp: A possible link to stress coping style. Behavioural Processes 115, 25–29. https://doi.org/10.1016/j.beproc.2015.02.017

Meuthen, D., Ferrari, M.C.O., Lane, T., Chivers, D.P., 2019. Plasticity of boldness: high perceived risk eliminates a relationship between boldness and body size in fathead minnows. Animal Behaviour 147, 25–32. https://doi.org/10.1016/j.anbehav.2018.11.003

michaelbolton, 2015. Rock 3D model . URL https://free3d.com/3d-model/rock-86533.html (accessed 2.2.22).

Miranda-Fuentes, A., Llorens, J., Gamarra-Diezma, J., Gil-Ribes, J., Gil, E., 2015. Towards an Optimized Method of Olive Tree Crown Volume Measurement. Sensors 15, 3671–3687. https://doi.org/10.3390/s150203671

Mirza, R.S., Chivers, D.P., 2003. Response of juvenile rainbow trout to varying concentrations of chemical alarm cue: response thresholds and survival during encounters with predators. Can. J. Zool. 81, 88–95. https://doi.org/10.1139/z02-216
Mitchell, David Joseph, Lefèvre, J., Vega-Trejo, R., Vila Pouca, C., Kotrschal, A., 2020. Visual and olfactory cues of predation affect body and brain growth in the guppy. https://doi.org/10.32942/osf.io/vxrq4
Mitchell, David J., Vega-Trejo, R., Kotrschal, A., 2020. Experimental translocations to low predation lead to non-parallel increases in relative brain size. Biol. Lett. 16, 20190654. https://doi.org/10.1098/rsbl.2019.0654
Mitteroecker, P., Gunz, P., Windhager, S., Schaefer, K., 2013. A brief review of shape, form, and allometry in geometric morphometrics, with applications to human facial morphology. Hystrix, the Italian Journal of Mammalogy 24. https://doi.org/10.4404/hystrix-24.1-6369
Mohammed, A.H., Zhu, S.W., Darmopil, S., Hjerling-Leffler, J., Ernfors, P., Winblad, B., Diamond, M.C., Eriksson, P.S., Bogdanovic, N., 2002. Environmental enrichment and the brain, in: Progress in Brain Research. Elsevier, pp. 109–133. https://doi.org/10.1016/S0079-6123(02)38074-9
Monkman, G.G., Hyder, K., Kaiser, M.J., Vidal, F.P., 2020. Accurate estimation of fish length in single camera photogrammetry with a fiducial marker. ICES Journal of Marine Science 77, 2245–2254. https://doi.org/10.1093/icesjms/fsz030
Moran, D., Softley, R., Warrant, E.J., 2015. The energetic cost of vision and the evolution of eyeless Mexican cavefish. Sci. Adv. 1, e1500363. https://doi.org/10.1126/sciadv.1500363
Muir, A.M., Vecsei, P., Krueger, C.C., 2012. A Perspective on Perspectives: Methods to Reduce Variation in Shape Analysis of Digital Images. Transactions of the American Fisheries Society 141, 1161–1170. https://doi.org/10.1080/00028487.2012.685823
Murren, C.J., Auld, J.R., Callahan, H., Ghalambor, C.K., Handelsman, C.A., Heskel, M.A., Kingsolver, J.G., Maclean, H.J., Masel, J., Maughan, H., Pfennig, D.W., Relyea, R.A., Seiter, S., Snell-Rood, E., Steiner, U.K., Schlichting, C.D., 2015. Constraints on the evolution of phenotypic plasticity: limits and costs of phenotype and plasticity. Heredity 115, 293–301. https://doi.org/10.1038/hdy.2015.8
Naish, K.A., Taylor, J.E., Levin, P.S., Quinn, T.P., Winton, J.R., Huppert, D., Hilborn, R., 2007. An Evaluation of the Effects of Conservation and Fishery Enhancement Hatcheries on Wild Populations of Salmon, in: Advances in Marine Biology. Elsevier, pp. 61–194. https://doi.org/10.1016/S0065-2881(07)53002-6
Nakajima, M., Taniguchi, N., 2001. Genetics of the guppy as a model for experiment in aquaculture. Genetica 111, 279–289. https://doi.org/10.1023/A:1013717516234
Näslund, J., 2018. Relative Mass of Brain- and Intestinal Tissue in Juvenile Brown Trout: No Long-Term Effects of Compensatory Growth; with Additional Notes on Emerging Sex-Differences. Fishes 3, 38. https://doi.org/10.3390/fishes3040038
Näslund, J., 2014. A simple non-invasive method for measuring gross brain size in small live fish with semi-transparent heads. PeerJ 2, e586. https://doi.org/10.7717/peerj.586
Näslund, J., Aarestrup, K., Thomassen, S.T., Johnsson, J.I., 2012. Early enrichment effects on brain development in hatchery-reared Atlantic salmon (*Salmo salar*): no evidence for a critical period. Can. J. Fish. Aquat. Sci. 69, 1481–1490. https://doi.org/10.1139/f2012-074

Näslund, J., Johnsson, J.I., 2016. Environmental enrichment for fish in captive environments: effects of physical structures and substrates. Fish Fish 17, 1–30. https://doi.org/10.1111/faf.12088
Näslund, J., Larsen, M.H., Thomassen, S.T., Aarestrup, K., Johnsson, J.I., 2017. Environment-dependent plasticity and ontogenetic changes in the brain of hatchery-reared Atlantic salmon. J Zool 301, 75–82. https://doi.org/10.1111/jzo.12392
Näslund, J., Rosengren, M., Johnsson, J.I., 2019. Fish density, but not environmental enrichment, affects the size of cerebellum in the brain of juvenile hatchery-reared Atlantic salmon. Environ Biol Fish 102, 705–712. https://doi.org/10.1007/s10641-019-00864-9
Naud, M., Magnan, P., 1988. Diel onshore–offshore migrations in northern redbelly dace, *Phoxinus eos* (Cope), in relation to prey distribution in a small oligotrophic lake. Can. J. Zool. 66, 1249–1253. https://doi.org/10.1139/z88-182
Nicholson, D.J., 2018. Reconceptualizing the Organism: From Complex Machine to Flowing Stream, in: Dupré, J. (Ed.), Everything Flows: Towards a Processual Philosophy of Biology. Presented at the Process Philosophy of Biology, Oxford University Press, Oxford, United Kingdom.
Niven, J.E., Laughlin, S.B., 2008. Review Energy limitation as a selective pressure on the evolution of sensory systems. The Journal of Experimental Biology 211, 1792–1804. https://doi.org/doi:10.1242/jeb.017574
Noguera, P, Ubeda, C, Bruno, D, Semenas, L, 2015. The Fish Necropsy Manual . URL https://www.necropsymanual.net/en/ (accessed 12.11.22).
Noreikiene, K., Herczeg, G., Gonda, A., Balázs, G., Husby, A., Merilä, J., 2015. Quantitative genetic analysis of brain size variation in sticklebacks: support for the mosaic model of brain evolution. Proc. R. Soc. B. 282, 20151008. https://doi.org/10.1098/rspb.2015.1008
Olivera-Pasilio, V., Lasserre, M., Castelló, M.E., 2017. Cell Proliferation, Migration, and Neurogenesis in the Adult Brain of the Pulse Type Weakly Electric Fish, *Gymnotus omarorum*. Front. Neurosci. 11, 437. https://doi.org/10.3389/fnins.2017.00437
O'Neill, S.J., Williamson, J.E., Tosetto, L., Brown, C., 2018. Effects of acclimatisation on behavioural repeatability in two behaviour assays of the guppy *Poecilia reticulata*. Behav Ecol Sociobiol 72, 166. https://doi.org/10.1007/s00265-018-2582-7
Oswald, M.E., Drew, R.E., Racine, M., Murdoch, G.K., Robison, B.D., 2012. Is Behavioral Variation along the Bold-Shy Continuum Associated with Variation in the Stress Axis in Zebrafish? Physiological and Biochemical Zoology 85, 718–728. https://doi.org/10.1086/668203
Park, P.J., Bell, M.A., 2010. Variation of telencephalon morphology of the threespine stickleback (*Gasterosteus aculeatus*) in relation to inferred ecology: Threespine stickleback telencephalon evolution. Journal of Evolutionary Biology 23, 1261–1277. https://doi.org/10.1111/j.1420-9101.2010.01987.x
Park, P.J., Chase, I., Bell, M.A., 2012. Phenotypic plasticity of the threespine stickleback *Gasterosteus aculeatus* telencephalon in response to experience in captivity. Current Zoology 58, 189–210. https://doi.org/10.1093/czoolo/58.1.189
Paskin, T.R., Iqbal, T.R., Byrd-Jacobs, C.A., 2011. Olfactory bulb recovery following reversible deafferentation with repeated detergent application in the adult zebrafish. Neuroscience 196, 276–284. https://doi.org/10.1016/j.neuroscience.2011.09.005

Pereira, P., Puga, S., Cardoso, V., Pinto-Ribeiro, F., Raimundo, J., Barata, M., Pousão-Ferreira, P., Pacheco, M., Almeida, A., 2016. Inorganic mercury accumulation in brain following waterborne exposure elicits a deficit on the number of brain cells and impairs swimming behavior in fish (white seabream—*Diplodus sargus*). Aquatic Toxicology 170, 400–412. https://doi.org/10.1016/j.aquatox.2015.11.031

Pereira, P.D.C., Henrique, E.P., Porfírio, D.M., Crispim, C.C. de S., Campos, M.T.B., de Oliveira, R.M., Silva, I.M.S., Guerreiro, L.C.F., da Silva, T.W.P., da Silva, A. de J.F., Rosa, J.B. da S., de Azevedo, D.L.F., Lima, C.G.C., Castro de Abreu, C., Filho, C.S., Diniz, D.L.W.P., Magalhães, N.G. de M., Guerreiro-Diniz, C., Diniz, C.W.P., Diniz, D.G., 2020. Environmental Enrichment Improved Learning and Memory, Increased Telencephalic Cell Proliferation, and Induced Differential Gene Expression in *Colossoma macropomum*. Front. Pharmacol. 11, 840. https://doi.org/10.3389/fphar.2020.00840

Peris Tamayo, A., Devineau, O., Præbel, K., Kahilainen, K.K., Østbye, K., 2020. A brain and a head for a different habitat: Size variation in four morphs of Arctic charr (*Salvelinus alpinus* (L.)) in a deep oligotrophic lake. Ecol Evol 10, 11335–11351. https://doi.org/10.1002/ece3.6771

Pettersson, L.B., Brönmark, C., 1999. Energetic consequences of an inducible morphological defence in crucian carp. Oecologia 121, 12–18. https://doi.org/10.1007/s004420050901

Pickup, M., 2016. A Situationalist Solution to the Ship of Theseus Puzzle. Erkenn 81, 973–992. https://doi.org/10.1007/s10670-015-9777-3

Pike, T.W., Ramsey, M., Wilkinson, A., 2018. Environmentally induced changes to brain morphology predict cognitive performance. Phil. Trans. R. Soc. B 373, 20170287. https://doi.org/10.1098/rstb.2017.0287

Pittman, K., Yúfera, M., Pavlidis, M., Geffen, A.J., Koven, W., Ribeiro, L., Zambonino-Infante, J.L., Tandler, A., 2013. Fantastically plastic: fish larvae equipped for a new world. Rev Aquacult 5, S224–S267. https://doi.org/10.1111/raq.12034

Planchart, A., 2016. Advancing toxicology research using in vivo high throughput toxicology with small fish models. ALTEX. https://doi.org/10.14573/altex.1601281

Pollen, A.A., Dobberfuhl, A.P., Scace, J., Igulu, M.M., Renn, S.C.P., Shumway, C.A., Hofmann, H.A., 2007. Environmental Complexity and Social Organization Sculpt the Brain in Lake Tanganyikan Cichlid Fish. Brain Behav Evol 70, 21–39. https://doi.org/10.1159/000101067

printable_models, 2018a. Brain Coral v1 3D model . URL https://free3d.com/3d-model/brain-coral-v1--165215.html (accessed 2.2.22).

printable_models, 2018b. Heart v1 3D model . URL https://free3d.com/3d-model/heart-v1--539992.html (accessed 2.2.22).

printable_models, 2018c. Christmas Light C9 Bulb v1 3D model . URL https://free3d.com/3d-model/christmas-light-c9-bulb-v1--241552.html (accessed 2.2.22).

printable_models, 2018d. Peach Free 3D model . URL https://free3d.com/3d-model/-peach--306929.html (accessed 2.2.22).

printable_models, 2018e. Pear Free 3D model . URL https://free3d.com/3d-model/-pear--324071.html (accessed 2.2.22).

printable_models, 2018f. JetSki 2 person V1 3D model . URL https://free3d.com/3d-model/jetski-2-person-v1--512594.html (accessed 2.2.22).

printable_models, 2018g. Puffer fish v1 3D model . URL https://free3d.com/3d-model/puffer-fish-v1--451445.html (accessed 2.2.22).
printable_models, 2018h. Rugby Ball v1 3D model . URL https://free3d.com/3d-model/rugby-ball-v1--585369.html (accessed 2.2.22).
printable_models, 2018i. German Sausage In Bun v1 3D model . URL https://free3d.com/3d-model/german-sausage-in-bun-v1--848770.html (accessed 2.2.22).
printable_models, 2018j. Sea Cucumber v1 3D model . URL https://free3d.com/3d-model/sea-cucumber-v1--695146.html (accessed 2.2.22).
printable_models, 2018k. Squash 3D model . URL https://free3d.com/3d-model/squash--699912.html (accessed 2.2.22).
printable_models, 2018l. Starfruit 3D model . URL https://free3d.com/3d-model/starfruit--892632.html (accessed 2.2.22).
printable_models, 2018m. Cooked Turkey v1 3D model . URL https://free3d.com/3d-model/cooked-turkey-v1--511939.html (accessed 2.2.22).
Puga, S., Cardoso, V., Pinto-Ribeiro, F., Pacheco, M., Almeida, A., Pereira, P., 2018. Brain morphometric profiles and their seasonal modulation in fish (Liza aurata) inhabiting a mercury contaminated estuary. Environmental Pollution 237, 318–328. https://doi.org/10.1016/j.envpol.2018.02.047
Puga, S., Pereira, P., Pinto-Ribeiro, F., O'Driscoll, N.J., Mann, E., Barata, M., Pousão-Ferreira, P., Canário, J., Almeida, A., Pacheco, M., 2016. Unveiling the neurotoxicity of methylmercury in fish (*Diplodus sargus*) through a regional morphometric analysis of brain and swimming behavior assessment. Aquatic Toxicology 180, 320–333. https://doi.org/10.1016/j.aquatox.2016.10.014
Puschina, E.V., Obukhov, D.K., 2011. Processes of Proliferation and Apoptosis in the Brain of the Amur Sturgeon. Neurophysiology 43, 271–286. https://doi.org/10.1007/s11062-011-9227-z
Pushchina, E.V., Obukhov, D.K., 2012. Nitric oxide-factor, which regulates proliferation and apoptosis in the adult brain of amur sturgeon (*Acipenser schrenckii*). ABB 03, 788–804. https://doi.org/10.4236/abb.2012.326099
Raoult, V., Brown, C., Zuberi, A., Williamson, J.E., 2012. Blood cortisol concentrations predict boldness in juvenile mulloway (*Argyosomus japonicus*). J Ethol 30, 225–232. https://doi.org/10.1007/s10164-011-0314-9
Reddon, A.R., Chouinard-Thuly, L., Leris, I., Reader, S.M., 2018. Wild and laboratory exposure to cues of predation risk increases relative brain mass in male guppies. Funct Ecol 32, 1847–1856. https://doi.org/10.1111/1365-2435.13128
Reid, K., Bell, M.A., Veeramah, K.R., 2021. Threespine Stickleback: A Model System For Evolutionary Genomics. Annu. Rev. Genom. Hum. Genet. 22, 357–383. https://doi.org/10.1146/annurev-genom-111720-081402
Relyea, R.A., 2002. Costs of Phenotypic Plasticity. The American Naturalist 159, 272–282. https://doi.org/10.1086/338540
Relyea, R.A., Auld, J.R., 2004. Having the guts to compete: how intestinal plasticity explains costs of inducible defences: Gut plasticity in tadpoles. Ecology Letters 7, 869–875. https://doi.org/10.1111/j.1461-0248.2004.00645.x

Reznick, D.N., Travis, J., 2019. Experimental Studies of Evolution and Eco-Evo Dynamics in Guppies (*Poecilia reticulata*). Annu. Rev. Ecol. Evol. Syst. 50, 335–354. https://doi.org/10.1146/annurev-ecolsys-110218-024926

Richard Stasiak, 2006. Northern Redbelly Dace (*Phoxinus eos*): A Technical Conservation Assessment (USDA Forest Service). USDA Forest Service.

RISD Nature Lab, 2020. Thika Pod 3D model . URL https://sketchfab.com/models/ae441e1425034575a7461f2daa2677b3/embed?autostart=1 (accessed 2.2.22).

Rohlf, F.J., 2018. TPSDig - Digitize Landmarks and Outlines, Version 2.05.

Salvanes, A.G.V., Moberg, O., Ebbesson, L.O.E., Nilsen, T.O., Jensen, K.H., Braithwaite, V.A., 2013. Environmental enrichment promotes neural plasticity and cognitive ability in fish. Proc. R. Soc. B. 280, 20131331. https://doi.org/10.1098/rspb.2013.1331

Samuk, K., Iritani, D., Schluter, D., 2014. Reversed brain size sexual dimorphism accompanies loss of parental care in white sticklebacks. Ecol Evol 4, 3236–3243. https://doi.org/10.1002/ece3.1175

Samuk, K., Xue, J., Rennision, D.J., 2018. Exposure to predators does not lead to the evolution of larger brains in experimental populations of threespine stickleback: Experimental Predation And Brain Size. Evolution 72, 916–929. https://doi.org/10.1111/evo.13444

Sanogo, Y.O., Hankison, S., Band, M., Obregon, A., Bell, A.M., 2011. Brain Transcriptomic Response of Threespine Sticklebacks to Cues of a Predator. Brain Behav Evol 77, 270–285. https://doi.org/10.1159/000328221

Schauber, E.M., Connors, M.J., Goodwin, B.J., Jones, C.G., Ostfeld, R.S., 2009. Quantifying a dynamic risk landscape: heterogeneous predator activity and implications for prey persistence. Ecology 90, 240–251. https://doi.org/10.1890/07-0980.1

Schmitz, J., Güntürkün, O., Ocklenburg, S., 2019. Building an Asymmetrical Brain: The Molecular Perspective. Front. Psychol. 10, 982. https://doi.org/10.3389/fpsyg.2019.00982

Schneider, C.A., Rasband, W.S., Eliceiri, K.W., 2012. NIH Image to ImageJ: 25 years of image analysis. Nature Methods 9, 671–675. https://doi.org/10.1038/nmeth.2089

Schnitzlein, H.N., 1964. Correlation of habit and structure in the fish brain. Am Zool 4, 21–32. https://doi.org/10.1093/icb/4.1.21

Schulz-Mirbach, T., Riesch, R., García de León, F.J., Plath, M., 2011. Effects of extreme habitat conditions on otolith morphology – a case study on extremophile livebearing fishes (*Poecilia mexicana*, *P. sulphuraria*). Zoology 114, 321–334. https://doi.org/10.1016/j.zool.2011.07.004

Sebastiani, A., Hirnet, T., Jahn-Eimermacher, A., Thal, S.C., 2017. Comparison of speed-vacuum method and heat-drying method to measure brain water content of small brain samples. Journal of Neuroscience Methods 276, 73–78. https://doi.org/10.1016/j.jneumeth.2016.11.012

Shen, W., Wang, Z., Tang, H., Heshka, S., Punyanitya, M., Zhu, S., Lei, J., Heymsfield, S.B., 2003. Volume Estimates by Imaging Methods: Model Comparisons with Visible Woman as the Reference. Obesity Research 11, 217–225. https://doi.org/10.1038/oby.2003.34

Sherratt, E., 2014. Quick guide to geomorph v.2.0.

Simonpk, 2019. Submarine 3D model . URL https://www.thingiverse.com/thing:3589230 (accessed 2.2.22).

Sîrbulescu, R.F., Zupanc, G.K.H., 2011. Spinal cord repair in regeneration-competent vertebrates: Adult teleost fish as a model system. Brain Research Reviews 67, 73–93. https://doi.org/10.1016/j.brainresrev.2010.11.001
Snell-Rood, E.C., 2013. An overview of the evolutionary causes and consequences of behavioural plasticity. Animal Behaviour 85, 1004–1011. https://doi.org/10.1016/j.anbehav.2012.12.031
Soares, D., Niemiller, M.L., 2013. Sensory Adaptations of Fishes to Subterranean Environments. BioScience 63, 274–283. https://doi.org/10.1525/bio.2013.63.4.7
Soengas, J.L., Aldegunde, M., 2002. Energy metabolism of fish brain. Comparative Biochemistry and Physiology Part B: Biochemistry and Molecular Biology 131, 271–296. https://doi.org/10.1016/S1096-4959(02)00022-2
Sørensen, C., Øverli, Ø., Summers, C.H., Nilsson, G.E., 2007. Social Regulation of Neurogenesis in Teleosts. Brain Behav Evol 70, 239–246. https://doi.org/10.1159/000105487
SPSS Statistics for Windows, 2020.
Sreekala, S., 2011. Correlation between medulla oblongata and feeding habits in two teleosts. IJST 4, 1693–1695. https://doi.org/10.17485/ijst/2011/v4i12.26
Thomson, J.S., Watts, P.C., Pottinger, T.G., Sneddon, L.U., 2016. HPI reactivity does not reflect changes in personality among trout introduced to bold or shy social groups. Behav 153, 1589–1610. https://doi.org/10.1163/1568539X-00003398
Toli, E.A., Noreikiene, K., DeFaveri, J., Merilä, J., 2017. Environmental enrichment, sexual dimorphism, and brain size in sticklebacks. Ecol Evol 7, 1691–1698. https://doi.org/10.1002/ece3.2717
Toms, C.N., Echevarria, D.J., Jouandot, D.J., 2010. A Methodological Review of Personality-Related Studies in Fish: Focus on the Shy-Bold Axis of Behavior. International Journal of Comparative Psychology 23, 25.
Tort, L., 2011. Stress and immune modulation in fish. Developmental & Comparative Immunology 35, 1366–1375. https://doi.org/10.1016/j.dci.2011.07.002
Tran, M.T., Nguyen, H.H., Rantung, J., Kim, H.K., Oh, S.J., Kim, S.B., 2017. A new approach of 2D measurement of injury rate on fish by a modified K-means clustering algorithm based on L* A* B* color space, in: International Conference on Advanced Engineering Theory and Applications. Springer, pp. 324–333.
Triki, Z., Levorato, E., McNeely, W., Marshall, J., Bshary, R., 2019. Population densities predict forebrain size variation in the cleaner fish *Labroides dimidiatus*. Proc. R. Soc. B. 286, 20192108. https://doi.org/10.1098/rspb.2019.2108
Trudeau, V.L., Somoza, G.M., 2020. Multimodal hypothalamo-hypophysial communication in the vertebrates. General and Comparative Endocrinology 293, 113475. https://doi.org/10.1016/j.ygcen.2020.113475
Tsuboi, M., Husby, A., Kotrschal, A., Hayward, A., Buechel, S.D., Zidar, J., Løvlie, H., Kolm, N., 2015. Comparative support for the expensive tissue hypothesis: Big brains are correlated with smaller gut and greater parental investment in Lake Tanganyika cichlids. Evolution 69, 190–200. https://doi.org/10.1111/evo.12556
Tsuboi, M., Shoji, J., Sogabe, A., Ahnesjö, I., Kolm, N., 2016. Within species support for the expensive tissue hypothesis: a negative association between brain size and visceral fat

storage in females of the P acific seaweed pipefish. Ecol Evol 6, 647–655. https://doi.org/10.1002/ece3.1873
Turschwell, M.P., White, C.R., 2016. The effects of laboratory housing and spatial enrichment on brain size and metabolic rate in the eastern mosquitofish, *Gambusia holbrooki*. Biology Open 5, 205–210. https://doi.org/10.1242/bio.015024
Udagawa, S., Miyara, K., Takekata, H., Takeuchi, Y., Takemura, A., 2019. Investigation on the validity of 3D micro-CT imaging in the fish brain. Journal of Neuroscience Methods 328, 108416. https://doi.org/10.1016/j.jneumeth.2019.108416
Ullmann, J.F.P., Cowin, G., Collin, S.P., 2010. Quantitative Assessment of Brain Volumes in Fish: Comparison of Methodologies. Brain Behav Evol 76, 261–270. https://doi.org/10.1159/000321467
Ullmann, J.F.P., Cowin, G., Kurniawan, N.D., Collin, S.P., 2009. Magnetic resonance histology of the adult zebrafish brain: optimization of fixation and gadolinium contrast enhancement. NMR Biomed.. https://doi.org/10.1002/nbm.1465
umar6419, 2011. Humpback 3D model . URL https://free3d.com/3d-model/humpback-fish-50109.html (accessed 2.2.22).
Vallortigara, G., 2006. The evolutionary psychology of left and right: Costs and benefits of lateralization. Dev. Psychobiol. 48, 418–427. https://doi.org/10.1002/dev.20166
van Praag, H., Kempermann, G., Gage, F.H., 2000. Neural consequences of enviromental enrichment. Nat Rev Neurosci 1, 191–198. https://doi.org/10.1038/35044558
Vavrek, M.A., Elvidge, C.K., DeCaire, R., Belland, B., Jackson, C.D., Brown, G.E., 2008. Disturbance cues in freshwater prey fishes: do juvenile convict cichlids and rainbow trout respond to ammonium as an 'early warning' signal? Chemoecology 18, 255–261. https://doi.org/10.1007/s00049-008-0412-5
Vega-Trejo, R., Vila-Pouca, C., Mitchell, D.J., Kotrschal, A., 2022. Predation impacts brain allometry in female guppies (*Poecilia reticulata*). Evol Ecol. https://doi.org/10.1007/s10682-022-10191-8
Versteeg, E.J., Fernandes, T., Guzzo, M.M., Laberge, F., Middel, T., Ridgway, M., McMeans, B.C., 2021. Seasonal variation of behavior and brain size in a freshwater fish. Ecol Evol 11, 14950–14959. https://doi.org/10.1002/ece3.8179
Vindas, M.A., Gorissen, M., Höglund, E., Flik, G., Tronci, V., Damsgård, B., Thörnqvist, P.-O., Nilsen, T.O., Winberg, S., Øverli, Ø., Ebbesson, L.O.E., 2017a. How do individuals cope with stress? Behavioural, physiological and neuronal differences between proactive and reactive coping styles in fish. Journal of Experimental Biology jeb.153213. https://doi.org/10.1242/jeb.153213
Vindas, M.A., Magnhagen, C., Brännäs, E., Øverli, Ø., Winberg, S., Nilsson, J., Backström, T., 2017b. Brain cortisol receptor expression differs in Arctic charr displaying opposite coping styles. Physiology & Behavior 177, 161–168. https://doi.org/10.1016/j.physbeh.2017.04.024
Vinterstare, J., Hulthén, K., Nilsson, D.E., Nilsson, P.A., Brönmark, C., 2020. More than meets the eye: Predator-induced pupil size plasticity in a teleost fish. J Anim Ecol 89, 2258–2267. https://doi.org/10.1111/1365-2656.13303
Vollestad, L.A., Varreng, K., Poleo, A.B.S., 2004. Body depth variation in crucian carp *Carassius carassius*: an experimental individual-based study. Ecology Freshwater Fish 13, 197–202. https://doi.org/10.1111/j.1600-0633.2004.00048.x

Walsh, M.R., Broyles, W., Beston, S.M., Munch, S.B., 2016. Predator-driven brain size evolution in natural populations of Trinidadian killifish (*Rivulus hartii*). Proc. R. Soc. B. 283, 20161075. https://doi.org/10.1098/rspb.2016.1075

Watz, J., Aldvén, D., Andreasson, P., Aziz, K., Blixt, M., Calles, O., Lund Bjørnås, K., Olsson, I., Österling, M., Stålhammar, S., Tielman, J., Piccolo, J.J., 2022. Atlantic salmon in regulated rivers: Understanding river management through the ecosystem services lens. Fish and Fisheries 23, 478–491. https://doi.org/10.1111/faf.12628

Webster, M., Sheets, H.D., 2010. A Practical Introduction to Landmark-Based Geometric Morphometrics. Paleontol. Soc. pap. 16, 163–188. https://doi.org/10.1017/S1089332600001868

Weinhardt, V., Shkarin, R., Wernet, T., Wittbrodt, J., Baumbach, T., Loosli, F., 2018. Quantitative morphometric analysis of adult teleost fish by X-ray computed tomography. Sci Rep 8, 16531. https://doi.org/10.1038/s41598-018-34848-z

Weisbecker, V., 2012. Distortion in formalin-fixed brains: using geometric morphometrics to quantify the worst-case scenario in mice. Brain Struct Funct 217, 677–685. https://doi.org/10.1007/s00429-011-0366-1

White, Gemma E., Brown, C., 2015. Variation in Brain Morphology of Intertidal Gobies: A Comparison of Methodologies Used to Quantitatively Assess Brain Volumes in Fish. Brain Behav Evol 85, 245–256. https://doi.org/10.1159/000398781

White, Gemma E, Brown, C., 2015. Microhabitat Use Affects Brain Size and Structure in Intertidal Gobies. Brain, Behavior and Evolution 85, 107–116.

Wilkinson, G.M., Walter, J., Fleck, R., Pace, M.L., 2020. Beyond the trends: The need to understand multiannual dynamics in aquatic ecosystems. Limnol Oceanogr Letters 5, 281–286. https://doi.org/10.1002/lol2.10153

Wilson, A.D.M., McLaughlin, R.L., 2010. Foraging behaviour and brain morphology in recently emerged brook charr, *Salvelinus fontinalis*. Behav Ecol Sociobiol 64, 1905–1914. https://doi.org/10.1007/s00265-010-1002-4

Wiper, M.L., Britton, S., Higgs, D.M., 2014. Early experience and reproductive morph both affect brain morphology in adult male Chinook salmon (*Oncorhynchus tshawytscha*). Can. J. Fish. Aquat. Sci. 71, 1430–1436. https://doi.org/10.1139/cjfas-2013-0624

Wisenden, B., 2008. Active space of chemical alarm cue in natural fish populations. Behav 145, 391–407. https://doi.org/10.1163/156853908783402920

Wisenden, B.D., Binstock, C.L., Knoll, K.E., Linke, A.J., Demuth, B.S., 2010. Risk-sensitive information gathering by cyprinids following release of chemical alarm cues. Animal Behaviour 79, 1101–1107. https://doi.org/10.1016/j.anbehav.2010.02.004

Wisenden, B.D., Rugg, M., Korpi, N., Fuselier, L., 2009. Lab and field estimates of active time of chemical alarm cues of a cyprinid fish and an amphipod crustacean. Behav 146, 1423–1442. https://doi.org/10.1163/156853909X440998

Wong, R.Y., French, J., Russ, J.B., 2019. Differences in stress reactivity between zebrafish with alternative stress coping styles. R. Soc. open sci. 6, 181797. https://doi.org/10.1098/rsos.181797

Wulfsohn, D., Gundersen, H.J.G., Vedel Jensen, E.B., Nyengaard, J.R., 2004. Volume estimation from projections. J Microsc 215, 111–120. https://doi.org/10.1111/j.0022-2720.2004.01358.x

Xu, C., He, Y., Khannan, N., Parra, A., Boushey, C., Delp, E., 2013. Image-based food volume estimation, in: Proceedings of the 5th International Workshop on Multimedia for Cooking & Eating Activities - CEA '13. Presented at the the 5th international workshop, ACM Press, Barcelona, Spain, pp. 75–80. https://doi.org/10.1145/2506023.2506037

Yamamoto, N., 2009. Studies on the teleost brain morphology in search of the origin of cognition: Teleost brain morphology. Japanese Psychological Research 51, 154–167. https://doi.org/10.1111/j.1468-5884.2009.00397.x

Ye, C., Xu, S., Hu, Q., Hu, M., Zhou, L., Qin, X., Jia, J., Hu, G., 2020. Structure and function analysis of various brain subregions and pituitary in grass carp (*Ctenopharyngodon idellus*). Comparative Biochemistry and Physiology Part D: Genomics and Proteomics 33, 100653. https://doi.org/10.1016/j.cbd.2019.100653

Yin, L., Liu, H., Cui, H., Chen, B., Li, L., Wu, F., 2019. Impacts of polystyrene microplastics on the behavior and metabolism in a marine demersal teleost, black rockfish (*Sebastes schlegelii*). Journal of Hazardous Materials 380, 120861. https://doi.org/10.1016/j.jhazmat.2019.120861

Yokoyama, Y., Yamada, Y., Kosugi, K., Yamada, M., Narita, K., Nakahara, T., Fujiwara, H., Toda, M., Jinzaki, M., 2021. Effect of gravity on brain structure as indicated on upright computed tomography. Sci Rep 11, 392. https://doi.org/10.1038/s41598-020-79695-z

Zaaf, A., Herrel, A., Aerts, P., De Vree, F., 1999. Morphology and morphometrics of the appendicular musculature in geckoes with different locomotor habits (Lepidosauria). Zoomorphology 119, 9–22. https://doi.org/10.1007/s004350050077

Zandonà, E., Dalton, C.M., El-Sabaawi, R.W., Howard, J.L., Marshall, M.C., Kilham, S.S., Reznick, D.N., Travis, J., Kohler, T.J., Flecker, A.S., Thomas, S.A., Pringle, C.M., 2017. Population variation in the trophic niche of the Trinidadian guppy from different predation regimes. Sci Rep 7, 5770. https://doi.org/10.1038/s41598-017-06163-6

Závorka, L., Koeck, B., Armstrong, T.A., Soğanci, M., Crespel, A., Killen, S.S., 2020. Reduced exploration capacity despite brain volume increase in warm acclimated common minnow. Journal of Experimental Biology jeb.223453. https://doi.org/10.1242/jeb.223453

Závorka, L., Wallerius, M.L., Kainz, M.J., Höjesjö, J., 2021. Linking brain size in wild stream-dwelling brown trout with dietary supply of omega-3 fatty acids. https://doi.org/10.22541/au.163407473.35960551/v2

Zelditch, M.L., Swiderski, D.L., Sheets, H.D., 2012. Geometric morphometrics for biologists: a primer., 2nd ed. Academic Press.

Zhang, Z., Zhang, Xuemei, Li, Z., Zhang, Xiumei, 2019. Effects of different levels of environmental enrichment on the sheltering behaviors, brain development and cortisol levels of black rockfish *Sebastes schlegelii*. Applied Animal Behaviour Science 218, 104825. https://doi.org/10.1016/j.applanim.2019.06.006

Ziegler, A., Kunth, M., Mueller, S., Bock, C., Pohmann, R., Schröder, L., Faber, C., Giribet, G., 2011. Application of magnetic resonance imaging in zoology. Zoomorphology 130, 227–254. https://doi.org/10.1007/s00435-011-0138-8

Zippel, H.P., Hofmann, M., Meyer, D.L., Zeman, S., 1993. Functional and morphological regeneration of olfactory tracts and subtracts in goldfish. J Comp Physiol A 172, 91–99. https://doi.org/10.1007/BF00214718

Zotero, (2011). GitHub repository. Retrieved from https://github.com/zotero/zotero

Zupanc, G.K.H., 2008. Adult neurogenesis and neuronal regeneration in the brain of teleost fish. Journal of Physiology-Paris 102, 357–373. https://doi.org/10.1016/j.jphysparis.2008.10.007
Zupanc, G.K.H., 2006. Neurogenesis and neuronal regeneration in the adult fish brain. J Comp Physiol A 192, 649–670. https://doi.org/10.1007/s00359-006-0104-y

Appendix A: Supplementary materials for Chapter 1

Table A – Intraspecific comparisons of teleost brain morphology published between 2001-2021; Comparison (Comp.): abiotic environment (AB), biotic environment (BI), ecotype (EC), endogenous factor (EN), environmental enrichment (EN), genetics (GE), habitats (HA), methodology (MT), rearing conditions (RC), season (SE), sex (SX), various (V); Type (of study): between populations (BP), within population (WP), experimental treatment (EX), wild caught versus captive (WC), common garden (CG), optimization (OP); Method (MTH): area (Ar), ellipsoid (EL), dry mass (DM), wet mass (WM), Histology (Hi), magnetic resonance imaging (MRI), computerized tomography (CT), morphometrics (M) – centroid size (cs), shape (s)

Species	Comp	Type	MTH	C_1	C_2	WB	OB	TE	OT	CE	HY	PT	MO	Notes	Ref.
Bathygobius cocosensis (Cocos frillgoby)	MT	OP	Va (mm^3)	-	-	≠	≠	≠	≠	≈	≈	≠	≠		1
Bathygobius krefftii (Krefft's frillgoby)	MT			-	-	≠	≠	≠	≠	≈	≈	≠	≠		1
Chrosomus eos (Redbelly dace)	BI	EX	Ar (mm^2)	pred. cues	controls	↑	↑	≈	↑	≈	-	-	-		2
	V	WC		wild	captive	-	-	-	-	-	↑*	-	-	*l more symmetric	3
Colossoma macropomum (Cachama)	ER	EX	Hi (mm^3)	enriched	simple	-	-	≈	≈	-	-	-	-		4
Coregonus clupeaformis (Lake Whitefish)	GE	WP	WM (g)	dwarf	normal	↑*	-	-	-	-	-	-	-	*controlled for body size	5
Danio rerio (Zebrafish)	ER	EX	MRI (mm^3)	enriched	simple	↑	-	↑*	-	-	-	-	-	*absolute size	6
				enriched	simple	-	-	-	-	-	-	-	-	chased with net	6
	MT	OP	Ar (mm^2)	brain in-situ	brain excised	≈	-	≈	≈	≈	-	-	-		7
Diplodus sargus (White Seabream)	EN	BP	EL (mm^3)	MeHg (water, 2 µg / L)	controls	-	-	-	≈	↓*	≈	-	-	*at 7 days, not evident at 14 days	8
		EX		MeHg (food, 8.7 µg / g)	controls	-	-	-	≈	≈	↑*	-	-		9
Epinephelus malabaricus (Malabar grouper)	MT	OP	CT/Hi (mm^3)	CT	histology	≠	≠	≠	≠	≠	≠	≠	≠		10
Favonigobius lentiginosus (Eastern longfin)	MT		Va (mm^3)	-	-	≠	≠	≠	≠	≈	≈	≠	≠		11
Gadus morhua (Atlantic Cod)	HA	WC	DW (g)	wild	farm raised	↑*	-	-	-	-	-	-	-		12
Gambusia affinis (Western Mosquitofish)	HA	BP	EL (mm^3)	high temp /precipitation	low temp /precipitation	↓	↓	-	↓	↓	-	-	-	north-south climactic gradient	13
		CG	EL (mm^3)	wild	f1/f2	↕	↕	↕	↕	≈	↕	-	-	varied with population	13
Gambusia holbrooki (Eastern mosquitofish)	ER	WC	Ar (mm^2)	enriched	simple	↓	-	-	-	-	-	-	-		14
	V		Ar (mm^2)	in lab < 2 wks.	in lab 6 wks.	↑	-	-	-	-	-	-	-		14

Species	Comp.	Type	MTH	C_1	C_2	WB	OB	TE	OT	CE	HY	PT	MO	Notes	Ref.
Gambusia hubbsi (Bahamas mosquitofish)	HA	BP	Ar (mm^2)	high complexity	low complexity	≈	-	≈	↑	↑	-	-	-		15
	SX			female	male	↑	-	↑	≈	↑	-	-	-		15
Gasterosteus aculeatus (Threespine Stickleback)	BI	EX	Ar (mm^2)	F2/F32 (post live pred.)	f2/f32 controls	↓	≈	↓	↓	≈	-	-	-	pond raised	16
				F3/F33 hybrids (pred.)	f3/f33 controls	↓	≈	≈	↓	≈	≈	-	-	ancestral predation, lab raised	16
	EC	BP	M (cs)	benthic	generalists	-	-	↓	-	-	-	-	-		17
			M (sh)	benthic/sea run	generalists	-	-	≠	-	-	-	-	-		17
			M (cs)	benthic feeders	limnetic feeders	-	-	↑	-	-	-	-	-		18
			M (sh)	benthic feeders	limnetic and sea-run	-	-	≠	-	-	-	-	-	benthic TE was rounder and less triangular	18
			MRI (mm^3)	benthic feeders	limnetic feeders	↑	↑	-	↓	-	-	-	-		19
	EN		EL (mm^3)	non-breeding	pre-breeding	↓	≈	↓	≈	↑	≈	-	≈		20
				pre-breeding	breeding	↓	↓	≈	≈	↓	≈	-	↓		20
	ER		EL (mm^3)	enriched	simple	≠	≠	≠	≠	≠	≠	≠	-	heritability study: large plastic component to brain architecture	21
		CG		enriched	simple	≈	-	-	≈	-	-	-	≈		22
		EX		enriched	simple	↑ *	↓ *	≈	≈	≈	≈	-	-	*males only	23
	HA	BP	M (cs)	lake fish	sea-run fish	-	-	↑	-	-	-	-	-		18
			WM (g)	lake populations	associated streams	↕	-	↕	↕	↕	-	-	-	variable 15 lake/stream sites	24
	SX	CG	WM (g)	females	male	↓	-	-	-	-	-	-	≈	'mud' and 'lava' morphs	25
		WP	M (cs)	female	male	-	-	↓	-	-	-	-	-		17
			M (sh)	female	male	-	-	≠	-	-	-	-	-		6
			WM (g)	female	male	↑	-	-	-	-	-	-	-	marine	26
				female	male	↓	-	-	-	-	-	-	-	"white" morph	26
			EL (mm^3)	female	male	↓	↑	≈	≈	≈	≈	-	≈		23
				female	male	↓	≈	↓	↓	↓	↓	-	-		22
				female	male	↓	≈	↓	≈	↓	≈	-	≈		20
	V	BP	M (sh)	wild caught freshwater	held in lab	-	-	≠	-	-	-	-	-	TE resembles lab bred morph	18
		WC	M(cs)	wild (lake)	lab bred (lake)	-	-	↑	-	-	-	-	-		18
				wild (sea-run)	lab bred (sea-run)	-	-	↓	-	-	-	-	-		18
				wild - freshwater	held in lab	-	-	↓	-	-	-	-	-		18
			M(sh)	wild - freshwater	held in lab	-	-	≈	-	-	-	-	-	TE resembles wild	18

Species	Comp.	Type	MTH	C_1	C_2	WB	OB	TE	OT	CE	HY	PT	MO	Notes	Ref.
Gnathonemus victoriae (Victoria stonebasher)	HA	BP	WM (g)	normoxia	hypoxia	↑	-	-	-	-	-	-	-	open-water vs swamp	27
Halichoeres trimaculatus (Threespot wrasse)	MT	OP	CT/Hi (mm^3)	CT	histology	≠	≠	≠	≠	≠	≠	≠	≠		10
Istigobius hoesei (Krefft's frillgoby)	MT	OP	Va	-	-	≠	≠	≠	≠	≈	≈	≠	≠	compares different methods	11
Labroides dimidiatus (Bluestreak cleaner wrasse)	V	BP	MRI (mm^3)	fish (1.6/100 m2)	fish (≤0.83/100 m2)	≈	≈	≈	≈	≈	↑ *	↑ *	-	* dien-cephelon	28
Lepomis gibbosus (Pumpkinseed sunfish)	EC	BP	EL (mm^3)	pelagic	littoral	↓	≈	≈	≈	≈	≈	-	-		29
		WP		pelagic ecotype	littoral ecotype	↓	≈	≈	≈	≈	≈	-	-		30
			WM (g)	pelagic ecotype	littoral ecotype	↓ *	≈	≈	≈	≈	≈	-	-		31
Lepomis macrochirus (Bluegill sunfish)	EC	BP	WM (g)	pelagic ecotype	littoral ecotype	≈	≈	↑	≈	≈	≈	-	-		31
			EL (mm^3)	pelagic	littoral	≈	≈	↑	≈	≈	≈	-	-		29
Lipophrys pholis (Shanty)	SX	WP	Hi (mm^3)	female	male	-	≈	↓ *	-	-	-	-	-	* dorsalis telencephali (TE)	32
Liza aurata (Wolden grey mullet)	EN	BP	EL (mm^3)	Hg+ site	Hg- site	-	-	≈ *	↑	↑	≈	-	-	*lateral pallium (TE)	9
	SE	WP	EL (mm^3)	summer Hg+	winter Hg+	-	-	≈ *	↑	↑	≈	-	-		9
				summer Hg-	winter Hg-	-	-	↓ *	≈	≈	≈	-	-		9
Neogobius melanostomus (Round Goby)	EN		WM (g)	reproductive	not reproductive	-	-	↑	-	-	-	-	-		33
	SE	BP		caught in June	caught in October	-	-	↑	-	-	-	-	-		33
Neolamprologus pulcher (Daffodil Cichlid)	HA	EX	EL (mm^3)	small group	large group	≈	≈	≈	↑	↓	↓	-	≈		34
				small group	large group	≈	≈	≈	↓	↑	↑	-	≈		34
Oncorhynchus kisutch (Coho Salmon)	ER		Hi (mm^3)	enriched	simple	-	-	≈ *	-	-	-	-	-	*controlling for body size	35
	GE	CG	EL (mm^3)	transgenic	wild type	↑	≈	↓	≈	↑	≈	-	≈		36
	HA	BP		hatchery	stream	↑	≈	↑	≈	≈	≈	-	≈		36
Oncorhynchus mykiss (Rainbow Trout)	ER	EX	Hi (mm^3)	enriched	hatchery	-	≈	≈ *	-	-	-	-	-	*controlling for body size	37
				enriched	hatchery	≈	≈	↑	≈	↑	≈	-	-		38
	HA	CG	EL (mm^3)	domesticated lines	wild-caught	↑	↑	≈	≈	≈	≈	-	-		39
				semi-wild	wild / domesticated	≈	≈	≈	≈	≈	≈	-	-	intermediary results	39
		WC	L&W (mm)	hatchery	wild	-	-	↓ *	↓ *	↓ *	-	-	-	*length or width	40

Species	Comp.	Type	MTH	C_1	C_2	WB	OB	TE	OT	CE	HY	PT	MO	Notes	Ref.
Oncorhynchus tshawytscha (Chinook salmon)	EN	WP	M/EL (g/mm^3)	hooknoses	jacks	↓*	-	↑	≈	≈	-	-	-	*correcting for body size	41
	ER	EX	Hi (mm^3)	enriched	hatchery	≈	↓*	≈	-	-	-	-	-	*absolute size	38
	GE		Ar (mm^2)	less inbred	more inbred	≈	-	-	-	≈*	-	-	-	*CE more lateralized (L/R)	41
	HA	WC	Hi (mm^3)	lab	wild	↓	≈	↓*	-	↓*	-	-	-		38
	RC	EX	M/EL (g/mm^3)	released & recaptured	hatchery	↑*	-	≈	≈	≈	-	-	-	*correcting for body size	41
Oryzias latipes (Medaka)	GE	BP	Hi (mm^3)	eyeless mutant	controls	≈	≈	≈	↓	≈	↓	↓	-		42
Parablennius parvicornis (Barramundi)	MT	OP	Va	comparison		≠	≠	≠	≠	≠	≠	≠	-		43
Parablennius parvicornis (Azorean rock-pool blenny)	SX	EX	Hi (mm^3)	female	male	-	≈	↑*	-	-	-	-	-	*dorsalis telencephali lateralis	11
Paralichthys olivaceus (Bastard halibut)	MT	OP	CT/Hi (mm^3)	CT	histology	≠	≠	≠	≠	≠	≠	≠	≠		10
Perissodus microlepis (Rusosuomunsyöjä)	EN	WP	EL (mm^3)	laterality index (-1 to 1)	ratio of left to right volume	→	-	≈	→	-	≈	-	-	right side was larger	44
Petrocephalus catostoma (Churchill)	HA	BP	WM (g)	normoxia	hypoxia	↑	-	-	-	-	-	-	-	open-water vs swamp	27
Phoxinus phoxinus (Common minnow)	AB	EX	EL (mm^3)	cold acclimated	warm acclimated	↓	≈	≈	≈	≈	≈	-	↓		45
Poecilia mexicana (Shortfin Molly)	EC		L&W (mm)	surface dwelling	cave dwelling	-	-	↑	↑	≈	-	-	-		46
	HA	CG	EL (mm^3)	surface dwelling	cave dwelling	↑	↓	↓	↑	↓	≈	-	-		47
				female	male	↓	≈	≈	↓	↓	≈	-	-		47
Poecilia reticulata (Trinidadian Guppy)	BI	BP	Ar (mm^2)	high pred.	low pred.	-	-	≈	≈	-	-	-	-	females only	48
			WM (g)	high pred.	low pred.	↑*	-	-	-	-	-	-	-	males only	49
		CG	M/EL (g/mm^3)	high pred.	translocated to low	↓	≈	≈	≈	≈	≈	-	-	8+ years selection; 2 yrs in CG	50
		EX	EL (mm^3)	same sex pair	cross sex pair	↓	≈	≈	≈	≈	≈	-	≈	in males	51
				same sex pair	cross sex pair	≈	≈	≈	↑	≈	≈	-	≈	in females	51
			WM (g)	pred. cues	lab controls	↑*	-	-	-	-	-	-	-	*males only	49
	EN	WP	Ar (mm^2)	high hastiness	low hastiness	-	-	↓	≈	-	-	-	-		48
			EL (mm^3)	learning trials*	controls	≈	≈	≈	≈	≈	≈	-	≈	* reversal or spatial learning	52
	ER	EX	Ar (mm^2)	enriched	simple	≈	-	≈	≈	-	-	-	-	*females only	53

Species	Comp.	Type	MTH	C_1	C_2	WB	OB	TE	OT	CE	HY	PT	MO	Notes	Ref.
Poecilia reticulata (Trinidadian Guppy) cont.			EL (mm^3)	enriched spatial-learning environment	no enrichment	↑	≈	≈	↑	≈	≈	-	-		52
	HA	WC	Ar (mm^2)	F2 lab bred	wild	-	-	↓*	↓*	-	-	-	-	*females	48
				lab bred (F1)	wild	↓	-	↓	↓	-	-	-	-	*females	53
	SX	WP	EL (mm^3)	female	male	≈	↑	-	-	↑	-	-	≈		51
			M/EL (g/mm^3)	female	male	≈	↑	↑	↓	-	-	-	↑		50
Pseudocrenilabrus multicolor (Egyptian mouthbrooder)	AB	CG	WM (g)	hypoxia	normoxia	↓	-	-	-	-	-	-	-	rivers vs lakes	54
				hypoxia	normoxia	≈	-	-	-	-	-	-	-	swamp	54
				hypoxia	normoxia	↓	-	-	-	-	-	-	-	rivers vs lakes	55
Pterophyllum scalare (Angelfish)	ER	EX	Hi (mm^3)	enriched	simple	-	-	≈	≈	-	-	-	-		56
Pungnitus pungnitus (Nine spine stickleback)	AB		EL (mm^3)	visually restricted (black dye)	visually unrestricted	≈	↑	≈	↓	≈	-	-	≈		57
	BI	CG		F1 - pred. cues	controls	≈	↑	≈	≈	≈	↓	-	-	freshwater	58
				F1 - pred. cues	controls	≈	≈	≈	≈	≈	↓	-	-	marine	58
		EX		individually reared	group rearing	↑	↑	≈	↓	≈	≈	-	-		59
				individually reared	group rearing	↓	↑	≈	↓	≈	≈	-	-		59
	HA	BP		freshwater ponds	marine	↑	-	↓	-	-	-	-	-		60
		CG		pond (F1)	marine (F1)	≈	↑	↑	-	≈	-	-	-		61
		WC		freshwater ponds	lab bred	↑	-	↑	↑	↑	↑	-	-		60
	SX	WP		female	male	≠	≠	≠	≈	≈	≠	-	-	reported not discussed	58
				female	male	↓	≈	≈	≈	≈	≈	≈	↓		57
Rivulus hartii (Trinidadian killifish)	BI	CG	WM (g)	F2 (high pred.)	f2 (low pred.)	↓*	-	-	↓*	-	-	-	-	*males only; OT length	62
				strong ancestral pred.	weak ancestral pred.	↓	-	-	-	-	-	-	-	F1	63
	HA			F2 (strong pred.)	f2 (weak pred.)	≈	-	-	-	-	-	-	-		64
	V	EX		high food	low food	↑	-	-	-	-	-	-	-	relative brain size	64
				high food	low food	↓	-	-	-	-	-	-	-	absolute brain size	64

Species	Comp.	Type	MTH	C_1	C_2	WB	OB	TE	OT	CE	HY	PT	MO	Notes	Ref.
Salmo salar (Atlantic Salmon)	BI		DW (g)	high density (1500/m2)	low density (500/m2)	≈	-	↑	-	↑	-	-	-		65
			M (sh)	pred. cues	controls	≈ *	≈	≈	↓	≈	-	-	-	*different shape	2
	EN	WP	EL (mm^3)	sneaker males	females / anadromous	↑	≈	↑	≈	↑	≈	-	↑		66
	ER	EX	Ar (mm^2)	enriched	hatchery	≈		≈	≈	≈	-	-	-		67
				enriched	hatchery	≈		≈	≈	≈	-	-	-		67
				enriched	hatchery	≈		≈	≈	≈	-	-	-		67
			DW (g)	enriched	simple	-	-	-	-	≈	-	-	-	CE only	68
	GE		EL (mm^3)	triploid	diploid	≈	↓	↑	≈	↑	≈	-	-		69
	HA		Ar (mm^2)	released	hatchery	↓		≈	≈	≈	-	-	-		67
	V		EL (mm^3)	ad libitum	restricted	↓	↓	≈	≈	≈	≈	-	-		18
				ad libitum feeding	restricted feeding	≈	≈	≈	≈	≈	≈	-	↑		66
			DW (g)	high density (150/m2)	low density (50/m2)	-	≈	-	≈	↑	≈	-	-		68
Salmo Trutta (Brown Trout)	BI	WP	EL (mm^3)	anadromous	precocious	↓	≈	≈	↑	≈	≈	-	-		70
	MT	OP	Ar (mm^2)	brain in-situ	brain excised	≈	-	≈	≈	≈	-	-	-		71
	SX	WP	EL (mm^3)	female	male	≈	≈	↓	≈	≈	≈	-	-		70
	V	EX	DW (g)	caught, starved & released	caught & released	≈	-	-	-	-	-	-	-		72
Salvelinus alpinus (Arctic charr)	EC	BP	EL (mm^3)	abyssal morph	other morphs	↓ *	↑	↓ *	↓ *	↓ *	↓ *	-	-	*absolute size	73
				piscivore/planktivore	other morphs	≈	≈	≈	↑ *	↑ *	≈	-	-	*absolute size;	73
Salvelinus confluentus (Bull trout)	ER	EX	MRI (mm^3)	enriched	simple	≈	-	≈	≈	≈	-	-	-		74
	HA	WC	MRI (mm^3)	raised in captivity	wild caught	≈	-	≈	≈	↓	-	-	-		74
Salvelinus fontinalis (Brook Charr)	EN	WP	Hi (mm^3)	move more	move less	-	-	↑ *	-	-	-	-	-	*controlled for body size	75

Species	Comp.	Type	MTH	C_1	C_2	WB	OB	TE	OT	CE	HY	PT	MO	Notes	Ref.
Salvelinus namaycush (Lake trout)	SE	BP	EL (mm^3)	fall/winter	spring/summer	↑	↑	↑	≈	↑	↑	-	-	*spring only	76
				spring	summer/fall/winter	↓	↓	↓	≈	↓	↓	-	-	*spring only	76
Sebastes schlegelii (Black rockfish)	EC		EL (mm^3)	no pelagic prey	pelagic prey	↕*	↑	↑	↑	↑	≈	-	-	*larger absolute, smaller relative	76
	EN		EL (mm^3)	many objects	few or no objects	≈	↑	≈	≈	≈	-	-	-		77
				few objects	many or no objects	≈	≈	≈	≈	↑	-	-	-		77
Seriola quinqueradiata (Yellowtail)	V		Hi (mm3)	control	OA, EPA and DHA	↑	-	-	↑	↑	-	-	-		78
				control and OA	EPA and DHA	↑	-	-	↓	↓	-	-	-		78
Syngnathus *schlegeli* (Pacific seaweed pipefish)	EN	WP	WM (g)	more visceral fat	less visceral fat	↑	-	-	-	-	-	-	-	body condition	79

References for Table A.1

1. White, G. E. & Brown, C. Variation in Brain Morphology of Intertidal Gobies: A Comparison of Methodologies Used to Quantitatively Assess Brain Volumes in Fish. *Brain Behav Evol* **85**, 245–256 (2015).
2. Joyce, B. J. & Brown, G. E. Rapid plastic changes in brain morphology in response to acute changes in predation pressure in juvenile Atlantic salmon (*Salmo salar*) and northern redbelly dace (*Phoxinus eos*). *Can. J. Zool.* **98**, 186–194 (2020).
3. Joyce, B. J. & Brown, G. E. Short-term captivity drives hypothalamic plasticity and asymmetry in wild-caught northern red bellied dace (Chrosomus eos). *J Fish Biol* **97**, 577–582 (2020).
4. Pereira, P. D. C. *et al.* Environmental Enrichment Improved Learning and Memory, Increased Telencephalic Cell Proliferation, and Induced Differential Gene Expression in Colossoma macropomum. *Front. Pharmacol.* **11**, 840 (2020).
5. Evans, M. L., Chapman, L. J., Mitrofanov, I. & Bernatchez, L. Variable extent of parallelism in respiratory, circulatory, and neurological traits across lake whitefish species pairs. *Ecol Evol* **3**, 546–557 (2013).
6. DePasquale, C., Neuberger, T., Hirrlinger, A. M. & Braithwaite, V. A. The influence of complex and threatening environments in early life on brain size and behaviour. *Proc. R. Soc. B.* **283**, 20152564 (2016).
7. Puga, S. *et al.* Unveiling the neurotoxicity of methylmercury in fish (*Diplodus sargus*) through a regional morphometric analysis of brain and swimming behavior assessment. *Aquatic Toxicology* **180**, 320–333 (2016).
8. Pereira, P. *et al.* Inorganic mercury accumulation in brain following waterborne exposure elicits a deficit on the number of brain cells and impairs swimming behavior in fish (white seabream—Diplodus sargus). *Aquatic Toxicology* **170**, 400–412 (2016).
9. Puga, S. *et al.* Brain morphometric profiles and their seasonal modulation in fish (Liza aurata) inhabiting a mercury contaminated estuary. *Environmental Pollution* **237**, 318–328 (2018).
10. Udagawa, S., Miyara, K., Takekata, H., Takeuchi, Y. & Takemura, A. Investigation on the validity of 3D micro-CT imaging in the fish brain. *Journal of Neuroscience Methods* **328**, 108416 (2019).
11. White, G. E. & Brown, C. Microhabitat Use Affects Brain Size and Structure in Intertidal Gobies. *Brain, Behavior and Evolution* **85**, 107–116 (2015).
12. Mayer, I. *et al.* Domestication causes rapid changes in heart and brain morphology in Atlantic cod (Gadus morhua). *Environ Biol Fish* **92**, 181–186 (2011).
13. Liu, M., Liu, Y., Wang, X. & Wang, H. Brain morphological adaptations of *Gambusia affinis* along climatic gradients in China. *J Zool Syst Evol Res* **59**, 2150–2160 (2021).
14. Turschwell, M. P. & White, C. R. The effects of laboratory housing and spatial enrichment on brain size and metabolic rate in the eastern mosquitofish, *Gambusia holbrooki*. *Biology Open* **5**, 205–210 (2016).

15. Jenkins, M. R. *et al.* Natural and anthropogenic sources of habitat variation influence exploration behaviour, stress response, and brain morphology in a coastal fish. *J Anim Ecol* **90**, 2446–2461 (2021).
16. Samuk, K., Xue, J. & Rennision, D. J. Exposure to predators does not lead to the evolution of larger brains in experimental populations of threespine stickleback: EXPERIMENTAL PREDATION AND BRAIN SIZE. *Evolution* **72**, 916–929 (2018).
17. Park, P. J. & Bell, M. A. Variation of telencephalon morphology of the threespine stickleback (*Gasterosteus aculeatus*) in relation to inferred ecology: Threespine stickleback telencephalon evolution. *Journal of Evolutionary Biology* **23**, 1261–1277 (2010).
18. Park, P. J., Chase, I. & Bell, M. A. Phenotypic plasticity of the threespine stickleback *Gasterosteus aculeatus* telencephalon in response to experience in captivity. *Current Zoology* **58**, 189–210 (2012).
19. Keagy, J., Braithwaite, V. A. & Boughman, J. W. Brain differences in ecologically differentiated sticklebacks. *Current Zoology* **64**, 243–250 (2018).
20. Buechel, S. D. *et al.* Variation in sexual brain size dimorphism over the breeding cycle in the three-spined stickleback. *Journal of Experimental Biology* **222**, jeb194464 (2019).
21. Noreikiene, K. *et al.* Quantitative genetic analysis of brain size variation in sticklebacks: support for the mosaic model of brain evolution. *Proc. R. Soc. B.* **282**, 20151008 (2015).
22. Toli, E. A., Noreikiene, K., DeFaveri, J. & Merilä, J. Environmental enrichment, sexual dimorphism, and brain size in sticklebacks. *Ecol Evol* **7**, 1691–1698 (2017).
23. Herczeg, G., Gonda, A., Balázs, G., Noreikiene, K. & Merilä, J. Experimental evidence for sex-specific plasticity in adult brain. *Front Zool* **12**, 38 (2015).
24. Ahmed, N. I., Thompson, C., Bolnick, D. I. & Stuart, Y. E. Brain morphology of the threespine stickleback (*Gasterosteus aculeatus*) varies inconsistently with respect to habitat complexity: A test of the Clever Foraging Hypothesis. *Ecology and Evolution.* 3372–3380 (2017) doi:10.1002/ece3.2918.
25. Kotrschal, A., Räsänen, K., Kristjánsson, B. K., Senn, M. & Kolm, N. Extreme Sexual Brain Size Dimorphism in Sticklebacks: A Consequence of the Cognitive Challenges of Sex and Parenting? *PLoS ONE* **7**, e30055 (2012).
26. Samuk, K., Iritani, D. & Schluter, D. Reversed brain size sexual dimorphism accompanies loss of parental care in white sticklebacks. *Ecol Evol* **4**, 3236–3243 (2014).
27. Chapman, L. J. & Hulen, K. G. Implications of hypoxia for the brain size and gill morphometry of mormyrid fishes. *J. Zoology* **254**, 461–472 (2001).
28. Triki, Z., Levorato, E., McNeely, W., Marshall, J. & Bshary, R. Population densities predict forebrain size variation in the cleaner fish *Labroides dimidiatus*. *Proc. R. Soc. B.* **286**, 20192108 (2019).
29. Axelrod, C. J., Laberge, F. & Robinson, B. W. Interspecific and intraspecific comparisons reveal the importance of evolutionary context in sunfish brain form divergence. *J Evol Biol* **34**, 639–652 (2021).
30. Axelrod, C. J., Laberge, F. & Robinson, B. W. Intraspecific brain size variation between coexisting sunfish ecotypes. *Proc. R. Soc. B.* **285**, 20181971 (2018).
31. Axelrod, C. J., Laberge, F. & Robinson, B. W. Isolating the effects of ontogenetic niche shift on brain size development using pumpkinseed sunfish ecotypes. *Evolution & Development* **22**, 312–322 (2020).
32. Costa, S. S. *et al.* Sex Differences in the Dorsolateral Telencephalon Correlate with Home Range Size in Blenniid Fish. *Brain Behav Evol* **77**, 55–64 (2011).
33. McCallum, E. S., Capelle, P. M. & Balshine, S. Seasonal plasticity in telencephalon mass of a benthic fish: seasonal plasticity in telencephalon mass. *J Fish Biol* **85**, 1785–1792 (2014).
34. Fischer, S., Bessert-Nettelbeck, M., Kotrschal, A. & Taborsky, B. Rearing-Group Size Determines Social Competence and Brain Structure in a Cooperatively Breeding Cichlid. *The American Naturalist* **186**, 123–140 (2015).
35. Lema, S. C., Hodges, M. J., Marchetti, M. P. & Nevitt, G. A. Proliferation zones in the salmon telencephalon and evidence for environmental influence on proliferation rate. *Comp Biochem Physiol A Mol Integr Physio* **141**, 327–335 (2005).
36. Kotrschal, A., Sundström, L. F., Brelin, D., Devlin, R. H. & Kolm, N. Inside the heads of David and Goliath: environmental effects on brain morphology among wild and growth-enhanced coho salmon *Oncorhynchus kisutch*. *Journal of Fish Biology* **81**, 987–1002 (2012).
37. Kihslinger, R. L., Lema, S. C. & Nevitt, G. A. Environmental rearing conditions produce forebrain differences in wild Chinook salmon *Oncorhynchus tshawytscha*. *Comparative Biochemistry and Physiology Part A: Molecular & Integrative Physiology* **145**, 145–151 (2006).

38. Kihslinger, R. L. & Nevitt, G. A. Early rearing environment impacts cerebellar growth in juvenile salmon. *Journal of Experimental Biology* **209**, 504–509 (2006).
39. Campbell, J. M., Carter, P. A., Wheeler, P. A. & Thorgaard, G. H. Aggressive Behavior, Brain Size and Domestication in Clonal Rainbow Trout Lines. *Behav Genet* **45**, 245–254 (2015).
40. Marchetti, M. P. & Nevitt, G. A. Effects of Hatchery Rearing on Brain Structures of Rainbow Trout, *Oncorhynchus mykiss*. *Environmental Biology of Fishes* **66**, 9–14 (2003).
41. Wiper, M. L., Britton, S. & Higgs, D. M. Early experience and reproductive morph both affect brain morphology in adult male Chinook salmon (*Oncorhynchus tshawytscha*). *Can. J. Fish. Aquat. Sci.* **71**, 1430–1436 (2014).
42. Ishikawa, Y. *et al.* Brain Structures of a Medaka Mutant, *el(eyeless)*, in Which Eye Vesicles Do Not Evaginate. *Brain, Behavior and Evolution* **58**, 173–184 (2001).
43. Ullmann, J. F. P., Cowin, G. & Collin, S. P. Quantitative Assessment of Brain Volumes in Fish: Comparison of Methodologies. *Brain Behav Evol* **76**, 261–270 (2010).
44. Lee, H. J. *et al.* Lateralized Feeding Behavior is Associated with Asymmetrical Neuroanatomy and Lateralized Gene Expressions in the Brain in Scale-Eating Cichlid Fish. *Genome Biology and Evolution* **9**, 3122–3136 (2017).
45. Závorka, L. *et al.* Reduced exploration capacity despite brain volume increase in warm acclimated common minnow. *Journal of Experimental Biology* jeb.223453 (2020) doi:10.1242/jeb.223453.
46. Schulz-Mirbach, T., Riesch, R., García de León, F. J. & Plath, M. Effects of extreme habitat conditions on otolith morphology – a case study on extremophile livebearing fishes (*Poecilia mexicana*, P. sulphuraria). *Zoology* **114**, 321–334 (2011).
47. Eifert, C. *et al.* Brain size variation in extremophile fish: local adaptation versus phenotypic plasticity: Brain size variation in extremophile fish. *J Zool* **295**, 143–153 (2015).
48. Burns, J. G. & Rodd, F. H. Hastiness, brain size and predation regime affect the performance of wild guppies in a spatial memory task. *Animal Behaviour* **76**, 911–922 (2008).
49. Reddon, A. R., Chouinard-Thuly, L., Leris, I. & Reader, S. M. Wild and laboratory exposure to cues of predation risk increases relative brain mass in male guppies. *Funct Ecol* **32**, 1847–1856 (2018).
50. Mitchell, D. J., Vega-Trejo, R. & Kotrschal, A. Experimental translocations to low predation lead to non-parallel increases in relative brain size. *Biol. Lett.* **16**, 20190654 (2020).
51. Kotrschal, A., Rogell, B., Maklakov, A. A. & Kolm, N. Sex-specific plasticity in brain morphology depends on social environment of the guppy, *Poecilia reticulata*. *Behav Ecol Sociobiol* **66**, 1485–1492 (2012).
52. Fong, S., Buechel, S. D., Boussard, A., Kotrschal, A. & Kolm, N. Plastic changes in brain morphology in relation to learning and environmental enrichment in the guppy (*Poecilia reticulata*). *Journal of Experimental Biology* jeb.200402 (2019) doi:10.1242/jeb.200402.
53. Burns, J. G., Saravanan, A. & Helen Rodd, F. Rearing Environment Affects the Brain Size of Guppies: Lab-Reared Guppies have Smaller Brains than Wild-Caught Guppies. *Ethology* **115**, 122–133 (2009).
54. Chapman, L., Albert, J. & Galis, F. Developmental Plasticity, Genetic Differentiation, and Hypoxia-induced Trade-offs in an African Cichlid Fish. *TOEVOLJ* **2**, 75–88 (2008).
55. Crispo, E. & Chapman, L. J. Geographic variation in phenotypic plasticity in response to dissolved oxygen in an African cichlid fish: Variation in plasticity in an African cichlid. *Journal of Evolutionary Biology* **23**, 2091–2103 (2010).
56. Diniz, D. G. *et al.* Environmental enrichment increases the number of telencephalic but not tectal cells of angelfish (Pterophyllum scalare): an exploratory investigation using optical fractionator. *Environ Biol Fish* **103**, 847–857 (2020).
57. Pike, T. W., Ramsey, M. & Wilkinson, A. Environmentally induced changes to brain morphology predict cognitive performance. *Phil. Trans. R. Soc. B* **373**, 20170287 (2018).
58. Gonda, A., Välimäki, K., Herczeg, G. & Merilä, J. Brain development and predation: plastic responses depend on evolutionary history. *Biol. Lett.* **8**, 249–252 (2012).
59. Gonda, A., Herczeg, G. & Merilä, J. Habitat-dependent and -independent plastic responses to social environment in the nine-spined stickleback (*Pungitius pungitius*) brain. *Proc. R. Soc. B.* **276**, 2085–2092 (2009).
60. Gonda, A., Herczeg, G. & Merilä, J. Population variation in brain size of nine-spined sticklebacks (*Pungitius pungitius*) - local adaptation or environmentally induced variation? *BMC Evol Biol* **11**, 75 (2011).
61. Gonda, A., Herczeg, G. & Merilä, J. Adaptive brain size divergence in nine-spined sticklebacks (*Pungitius pungitius*)? *Journal of Evolutionary Biology* **22**, 1721–1726 (2009).

62. Walsh, M. R., Broyles, W., Beston, S. M. & Munch, S. B. Predator-driven brain size evolution in natural populations of Trinidadian killifish (*Rivulus hartii*). *Proc. R. Soc. B.* **283**, 20161075 (2016).
63. Dunlap, K. D., Corbo, J. H., Vergara, M. M., Beston, S. M. & Walsh, M. R. Predation drives the evolution of brain cell proliferation and brain allometry in male Trinidadian killifish, *Rivulus hartii*. *Proc. R. Soc. B.* **286**, 20191485 (2019).
64. Beston, S. M., Broyles, W. & Walsh, M. R. Increased juvenile predation is not associated with evolved differences in adult brain size in Trinidadian killifish (*Rivulus hartii*). *Ecol Evol* **7**, 884–894 (2017).
65. Näslund, J., Larsen, M. H., Thomassen, S. T., Aarestrup, K. & Johnsson, J. I. Environment-dependent plasticity and ontogenetic changes in the brain of hatchery-reared Atlantic salmon. *J Zool* **301**, 75–82 (2017).
66. Kotrschal, A. *et al.* The mating brain: early maturing sneaker males maintain investment into the brain also under fast body growth in Atlantic salmon (*Salmo salar*). *Evol Ecol* **28**, 1043–1055 (2014).
67. Näslund, J., Aarestrup, K., Thomassen, S. T. & Johnsson, J. I. Early enrichment effects on brain development in hatchery-reared Atlantic salmon (*Salmo salar*): no evidence for a critical period. *Can. J. Fish. Aquat. Sci.* **69**, 1481–1490 (2012).
68. Näslund, J., Rosengren, M. & Johnsson, J. I. Fish density, but not environmental enrichment, affects the size of cerebellum in the brain of juvenile hatchery-reared Atlantic salmon. *Environ Biol Fish* **102**, 705–712 (2019).
69. Fraser, T. W. K., Fjelldal, P. G., Skjaeraasen, J. E., Hansen, T. & Mayer, I. Triploidy alters brain morphology in pre-smolt Atlantic salmon ***Salmo salar*** : possible implications for behaviour. *Journal of Fish Biology* **81**, 2199–2212 (2012).
70. Kolm, N., Gonzalez-Voyer, A., Brelin, D. & Winberg, S. Evidence for small scale variation in the vertebrate brain: mating strategy and sex affect brain size and structure in wild brown trout (*Salmo trutta*). *Journal of Evolutionary Biology* **22**, 2524–2531 (2009).
71. Näslund, J. A simple non-invasive method for measuring gross brain size in small live fish with semi-transparent heads. *PeerJ* **2**, e586 (2014).
72. Näslund, J. Relative Mass of Brain- and Intestinal Tissue in Juvenile Brown Trout: No Long-Term Effects of Compensatory Growth; with Additional Notes on Emerging Sex-Differences. *Fishes* **3**, 38 (2018).
73. Peris Tamayo, A., Devineau, O., Præbel, K., Kahilainen, K. K. & Østbye, K. A brain and a head for a different habitat: Size variation in four morphs of Arctic charr (*Salvelinus alpinus* (L.)) in a deep oligotrophic lake. *Ecol Evol* **10**, 11335–11351 (2020).
74. Brignon, W. R. *et al.* Rearing environment influences boldness and prey acquisition behavior, and brain and lens development of bull trout. *Environ Biol Fish* **101**, 383–401 (2018).
75. Wilson, A. D. M. & McLaughlin, R. L. Foraging behaviour and brain morphology in recently emerged brook charr, Salvelinus fontinalis. *Behav Ecol Sociobiol* **64**, 1905–1914 (2010).
76. Versteeg, E. J. *et al.* Seasonal variation of behavior and brain size in a freshwater fish. *Ecol Evol* **11**, 14950–14959 (2021).
77. Zhang, Z., Zhang, X., Li, Z. & Zhang, X. Effects of different levels of environmental enrichment on the sheltering behaviors, brain development and cortisol levels of black rockfish Sebastes schlegelii. *Applied Animal Behaviour Science* **218**, 104825 (2019).
78. Ishizaki, Y. *et al.* The effect of dietary docosahexaenoic acid on schooling behaviour and brain development in larval yellowtail. *Journal of Fish Biology* **58**, 1691–1703 (2001).
79. Tsuboi, M. *et al.* Comparative support for the expensive tissue hypothesis: Big brains are correlated with smaller gut and greater parental investment in Lake Tanganyika cichlids. *Evolution* **69**, 190–200 (2015).

Appendix B: Abstract for Chapter 2

Abstract

Teleosts exhibit inter- and intra-specific variation in the size and shape of their brains. Interpopulation differences in gross brain morphology among numerous teleost fish species have been observed and have been partially attributed to plastic changes in response to their environment, including predation. These differences manifest themselves macroscopically, potentially because teleosts retain the capacity for active neuroproliferation into adulthood. Building on previous work, showing chronic exposure to predation can affect brain morphology, we sought to determine whether these differences manifest themselves on a time scale shown to induce phenotypically plastic behavioural changes. In separate trials, we held northern redbelly dace (Phoxinus eos (Cope, 1861) = Chrosomus eos Cope, 1861) and juvenile Atlantic salmon (Salmo salar Linnaeus, 1758) in semi-natural conditions and exposed them to conspecific skin extract as a proxy for predation risk over 2 weeks. After exposure, their brains were excised, photographed, and analyzed for size (multivariate ANOVA) and shape (Procrustes ANOVA). Despite their brief exposure to simulated predation pressure, subjects from both species developed significantly different brain morphologies. Compared with controls, the Atlantic salmon exhibited a different brain shape and smaller optic tecta, whereas the northern redbelly dace had larger brains with more developed olfactory bulbs and optic tecta. Our results highlight the rapidity with which external environment can alter patterns of growth in the brain.

Appendix C: Abstract for Chapter 3

Abstract

Teleost fish are neuroplastic and are known to alter their brain morphology and behaviour in response to environmental change such as an increase in predation pressure. The hypothalamus plays a key role in regulating behavioural responses to predation risk. In this study, wild-caught northern red bellied dace (*Chrosomus eos*) developed smaller and less symmetric hypothalami when held in captivity for 14 days; both measures correlated with boldness in a latency to emerge test. This study's results highlight the potential impact of short-term holding conditions on brains and behaviour

Appendix D: Abstract for Chapter 4

Abstract

Neuroplasticity enables teleosts to promote or downregulate the growth of their brains regionally. To compensate for the effects of predation pressure, teleosts may alter their brain morphology and behavioral responses to mitigate its impact on individual fitness. High-predation environments often promote specific patterns of brain growth and produce bolder and more proactive populations. Owing to the expense of maintaining neural tissue, relative size indicates the regions most relied upon. In northern redbelly dace *Chrosomus eos*, as little as 2 weeks of elevated predation pressure, resulted in increased investment in their olfactory bulbs and optic tecta, while the imposition of captivity produced smaller, less symmetric hypothalami. Taken together, these results suggest that an individual could potentially become better able to detect a threat, and simultaneously less inclined to react to it, making the impact of either change in isolation is difficult to discern. Here, we compared interindividual variation in gross brain morphology, risk-taking tactics in a novel arena (shy–bold personality), and responding to olfactory cues (proactive/reactive stress-coping style). We hypothesized that olfactory investment would positively correlate with response intensity to predator cue concentration and respond across a wider range of cue concentrations, while hypothalamus size would correlate with shyness and reactivity. Exposure to heightened risk produced more bold/proactive individuals, with larger olfactory bulbs and smaller hypothalami. However, the direction of the correlation between hypothalamus size and behavior varied by treatment, and olfactory investment only corresponded with response intensity amongst proactive individuals. Our findings illustrate the potential pitfalls of relating gross brain morphology to complex behavior and suggest that stress-coping style is a relevant consideration in future studies.

Appendix E: Abstract and Supplementary materials for Chapter 5

Abstract

The volume of a biological structure may be estimated from photographs using its apparent cross-sectional area (ACA), or by measuring its dimensions from orthogonal viewpoints and treating it as an ellipsoid. With ACA half as many photographs are required to achieve results comparable to the ellipsoid method (EM); potentially simplifying data collection by reducing specimen handling time. ACA also facilitates the collection of additional morphological data for analyzing the shape of specimens using geometric morphometrics. To characterize ACA's performance relative to EM, we carried out *in-silico* validations of ACA versus EM using virtual objects of known volume; first using a diversified set of 21 common objects, and subsequently, a set of 9 echinoderms scanned from wild-type specimens. The volume of each object was estimated twice, using pairs of images with orthogonal viewpoints. The relative and absolute performance (percent error) of both methods were evaluated. ACA performed comparably to EM across a broad range of object shapes and sizes. Both methods were sensitive to objects with low solidity and performed equally well for approximate spheres with high solidity. ACA tended to work as well or better than EM for objects with low circularity. Notably, in most cases, averaged ACA values also produced satisfactory or superior results relative to EM. Our results suggest that ACA represents a viable alternative to EM for estimating the volume of biological structures, especially those which deviate substantially from an ellipsoid form. Awareness of ACA's applications and limitations, coupled with its ease of implementation, may encourage the inclusion of morphological metrics in experimental designs.

Table E.1 - the distribution of methods for brain volume estimation used to study gross brain morphology in lower vertebrates published from 2020-2022

Method	Percentage	Reference
Photographic (2D Area)	17%	8, 9, 10, 15, 20
Photographic (Elliptical)	53%	1, 6, 11-14, 17, 19, 21-22, 24-26, 28, 29, 30
Weight	20%	2, 3, 7, 16, 23, 27
Histology	3%	18, 27
Computerized Tomography	2%	4, 5

We looked for intraspecific studies involving externally visible gross brain morphology in lower vertebrates. Using Web of Science and Google Scholar we searched using “brain morphology” along with the terms: “fish”, “teleost”, “shark”, “anuran”, “amphibian”, and “reptile”; published between January 2020 and April 2022. Based on titles and abstracts 30 papers were identified, of which 21 used some form of photographic volume estimation; 16 used the elliptical method while another 5 used some form of ACA.

Table E1 References

1. Abrahão, V. P., Ballen, G. A., Pastana, M. N. L., & Shibatta, O. A. (2021). Ontogeny of the brain of Microglanis garavelloi Shibatta and Benine 2005 (Teleostei: Siluriformes: Pseudopimelodidae). Journal of Morphology, 282(4), 489–499. https://doi.org/10.1002/jmor.21321
2. Axelrod, C. J., Laberge, F., & Robinson, B. W. (2020). Isolating the effects of ontogenetic niche shift on brain size development using pumpkinseed sunfish ecotypes. Evolution & Development, 22, 312–322. https://doi.org/10.1111/ede.12333
3. Axelrod, C. J., Laberge, F., & Robinson, B. W. (2021). Interspecific and intraspecific comparisons reveal the importance of evolutionary context in sunfish brain form divergence. Journal of Evolutionary Biology, 34(4), 639–652. https://doi.org/10.1111/jeb.13763
4. Camilieri-Asch, V., Shaw, J. A., Mehnert, A., Yopak, K. E., Partridge, J. C., & Collin, S. P. (2020). diceCT: A Valuable Technique to Study the Nervous System of Fish. Eneuro, 7(4), ENEURO.0076-20.2020. https://doi.org/10.1523/ENEURO.0076-20.2020
5. Camilieri-Asch, V., Shaw, J. A., Yopak, K. E., Chapuis, L., Partridge, J. C., & Collin, S. P. (2020). Volumetric analysis and morphological assessment of the ascending olfactory pathway in an elasmobranch and a teleost using diceCT. Brain Structure and Function, 225(8), 2347–2375. https://doi.org/10.1007/s00429-020-02127-1
6. Cha, E. S., Uhrin, M. T., McClelland, S. J., & Woodley, S. K. (2021). Brain plasticity in response to short-term exposure to corticosterone in larval amphibians. Canadian Journal of Zoology, 99(9), 839–844. https://doi.org/10.1139/cjz-2021-0031

7. Culumber, Z. W., Engel, N., Travis, J., & Hughes, K. A. (2020). Larger female brains do not reduce male sexual coercion. Animal Behaviour, 160, 15–24. https://doi.org/10.1016/j.anbehav.2019.11.018
8. Jenkins, M. R., Cummings, J. M., Cabe, A. R., Hulthén, K., Peterson, M. N., & Langerhans, R. B. (2021). Natural and anthropogenic sources of habitat variation influence exploration behaviour, stress response, and brain morphology in a coastal fish. Journal of Animal Ecology, 90(10), 2446–2461. https://doi.org/10.1111/1365-2656.13557
9. Joyce, B. J., & Brown, G. E. (2020a). Rapid plastic changes in brain morphology in response to acute changes in predation pressure in juvenile Atlantic salmon (*Salmo salar*) and northern redbelly dace (Phoxinus eos). Canadian Journal of Zoology, 98(3), 186–194. https://doi.org/10.1139/cjz-2019-0131
10. Joyce, B. J., & Brown, G. E. (2020b). Short-term captivity drives hypothalamic plasticity and asymmetry in WILD-CAUGHT northern red bellied dace (CHROSOMUS EOS). Journal of Fish Biology, 97(2), 577–582. https://doi.org/10.1111/jfb.14408
11. Laberge, F., Gutgesell, M., & McCann, K. S. (2021). Increased brain growth in escaped rainbow trout [Preprint]. Zoology. https://doi.org/10.1101/2021.06.17.448828
12. Liu, M., Jia, J., Wang, H., & Wang, L. (2022). Allometric model of brain morphology of Hemiculter leucisculus and its variation along climatic gradients. Journal of Anatomy, joa.13664. https://doi.org/10.1111/joa.13664
13. Liu, M., Liu, Y., Wang, X., & Wang, H. (2021). Brain morphological adaptations of Gambusia affinis along climatic gradients in China. Journal of Zoological Systematics and Evolutionary Research, 59(8), 2150–2160. https://doi.org/10.1111/jzs.12544
14. McNeil, R. M., Devigili, A., Kolm, N., & Fitzpatrick, J. L. (2021). Does brain size affect mate choice? An experimental examination in pygmy halfbeaks. Behavioral Ecology, 32(6), 1103–1113. https://doi.org/10.1093/beheco/arab046
15. Mitchell, D. J., Lefèvre, J., Vega-Trejo, R., Vila Pouca, C., & Kotrschal, A. (2020). Visual and olfactory cues of predation affect body and brain growth in the guppy [Preprint]. EcoEvoRxiv. https://doi.org/10.32942/osf.io/vxrq4
16. Mitchell, D. J., Vega-Trejo, R., & Kotrschal, A. (2020). Experimental translocations to low predation lead to non-parallel increases in relative brain size. Biology Letters, 16(1), 20190654. https://doi.org/10.1098/rsbl.2019.0654
17. Oliveira, R. C., & Graça, W. J. (2020). Encephalon gross morphology of the cichlid Geophagus sveni (Cichlidae: Geophagini): Comparative description and ecological perspectives. Journal of Fish Biology, 97(5), 1363–1374. https://doi.org/10.1111/jfb.14495
18. Pereira, P. D. C., Henrique, E. P., Porfírio, D. M., Crispim, C. C. de S., Campos, M. T. B., de Oliveira, R. M., Silva, I. M. S., Guerreiro, L. C. F., da Silva, T. W. P., da Silva, A. de J. F., Rosa, J. B. da S., de Azevedo, D. L. F., Lima, C. G. C., Castro de Abreu, C., Filho, C. S., Diniz, D. L. W. P., Magalhães, N. G. de M., Guerreiro-Diniz, C., Diniz, C. W. P., & Diniz, D. G. (2020). Environmental Enrichment Improved Learning and Memory, Increased Telencephalic Cell Proliferation, and Induced Differential Gene Expression in Colossoma macropomum. Frontiers in Pharmacology, 11, 840. https://doi.org/10.3389/fphar.2020.00840
19. Peris Tamayo, A., Devineau, O., Præbel, K., Kahilainen, K. K., & Østbye, K. (2020). A brain and a head for a different habitat: Size variation in four morphs of Arctic charr (Salvelinus alpinus (L.)) in a deep oligotrophic lake. Ecology and Evolution, 10(20), 11335–11351. https://doi.org/10.1002/ece3.6771
20. Peters, H., Laberge, F., & Heyland, A. (2022). Latent effect of larval rearing environment on post-metamorphic brain growth in an anuran amphibian. Zoology, 152, 126011. https://doi.org/10.1016/j.zool.2022.126011
21. Roussos, I., & Megalofonou, P. (2021). Ontogenetic shifts and sexual dimorphism in the brain organization of the small-spotted catshark Scyliorhinus canicula. Journal of the Marine Biological Association of the United Kingdom, 101(1), 189–198. https://doi.org/10.1017/S0025315420001368

22. Sowersby, W., Eckerström-Liedholm, S., Kotrschal, A., Näslund, J., Rowiński, P., Gonzalez-Voyer, A., & Rogell, B. (2021). Fast life-histories are associated with larger brain size in killifishes. Evolution, 75(9), 2286–2298. https://doi.org/10.1111/evo.14310
23. Triki, Z., Aellen, M., van Schaik, C. P., & Bshary, R. (2021). Relative brain size and cognitive equivalence in fishes. Brain, Behavior and Evolution. https://doi.org/10.1159/000520741
24. Triki, Z., Emery, Y., Teles, M. C., Oliveira, R. F., & Bshary, R. (2020). Brain morphology predicts social intelligence in wild cleaner fish. Nature Communications, 11(1), 6423. https://doi.org/10.1038/s41467-020-20130-2
25. Versteeg, E. J., Fernandes, T., Guzzo, M. M., Laberge, F., Middel, T., Ridgway, M., & McMeans, B. C. (2021). Seasonal variation of behavior and brain size in a freshwater fish. Ecology and Evolution, 11(21), 14950–14959. https://doi.org/10.1002/ece3.8179
26. Yao, Z., Qi, Y., Yue, B., & Fu, J. (2021). Brain size variation along altitudinal gradients in the Asiatic Toad (Bufo gargarizans). Ecology and Evolution, 11(7), 3015–3027. https://doi.org/10.1002/ece3.7192
27. Ye, C., Xu, S., Hu, Q., Hu, M., Zhou, L., Qin, X., Jia, J., & Hu, G. (2020). Structure and function analysis of various brain subregions and pituitary in grass carp (Ctenopharyngodon idellus). Comparative Biochemistry and Physiology Part D: Genomics and Proteomics, 33, 100653. https://doi.org/10.1016/j.cbd.2019.100653
28. Závorka, L., Koeck, B., Armstrong, T. A., Soğanci, M., Crespel, A., & Killen, S. S. (2020). Reduced exploration capacity despite brain volume increase in warm acclimated common minnow. Journal of Experimental Biology, jeb.223453. https://doi.org/10.1242/jeb.223453
29. Závorka, L., Koene, J. P., Armstrong, T. A., Fehlinger, L., & Adams, C. E. (2022). Differences in brain morphology of brown trout across stream, lake, and hatchery environments. Ecology and Evolution, 12(3). https://doi.org/10.1002/ece3.8684
30. Závorka, L., Wallerius, M. L., Kainz, M. J., & Höjesjö, J. (2021). Linking brain size in wild stream-dwelling brown trout with dietary supply of omega-3 fatty acids [Preprint]. Preprints. https://doi.org/10.22541/au.163407473.35960551/v2

Category	Topic	Author	Year	DOI
Commentary	Good data behind clever analyses?	Cardini	2020	10.1002/ar.24397
Considerations	The impact of sample size	Cardini et al.	2015	10.1007/s00435-015-0253-z
	Measurement error in geometric morphometrics	Fruciano	2016	10.1007/s00427-016-0537-4
	Considerations of allometry in morphometrics	Klingenberg	2016	10.1007/s00427-016-0539-2
	Shape, size and allometry in Procrustes analysis	Mitteroecker et al.	2013	10.4404/hystrix-24.1-6369
	Ontogeny and phylogeny in morphometrics	Rohlf	1998	www.jstor.org/stable/2585239
Photography	Potential sources of error during photography	Muir et al.	2012	10.1080/00028487.2012.685823
	A discussion of common lens distortions	Neale et al.	2014	10.4271/2011-01-0286
Software	R package for geometric morphometrics	Adams & Otárola-Castillio	2013	10.1111/2041-210X.12035
	MorphoJ: To analyze morphology data	Klingenberg	2016	10.1111/j.1755-0998.2010.02924.x
	TPSDig and TPSUtil	Rohlf	2015	10.4404/hystrix-26.1-11264
	ImageJ from NIH	Schneider et al.	2012	10.1038/nmeth.2089
Methodology	Optimizing landmark digitalization	Evin et al.	2020	10.1093/biomethods/bpaa023
	Using ImageJ for efficent measurements	Andrialovanirina et al.	2020	j.fishres.2019.105425
	Measurements from historical data sets	Black et al.	2019	10.1186/s12983-019-0309-x
	Comparing 2D versus 3D morphometrics	Cardini	2014	10.4404/hystrix-25.2-10993
	Testing the goodness of fit of 2D models	McWhinnie & Parsons	2019	10.1007/s10641-019-00879-2
	Suggestions for doing photography in the field	Meise et al.	2014	10.1371/journal.pone.0101197
	A modernized approach to landmark detection	Vandaele et al.	2018	10.1038/s41598-017-18993-5
	Introductory guide to landmarks	Webster & Sheets	2010	10.1017/S1089332600001868
	Introduction to geometric morphometrics	Zelditch	2012	ISBN 978-0-12-386903-6

Table .E2 – A collection of resources regarding experimental design, data collection, shape analysis and geomorphic morphometrics

Table E.2 References

1. Adams, D. C., & Otárola-Castillo, E. (2013). geomorph: An R package for the collection and analysis of geometric morphometric shape data. *Methods in Ecology and Evolution*, *4*(4), 393–399. https://doi.org/10.1111/2041-210X.12035
2. Andrialovanirina, N., Ponton, D., Behivoke, F., Mahafina, J., & Léopold, M. (2020). A powerful method for measuring fish size of small-scale fishery catches using ImageJ. *Fisheries Research*, *223*, 105425. https://doi.org/10.1016/j.fishres.2019.105425
3. Black, C. E., Mumby, H. S., & Henley, M. D. (2019). Mining morphometrics and age from past survey photographs. *Frontiers in Zoology*, *16*(1), 14. https://doi.org/10.1186/s12983-019-0309-x
4. Cardini, A. (2014). Missing the third dimension in geometric morphometrics: How to assess if 2D images really are a good proxy for 3D structures? *Hystrix, the Italian Journal of Mammalogy*, *25*(2). https://doi.org/10.4404/hystrix-25.2-10993
5. Cardini, A. (2020). Modern morphometrics and the study of population differences: Good data behind clever analyses and cool pictures? *The Anatomical Record*, *303*(11), 2747–2765. https://doi.org/10.1002/ar.24397
6. Cardini, A., Seetah, K., & Barker, G. (2015). How many specimens do I need? Sampling error in geometric morphometrics: testing the sensitivity of means and variances in simple randomized selection experiments. *Zoomorphology*, *134*(2), 149–163. https://doi.org/10.1007/s00435-015-0253-z
7. Evin, A., Bonhomme, V., & Claude, J. (2020). Optimizing digitalization effort in morphometrics. *Biology Methods and Protocols*, *5*(1), bpaa023. https://doi.org/10.1093/biomethods/bpaa023
8. Fruciano, C. (2016). Measurement error in geometric morphometrics. *Development Genes and Evolution*, *226*(3), 139–158. https://doi.org/10.1007/s00427-016-0537-4
9. Klingenberg, C. P. (2016). Size, shape, and form: Concepts of allometry in geometric morphometrics. *Development Genes and Evolution*, *226*(3), 113–137. https://doi.org/10.1007/s00427-016-0539-2
10. McWhinnie, K. C., & Parsons, K. J. (2019). Shaping up? A direct comparison between 2D and low-cost 3D shape analysis using African cichlid mandibles. *Environmental Biology of Fishes*, *102*(7), 927–938. https://doi.org/10.1007/s10641-019-00879-2
11. Meise, K., Mueller, B., Zein, B., & Trillmich, F. (2014). Applicability of Single-Camera Photogrammetry to Determine Body Dimensions of Pinnipeds: Galapagos Sea Lions as an Example. *PLoS ONE*, *9*(7), e101197. https://doi.org/10.1371/journal.pone.0101197
12. Mitteroecker, P., Gunz, P., Windhager, S., & Schaefer, K. (2013). A brief review of shape, form, and allometry in geometric morphometrics, with applications to human facial morphology. *Hystrix, the Italian Journal of Mammalogy*, *24*(1). https://doi.org/10.4404/hystrix-24.1-6369
13. Muir, A. M., Vecsei, P., & Krueger, C. C. (2012). A Perspective on Perspectives: Methods to Reduce Variation in Shape Analysis of Digital Images. *Transactions of the American Fisheries Society*, *141*(4), 1161–1170. https://doi.org/10.1080/00028487.2012.685823
14. Neale, W. T., Hessel, D., & Terpstra, T. (2011). *Photogrammetric Measurement Error Associated with Lens Distortion*. 2011-01–0286. https://doi.org/10.4271/2011-01-0286
15. Rohlf, F. (2015). The tps series of software. *Hystrix, the Italian Journal of Mammalogy*, *26*(1). https://doi.org/10.4404/hystrix-26.1-11264
16. Rohlf, F. J. (1998). On Applications of Geometric Morphometrics to Studies of Ontogeny and Phylogeny. *Systematic Biology*, *47*(1), 147–158. https://doi.org/10.1080/106351598261094
17. Schneider, C. A., Rasband, W. S., & Eliceiri, K. W. (2012). NIH Image to ImageJ: 25 years of image analysis. *Nature Methods*, *9*(7), 671–675. https://doi.org/10.1038/nmeth.2089
18. Vandaele, R., Aceto, J., Muller, M., Péronnet, F., Debat, V., Wang, C.-W., Huang, C.-T., Jodogne, S., Martinive, P., Geurts, P., & Marée, R. (2018). Landmark detection in 2D bioimages for geometric morphometrics: A multi-resolution tree-based approach. *Scientific Reports*, *8*(1), 538. https://doi.org/10.1038/s41598-017-18993-5
19. Webster, M., & Sheets, H. D. (2010). A Practical Introduction to Landmark-Based Geometric Morphometrics. *The Paleontological Society Papers*, *16*, 163–188. https://doi.org/10.1017/S1089332600001868
20. Zelditch, M. L., Swiderski, D. L., & Sheets, H. D. (2012). *Geometric morphometrics for biologists: A primer.* (2nd ed.). Academic Press.

Table E.3 – Supplementary data for the echinoderm set: shape metrics of circularity (C)/solidity (S); equivalent radius (R), known volume, and estimates based on: EM half-ellipsoid (H) / full-ellipsoid (F) and ACA top-down (T) and side-on (S) volume estimate comparisons

Species	CT	CS	ST	SS	R_{Vol}[a]	RT	R_S[a]	R_F[a]	R_H[a]	Vol[b]	EM_F[b]	EM_H[b]	ACA_T[b]	ACA_S[b]
O. japonicus	0.03	0.04	0.16	0.26	0.21	0.28	0.44	0.87	1.17	-1.39	0.43	-0.44	-0.55	-0.35
A. scoparius	0.05	0.12	0.37	0.74	128.91	122.82	54.83	148.33	155.17	6.95	7.14	5.84	2.09	1.74
P. helianthoides	0.05	0.13	0.62	0.85	86.27	130.36	47.16	118.17	122.83	6.43	6.84	5.64	2.12	1.67
P. pectinifera	0.20	0.31	0.44	0.93	72.14	103.04	63.84	121.17	51.33	6.20	6.87	6.04	2.01	1.81
O. reticulatus	0.31	0.32	0.62	0.88	90.27	131.04	79.47	146.33	176.83	6.49	7.12	6.32	2.12	1.90
C. schmideliana	0.67	0.56	0.97	0.96	155.12	156.97	107.37	133.33	158.33	7.19	7.00	6.71	2.20	2.03
E. antillarum	0.80	0.65	0.99	0.98	110.23	124.72	90.81	107.33	129.50	6.75	6.71	6.50	2.10	1.96
C. albogalerus	0.88	0.74	0.99	0.98	98.11	99.31	89.65	96.83	126.33	6.60	6.58	6.48	2.00	1.95
S. purpuratus	0.89	0.83	0.99	0.99	124.31	120.08	107.74	112.67	144.83	6.91	6.78	6.72	2.08	2.03

a) radius of the sphere corresponding to the estimate, b) $\log_{10}$ transformed